AN ATTEMPT TOWARDS AN INTERPRETATION OF A CONTINUOUS CRUSTAL SEISMIC REFRACTION SURVEY IN MANITOBA

A Thesis
Presented to
The Faculty of Graduate Studies and Research
University of Manitoba

In Partial Fulfillment
of the Requirements for the Degree
Master of Science

By
Rebecca R. Santos
October, 1976

"AN ATTEMPT TOWARDS AN INTERPRETATION OF A CONTINUOUS CRUSTAL SEISMIC REFRACTION SURVEY IN MANITOBA"

by

REBECCA R. SANTOS.

A dissertation submitted to the Faculty of Graduate Studies of the University of Manitoba in partial fulfillment of the requirements of the degree of

MASTER OF SCIENCE

ACKNOWLEDGEMENTS

This writer wishes to thank Drs. A. G. Green and D. H. Hall for their comments and general supervision. Funds supporting this research came from the National Research Council of Canada. Financial assistance for the support of this writer also came from the Student Aid Branch, Department of Colleges and Universities Affairs, the Government of Manitoba.

ABSTRACT

The objective of this thesis is to test the usefulness of a new processing technique in enhancing seismic events. The principal technique is a weighted differential stack (WDS) assuming uniform moveout for the expected arrivals. This technique is applied to selected records from a near-continuous crustal seismic refraction survey conducted near the Manitoba-Ontario boundary to the east of Lake Winnipeg, during the periods of June to July, 1967 and May to June, 1968. The records are obtained from stations P30 to P40 and P48 to P59 (as indicated in the field books of this survey) which were previously digitized, filtered, and recorded on two separate 800 bpi tapes. The results obtained are very satisfactory. There is a definite improvement in the resolution of the arrivals over those observed on the original playback records and the sections given by Hajnal (1970). The WDS traces not only confirm the existence of the events interpreted as Pg, P*, PP, Pn, and PPPP by Hajnal (1970) on the records but also show the presence of two other events, referrred to as X1 and X2, not previously identified by Hajnal on the same records.

TABLE OF CONTENTS

LIST OF FIGURES

LIST OF TABLES

CHAPTER I

A SHORT DESCRIPTION OF THE DATA USED IN THIS STUDY

1.1 Introduction

Explosion seismology has increasingly become an important field in the study of the earth's crust. Here in Manitoba, such studies began in the early 1960's. Since then a number of surveys have been made and their results published. A compilation of all previous seismic work by the University of Manitoba crustal study group since 1961 is given by Hall and Hajnal (1973). Dorn (1974) traces the development of the seismic method in this university.

1.2 A Review of the Survey

In the summers of 1967 and 1968 (June-July, 1967 and May-June, 1968) a near-continuous refraction survey was conducted near the Manitoba-Ontario boundary to the east of Lake Winnipeg (Figure 1). The data gathered in this survey together with the data from two other surveys conducted over the same area (a regional refraction survey and a near-vertical reflection survey) were analyzed by Hajnal (1970). The near-continuous refraction survey is the main subject of the present investigation. However, only those records of good quality are used here. These are the recordings from stations P30 to P40 and P48 to P59 as denoted in the field books of the survey and which Hajnal referred to as stations A-30 to A-40 and A-48 to A-59. These data were previously digitized, filtered, and recorded by Hajnal on two separate 800 bpi magnetic tapes. The amplitude response of the applied 5-25 Hz bandpass filter is given in Figure 2. The set of

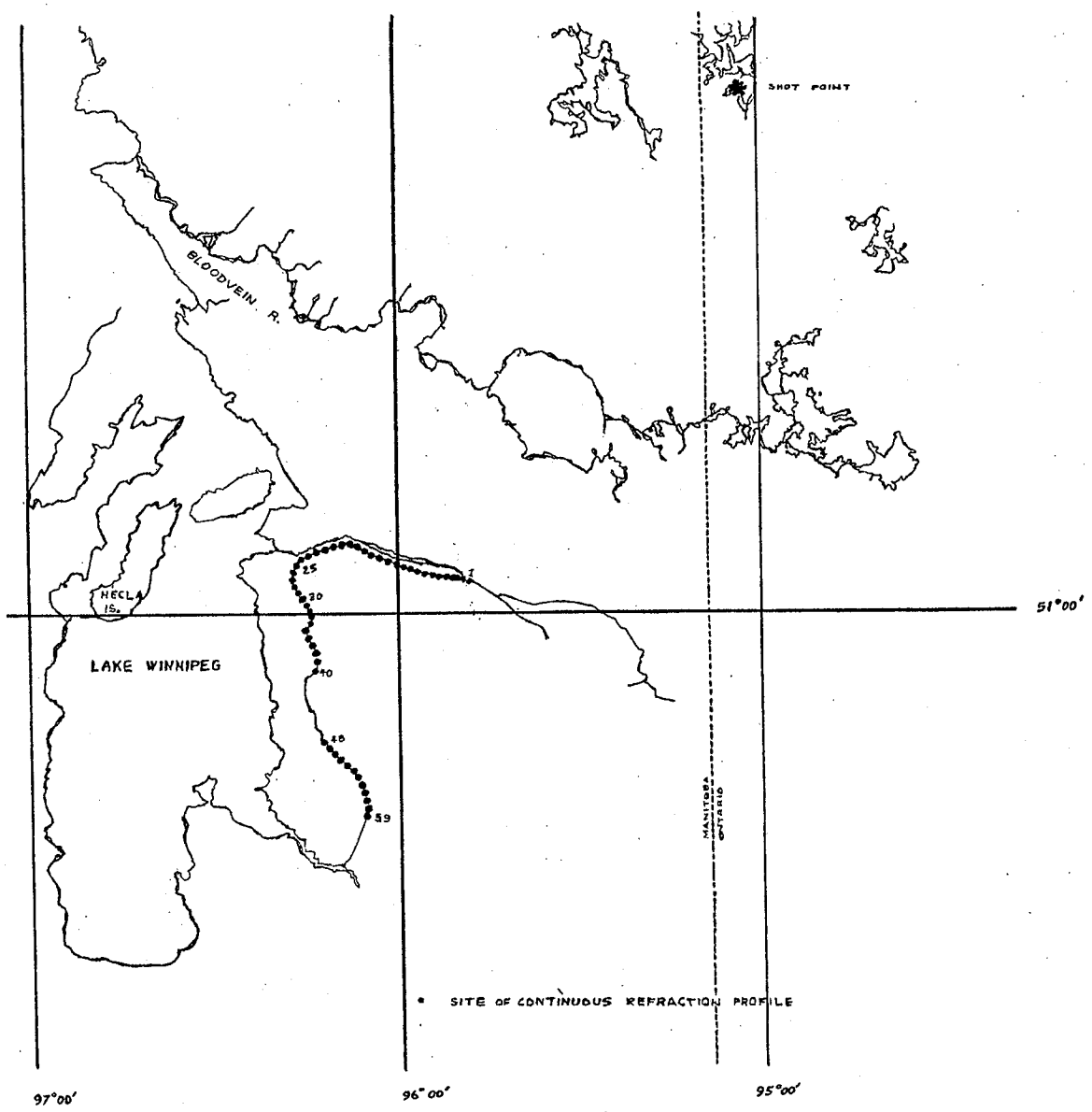

Figure 1. A schematic diagram showing the location sites of the continuous refraction survey.

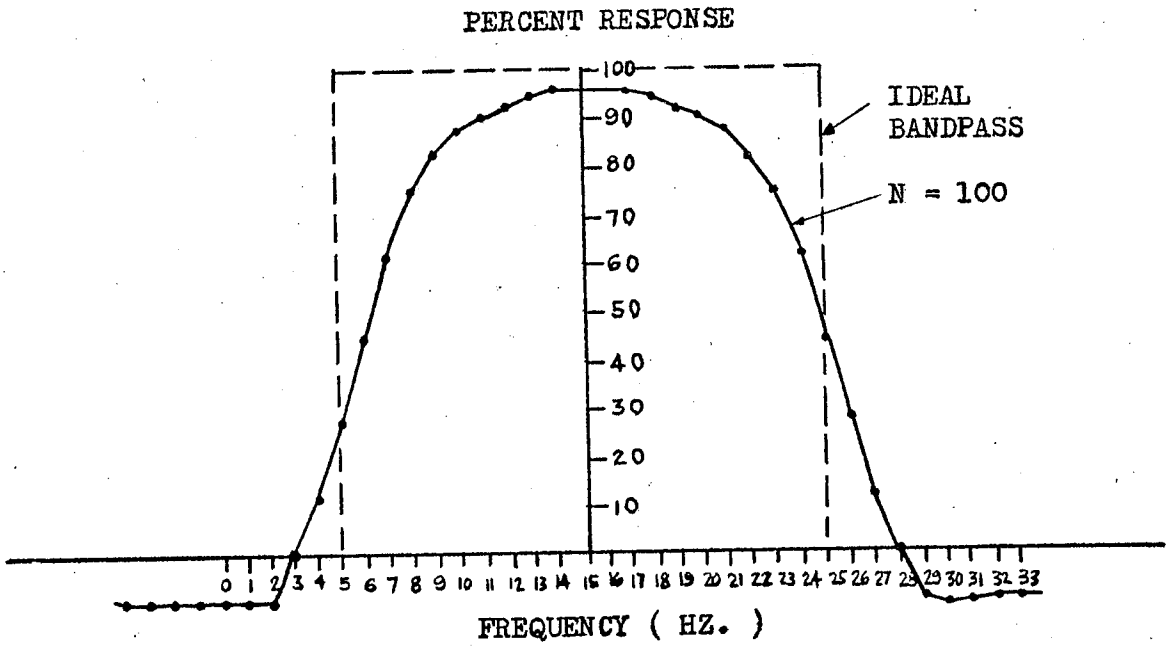

Figure 2. Amplitude response of a 100-point, 5-25 Hz bandpass filter modified from Hajnal (1970).

recordings corresponding to stations P30 to P40 of the field books is indexed 30 to 40 on the tape; the other set corresponding to P48 to P59 is indexed 41 to 52. Since information for more than just one station is contained in each data set, the indices are used to distinguish one record from another within that set. A 'record' contains the complete set of digitized information from the twelve channels at a recording site. Thus 'record' will be used to refer to the set of logical records on tape which begin with the same index number. Henceforth 'record' and 'station' will be used interchangeably. For future reference, a description of these tapes, information regarding the data stored here, and comparison of the notation used in designating these records are given in Appendix A.

The recordings were made along the provincial highway 304 using

seismometers of the Geo-Space HS-10-1 type with a natural resonant frequency of 1 Hz. The reader is referred to Homeniuk (1972) for a diagram of the response characteristics of this instrument. At each site an effort was made to lay out the one-mile spread of 12 geophones as closely in line with the shot point - station direction as possible. The field books show that there was difficulty in achieving this as the linear array commonly formed angles θ with respect to this direction of about 40° to 70°. Other stations, however, were aligned to within 6°. The array geometry is shown in Figure 3. The geophone spacing was approximately 144 ft (0.132 km). Continuity in this survey was achieved by making the last geophone in each one-mile spread the position of the first geophone in the next one-mile spread that is laid out. Of the twelve seismometers, four were used to record horizontal motion in channels 2, 3, 10, and 11; the rest were used to record vertical ground motion. Each seismometer was connected to a single takeout. In this investigation, only the vertical channels were used and interpreted. Hajnal gives an excellent discussion of the instrumentation, digitization, and filtering of the data. Hence no further discussion of these is needed.

The data on the magnetic tapes have not been corrected for dc-shift and modulation difference. The appropriate corrections were therefore made. For each record, the dc-shift correction was achieved by subtracting the average of each trace, corresponding to each channel, from each trace element in that channel. Modulation differences between channels were corrected by simply scaling the traces to a common maximum amplitude value. Only the first eight

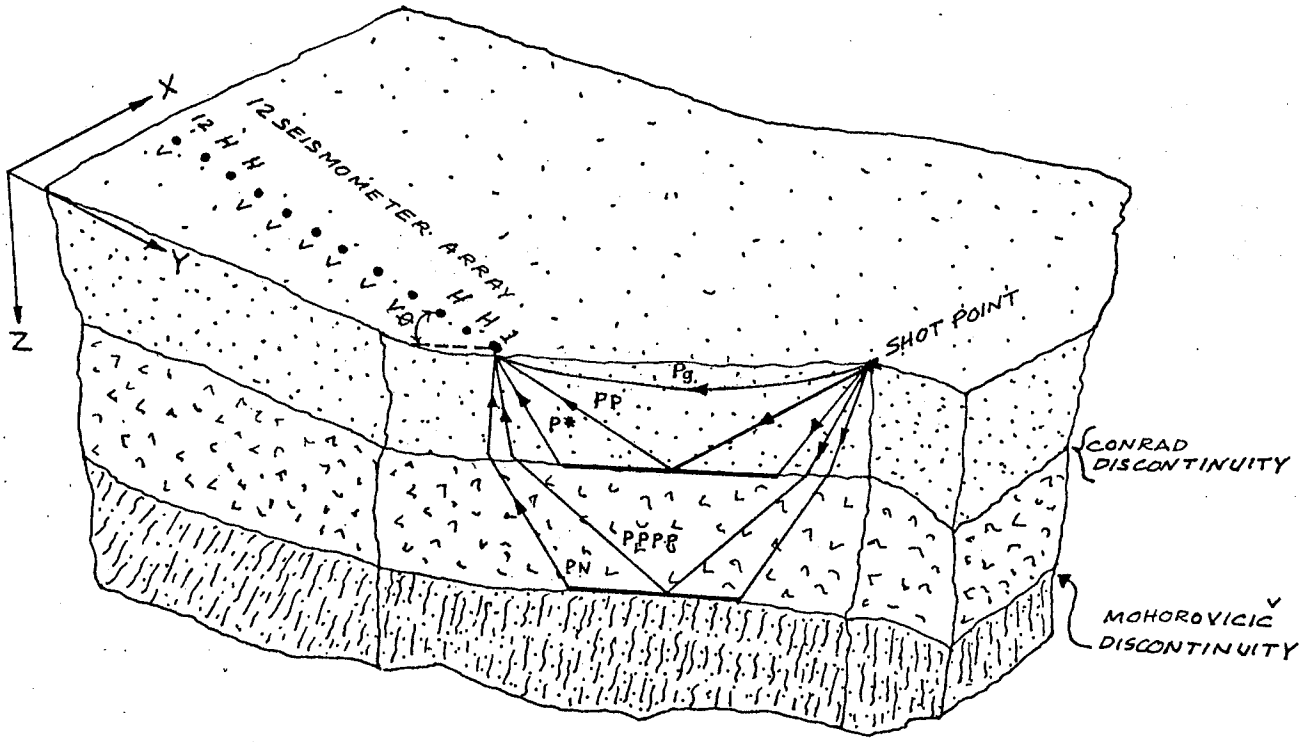

Figure 3. A cut-away diagram showing the shot point - station geometry. The definitions of the arrivals Pg, P*, PP, Pn, and PPPP are also illustrated using uniformly - and horizontally - layered subsurface. This diagram is not drawn to scale.

seconds of each record were used and edited as described above. These edited data were then written on magnetic tapes at 6250 bpi.

1.3 Timing

The times t_{oi} of the beginning of the digitized records on tapes for the stations P_i relative to the explosion of the charges at the shot point were redetermined. According to Hajnal, this information is in the digital tape file book which he started, but this was not available for this investigation. The early part of each record was plotted according to a known scale. At least three very sharp peaks which fall on the division lines of the analog playback of the best

quality single channel trace were chosen. The times $t_{i,j}$ of the peaks were then read as accurately as possible. It was found possible to read each $t_{i,j}$ up to three significant decimal figures with an estimated average error of $\pm$ 0.005 sec. The computer plots were later compared with the analog records and used to locate the sample number and logical record number* of these peaks. The times $\tilde{t}_{i,j}$ of these peaks from the beginning of the digitized record were calculated. Thus the time of the beginning of the digitized record P_i was found using

$$(1) \qquad t_{oi} = \left(\sum_{j=1}^{n} t_{i,j} - \tilde{t}_{i,j} \right) (n)^{-1}$$

where n = number of peaks used in the measurement. This method differs from that applied by Hajnal who used first break information. Since the first break may not be clear on either the analog or the digital record in the case of noisy channels, the present method is considered more reliable. The use of the peaks in this measurement was made possible by the availability of the Calcomp plotter in the present computer system.

Since the time of explosion of the charge can usually be determined only up to one or two significant decimal figures, the error estimate of $\pm$ 0.005 sec represents the minimum error in

---

* Hajnal referred to each logical record as a block in his discussion of the timing of digitization. In this particular case this is possible as on these tapes, each physical block contains only one logical record. However, the terms 'block' and 'logical record' will not be synonymous if the recording is made on tape such that more than one logical record is put in one physical block, i.e., a blocked format is used.

determining the times of the start of the digitized records. This must be counted when estimating the error in the times of the arrivals in any record. In this thesis, error estimates are made whenever possible as an aid in comparing results.

1.4 Digitization

In Chapter V of Hajnal (1970), a fairly complete description of the digitization process is given. However, the manner in which the data is written onto the magnetic tape during the digitization is not mentioned there. Since this affects the relative shifts of the channels required for the weighted differential stack, particularly at high velocities, this process will be discussed here.

The analog to digital process is illustrated schematically in Figure 4. In this figure, channel 1 is sampled at time τ. This sample is then written onto the magnetic tape as 1 byte of information. Then channel 2 is sampled at time $\tau + \Delta/12$, where Δ is equal to the sampling interval of 0.0017143 sec. This sample is written onto the tape as the next byte and so on. Sampling of the twelve traces, therefore, is not along $\overline{AB}$ but along $\overline{AC}$. The next sample from analog trace 1 is taken Δ sec later than the previous sample taken from the same trace and is $\Delta/12$ sec later than the sample from the analog trace 12. The process is repeated.

1.5 Example of a Digitized Record without Weighted Differential Stack

A plot of the first seven seconds of data for station P37 stored on an 800 bpi tape is shown in Figure 5. This is a replica of the analog playback for the same station. The arrivals identified by

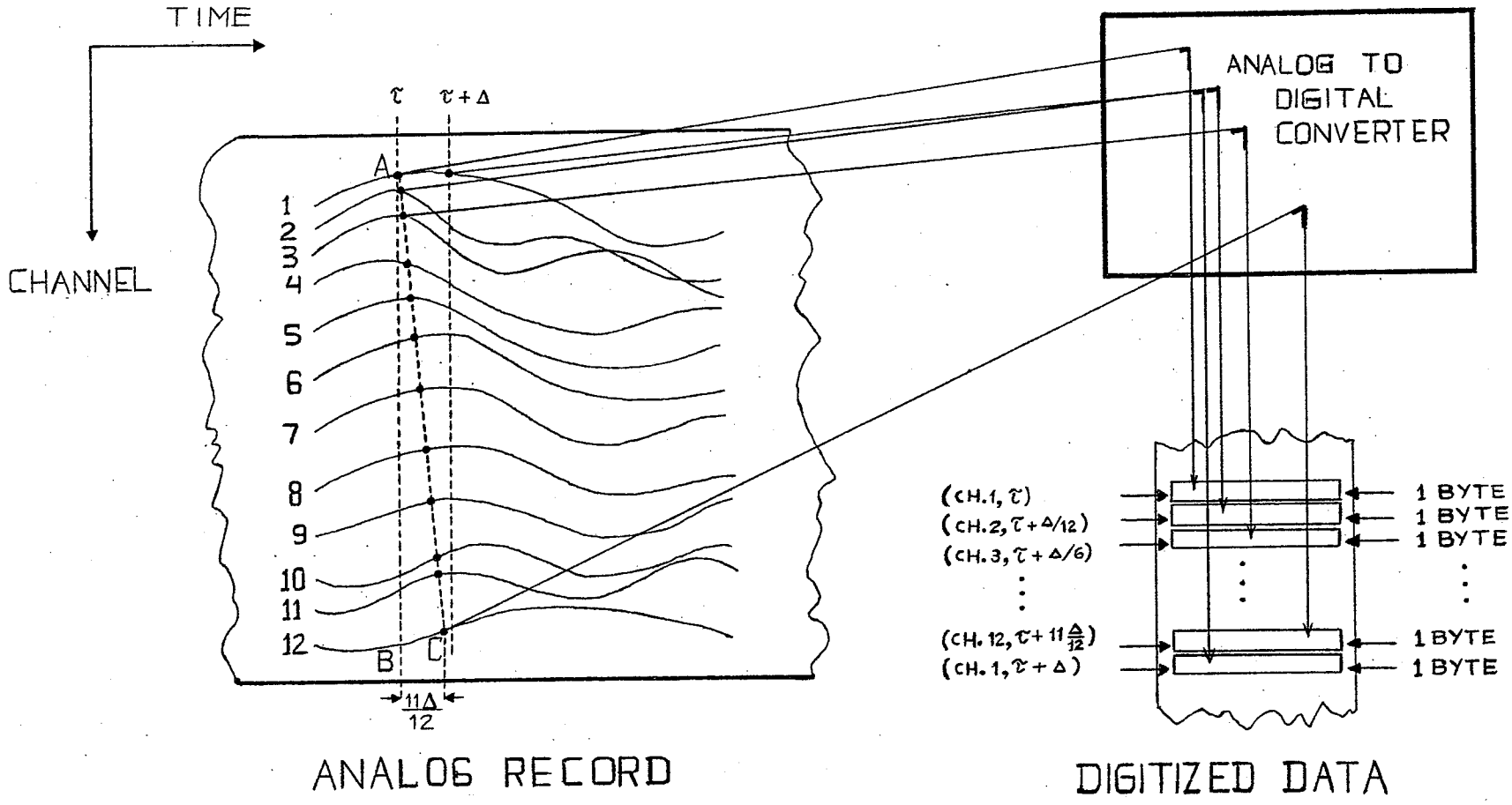

Figure 4. Diagram showing how samples are taken from the analog records and written onto the magnetic tape. The time axis is exagerated to show Δ.

Hajnal are indicated. Clearly, picking out the important events is not easy. In this thesis, it is shown that the application of a weighted differential stack on this and other records improves the signal to noise ratio and greatly improves the resolution of the events.

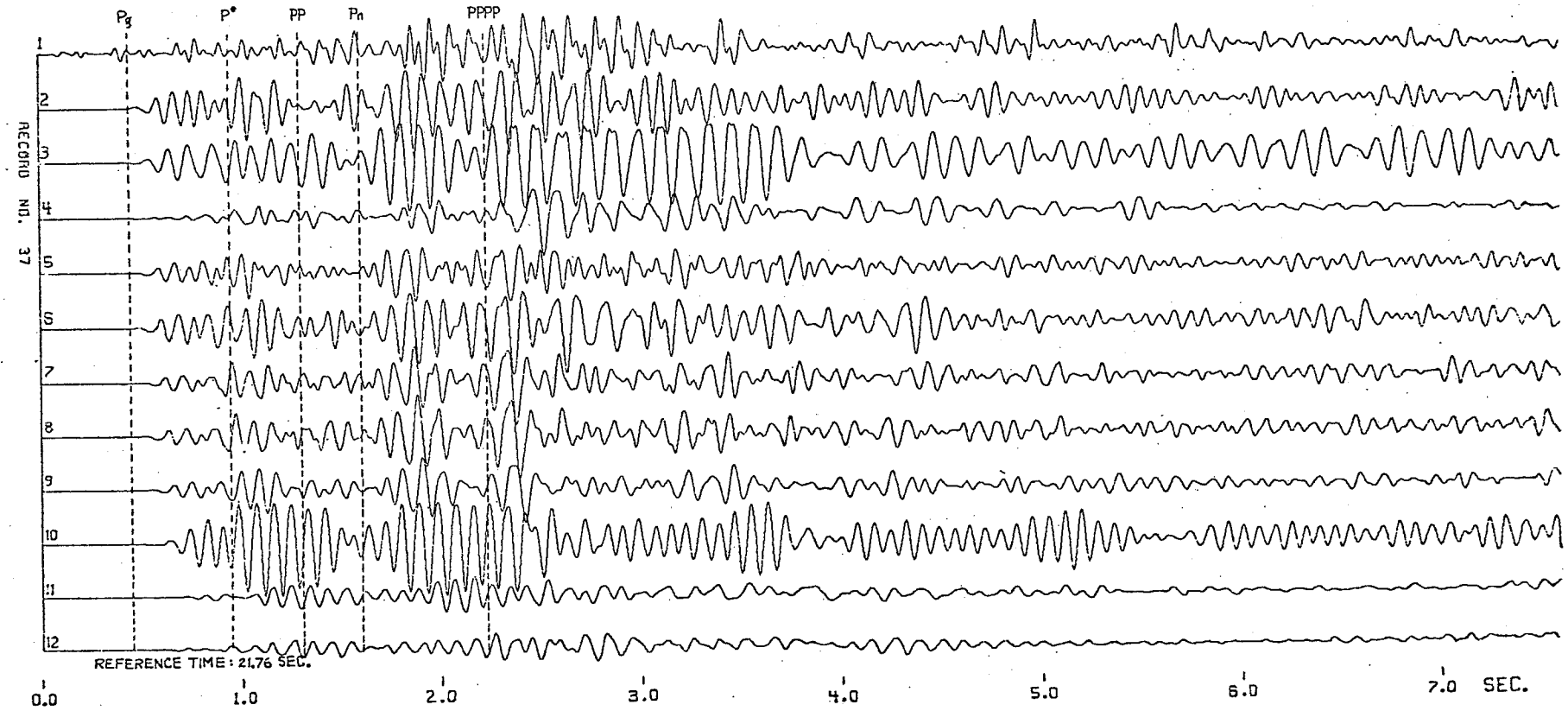

Figure 5. Plot of the first seven seconds of record P37 showing the arrivals Pg, P*, PP, Pn, and PPPP as identified by Hajnal (1970).

CHAPTER 2

PROCESSING OF DATA

2.1 Description of the Principal Processing Technique

The principal technique used in this study is a weighted differential stack (WDS). In this method, the seismic traces in each record are weighted according to their calculated signal to noise ratios. The traces are then shifted relative to each other according to the apparent velocity of an event being investigated. If the apparent velocity is assumed uniform for each geophone spread then the relative shifts from trace to trace are also uniform. The traces are then stacked or summed vertically into a single trace. This is illustrated in the following example.

Suppose 12 traces of record length 25 samples are read into a (12,25) matrix where each element $x_{i,j}$ (i=1,12 ; j=1,25) is represented by a half-word.* Let channel 1 be the reference channel with respect to which all other channels are shifted. For simplicity, assume that digital sampling of the 12 traces is taken simultaneously at any time $\tau = n\Delta$ for some value of n. The more complicated situation which involves the point raised in section 1.4 will be treated later. Also consider positive apparent velocity v for the p^{th} element of the stack trace, i.e., the single trace which results from WDS:

*The maximum decimal figure in a half-word is 32000.

$$(2) \qquad z_p^v = \sum_{i=1}^{12} \tilde{w}_i \, x_{i,p+k(i)} \qquad 1 \leq p \leq 25$$

$$(3) \qquad k(i) = \text{Int} \left[\frac{(i-1)d \cos \theta}{v \Delta} \right]$$

where z_p^v = $p^{\underline{th}}$ element of the stack trace for velocity v

Int (α) = α rounded off to an integer

v = apparent velocity

d = geophone separation

θ = angle shown in Figure 3

Δ = sampling interval

$\tilde{w}_i$ = modified weight of the $i^{\underline{th}}$ trace

$\tilde{w}_2 = \tilde{w}_3 = \tilde{w}_{10} = \tilde{w}_{11} = 0$ (eliminates horizontal traces from the stack)

In this example,

$$z_1^v = \tilde{w}_1 \, x_{1,1} + \tilde{w}_2 \, x_{2,1+k(2)} + \cdots + \tilde{w}_{12} \, x_{12,1+k(12)}$$

$$z_2^v = \tilde{w}_1 \, x_{1,2} + \tilde{w}_2 \, x_{2,2+k(2)} + \cdots + \tilde{w}_{12} \, x_{12,2+k(12)}$$

$$\vdots$$

The elements $x_{i,1}$ to $x_{i,k(i)}$ of the $i^{\underline{th}}$ channel ($2 \leq i \leq 12$) are discarded while an equal number of zeroes are added at the end of the trace to maintain the length of 25 samples. An illustration is given in Figure 6.

Each weight $\tilde{w}_i$ is calculated using the average power of the signal and average power of the noise in the $i^{\underline{th}}$ trace. Denote an element of the signal window as $x^s_{i,j}$ and an element of the noise window as $x^n_{i,j}$.

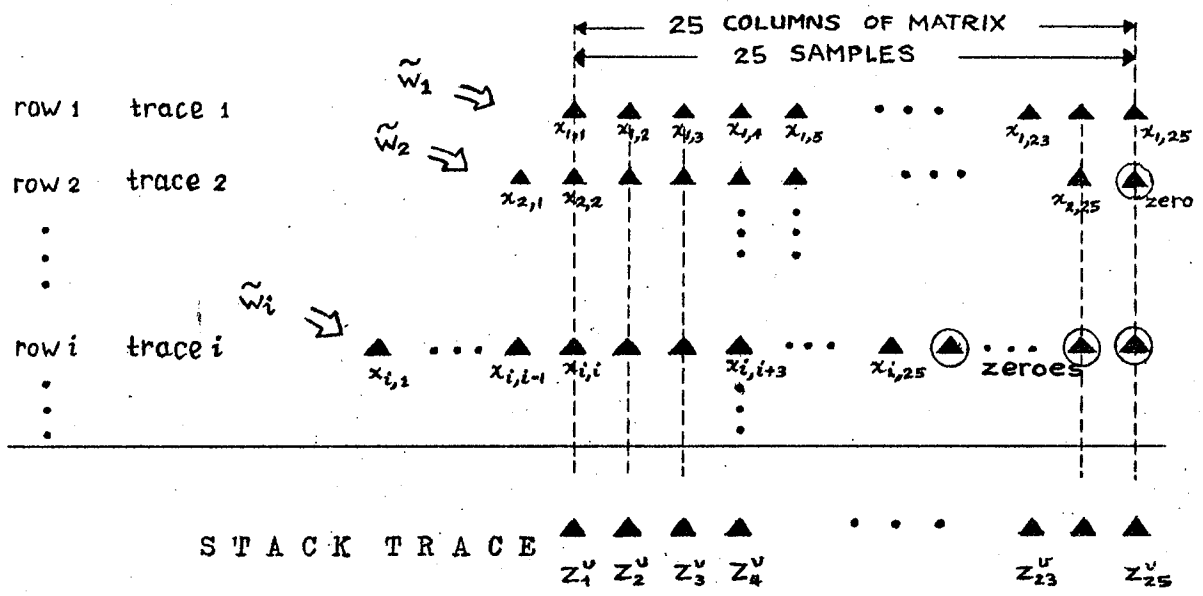

Figure 6. Illustration of weighted differential stack using $k(i)=(i-1)$ for all i. Each z_p^v is the sum of the elements in the column p of the matrix.

The noise window is taken from the section of the data before the first break while the signal window is taken from the section of the data with maximum and approximately uniform signal amplitude on all the traces.@

From Parseval's theorem, the mean square value or average power in the signal window in the i^{th} trace is

$$P_i^s = \frac{1}{M}\sum_{j=1}^{M}(x_{i,j}^s)^2 \qquad (4)$$

while the average power in the noise window is

$$P_i^n = \frac{1}{M}\sum_{j=1}^{M}(x_{i,j}^n)^2 \qquad (5)$$

where M is the number of samples in either window.* The length of the

---

@ A discussion on the choice of the signal and noise windows is given by Friesen (1974).

* Jenkins and Watts, Spectral Analysis and its Application (Holden-Day, 1968).

noise and signal windows in a trace must be the same to avoid biasing the signal to noise ratio estimate. This ratio may then be calculated as

$$(6) \qquad P_i^s / P_i^n = \frac{\sum_{j=1}^{M-1} (x_{i,j}^s)^2}{\sum_{j=1}^{M-1} (x_{i,j}^n)^2}$$

for the $i^{\underline{th}}$ channel. From Friesen (1974) the optimum weight is given by

$$(7) \qquad w_i = \left[P_i^s / P_i^n - 1 \right]^{\frac{1}{2}} / (P_i^n)^{\frac{1}{2}}$$

Now it is desirable to have sufficiently large maximum value for elements of a trace to preserve sufficient detail in the waveforms. Since in the programs each trace element is stored in a half-word only, the weights w_i are modified to keep the product elements $w_i x_{i,j}$ of the weighted $i^{\underline{th}}$ trace, and also the sums of these product elements (which sums are the elements of the stack trace) below 32000. These modified weights are denoted $\tilde{w}_i$.

WDS may be classified as a velocity filter because the traces in a record are shifted relative to each other according to the apparent velocity of the desired event. However, compared to the velocity filter used by Hajnal (1970), Baer (1972) and Homeniuk (1972) on seismic reflection data, this method has the clear advantage of the weighting factors $\tilde{w}_i$.

2.2 Stack using Uniform Moveout

The calculation of the weights was incorporated by Friesen (1974)

in the subroutine WEIGHT of the program NSTACK written by Friesen and Stephenson (University of Manitoba). The present writer subsequently modified the main program and renamed it MVSTACK in order to introduce changes in the manner of plotting and calculation of the relative shifts. The program MVSTACK used in this study is listed in Appendix B.

Uniform moveout is assumed in applying MVSTACK. The results obtained show that eight vertical traces stacked together give good enhancement of the arrivals, while 144 ft of geophone separation appears sufficient to permit resolution of arrivals falling in different velocity ranges provided the seismometer array is in close alignment with the shot point - station direction.

WDS is applied to the first seven seconds of each record. For each of records P30 to P40 a uniform scale is used in plotting the stack traces since the arrivals over the entire seven seconds have comparable amplitudes. For each of records P41 to P52 a first plot of the stack traces (length = 7 sec ; scale = s_1) show arrivals in the first half (first three or four seconds) with larger amplitude relative to later arrivals in the second half. Hence a second plot (scale = s_2 ; $s_2 > s_1$) of the second half of each of P41 to P52 is done for purposes of presentation. The original picks of the arrivals in a record are based on the first plot. However the times of these arrivals are based on the second plot. The choice of s_2 is subjective but as a general rule, it is chosen such that noise does not give rise to fictitious arrivals. The ratio $S = {}^{s_2}/_{s_1}$ is given in the labels of the figures. An example is given in Figure 7.

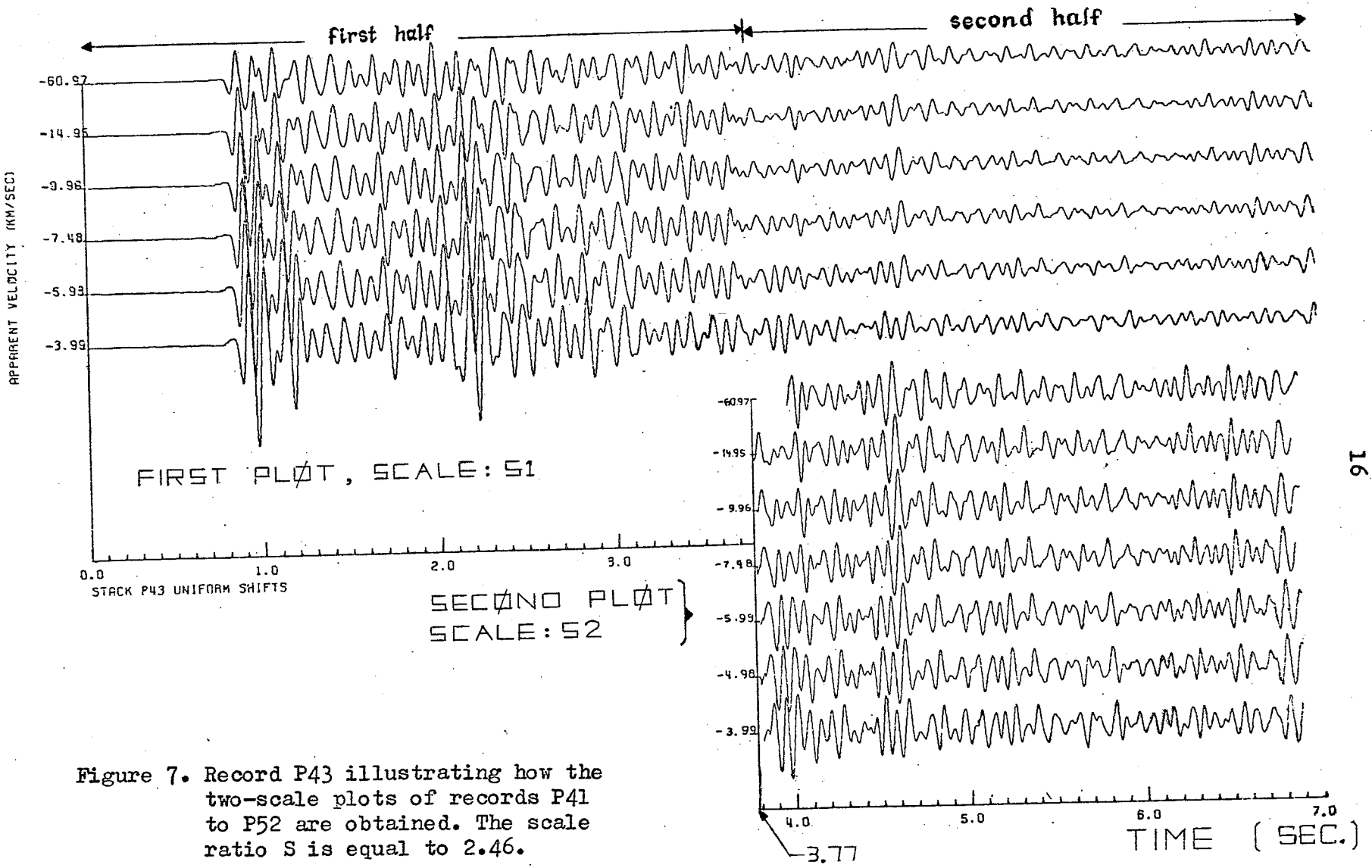

Figure 7. Record P43 illustrating how the two-scale plots of records P41 to P52 are obtained. The scale ratio S is equal to 2.46.

2.3 Calculation of Relative Shifts between Channels

When a set of 12 samples corresponding to 12 channels are stored in a column of the array DATA of program MVSTACK, these samples are assumed to have the same time coordinates; i.e., they were taken from the 12 analog traces simultaneously. In view of the discussion in section 1.4, this manner of storing information in the array DATA results in an automatic shift to the left of the samples corresponding to channels 2 to 12 by $\Delta/12$, $2\Delta/12$, . . ., and $11\Delta/12$, respectively. Call this shift the dh-shift, after data handling. This is illustrated in Figure 8.

A consequence of the digitization of data is the limitation of the relative shifts of the channels to only integral multiples of Δ. Without taking the dh-shift into account, the shift of channel i relative to channel 1 is given by equation (3) for assumed constant apparent velocity v. When the dh-shift is taken into account, the dh-shift is added to k(i) when v is positive. Thus for a chosen v, the resultant shift of channel i is

$$R_i = \frac{(i-1)\Delta}{12} + \text{Int}\left[\frac{(i-1)d\cos\theta}{v\Delta}\right] \qquad (8)$$

Define the effective apparent velocity for channel i by

$$\bar{v}_i = \frac{(i-1)d\cos\theta}{R_i\Delta} \qquad (9)$$

Clearly, $\bar{v}_i$ is different for each channel and is also different from v. From equations (3) and (9),

$$v - \bar{v}_i = \frac{v\,(i-1)\Delta}{12\,R_i} \qquad (10)$$

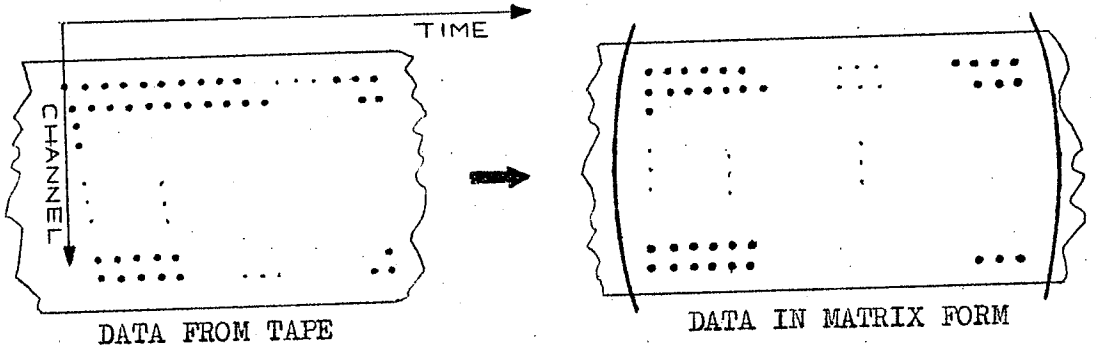

Figure 8. Diagram showing dh-shift effect that results from reading tape information into two dimensional array.

Since R_i is a function of $\cos\theta\ v^{-1}$ then $v - \bar{v}_i$ is approximately proportional to v^2 and inversely proportional to $\cos\theta$. Truncation by the function Int ( ) causes k(i) to vanish for certain values of v. For instance, k(4) vanishes when $v > \sim 230$ km/sec, $\theta \sim 10^\circ$; $v > \sim 180$ km/sec, $\theta \sim 40^\circ$; and when $v > \sim 80$ km/sec, $\theta \sim 70^\circ$. Consequently, the dh-shift dominates, the value of $\bar{v}_4$ jumps to $\frac{12d\cos\theta}{\Delta^2}$, and equation (10) ceases to hold. The velocity limits are greater for other channels. In the present study, only non-vanishing, integer values of k(i) are considered.

The use of R_i and $\bar{v}_i$ in the calculation of the relative shifts is shown in the following example. Suppose it is desired to plot three stack traces corresponding to chosen apparent velocities v: v^1 = 8.40 km/sec, v^2 = 15.00 km/sec, and v^3 = 70.00 km/sec. First, using equations (3), (8), and (9) construct a table of values of k(i) and $\bar{v}_i$ as shown in Appendix C. As these values may vary with θ, k(i) and $\bar{v}_i$ are calculated for $\theta = 6^\circ, 23^\circ$, and 72° in this example. The values of v are also given for comparison. Next, determine the relative shifts as follows. Consider v^1 in particular. The relative shift of channel i with respect to channel 1 is the value of k(i) at which $\bar{v}_i$ is closest

to v^1. When i = 2;3;10;11 set k(i) to zero. Then calculate the average effective apparent velocity V given by

$$V = \left(\sum_{i=2}^{12} \bar{v}_i \right) \Big/ 7 \qquad i \neq 2;3;10;11 \tag{11}$$

In this example, if $\theta = 6^\circ$, $V^1 = 8.43$ km/sec; if $\theta = 23^\circ$, $V^1 = 8.42$ km/sec; and if $\theta = 72^\circ$, $V^1 = 8.51$ km/sec.

At the appropriate value of θ, the values of k(i), i = 2,12, are read into the first row of the array ISHIFT of the program MVSTACK while V^1 is used to label stack trace 1.

Similar procedure is followed for v^2 and v^3.

CHAPTER 3

PRESENTATION AND EVALUATION OF RESULTS

3.1 Preliminary Remarks

In the following discussion, the events identified by Hajnal (1970) will be represented by the notation Pg, P*, PP, Pn, and PPPP. Their arrival times on each record were obtained from Table VI of Hajnal (1970, p.110).

The arrival times identified on the records in this study are denoted A_1, A_2, etc. in the order they appear in time on each record. They were identified independently of Hajnal's interpretation. They were picked solely on the basis of the observed changes in the waveform and amplitude on each stack trace. For this purpose, a graphing paper (density = 20 lines/inch) was used as an underlay and zero lines were drawn through the traces. The apparent velocity of an event A_i is the effective apparent velocity V of the stack trace on which it has maximum amplitude enhancement. The time of A_i was determined using the same trace. An error estimate of the time was also determined. The total timing error was then obtained by adding to this estimate 0.02 sec, the approximate error in the shot time, and 0.05 sec, the error in the timing of the start of a digital record. In this study, the time of an arrival was measured with respect to channel 1, as all the other vertical channels were shifted with respect to, and added to channel 1 in the stacking process.

The reference time indicated on each of Tables 1 to 22 refers to the time at which the plot in the accompanying figure begins

relative to the shot time. The starting time of all digital records (P30 to P52) are given in Appendix A.

The rules for the calculation of errors and the expressions used to estimate error in the intercept and slope of the linear least square fit to the data are given in Appendix D.

3.2 Results

(i) All the WDS records show definite improvement in their signal to noise ratios over the original unstacked traces. On many of these records, more arrivals can be picked and timed than on the analog playbacks or the sections given by Hajnal (i.e., the traces shown on pp.113-121 of Hajnal, 1970). Comparison of Figure 5 with Figure 16 and the section for P37 in Hajnal (1970, p.119) demonstrates this.

(ii) On the basis of seismic event enhancement, resolution, and effectiveness of apparent velocity discrimination, the WDS stacks of all records in this study may be classified into approximately four groups.

Group I includes records P30, P37, P46, P48, and P49 (Figures 10, 17, 25, 27, and 28, respectively). These records show good seismic event resolution and enhancement but only partially successful velocity discrimination. Some arrivals have maximum amplitudes at apparent velocities V within the expected ranges while other arrivals do not. For example, the arrivals A_3(P*) and A_5(Pn) of record P37 (Figure 17) have maximum amplitudes at apparent velocities 97.19 km/sec and 5.91 km/sec, respectively, instead of the expected 6.92 km/sec and 7.79 - 8.15 km/sec, respectively. On the other hand, events A_1(Pg), A_4(PP), and A_7(PPPP) of the same record have their maximum amplitudes at the expected apparent velocities. Although not

all of the events identified on the records in this group exhibit maximum amplitudes at their expected apparent velocities, many of the well identified events (e.g., Pg, Pn, etc.) have amplitudes near their expected velocities that are not significantly different from the maximum amplitudes. Compared to the results from other records in this study, the stacks in this group are of good quality.

The poorest results are obtained from Group IV records P31, P33, ans P52 (Figures 11, 13, and 31, respectively). The stack traces from each of these records are almost identical for a wide range of apparent velocities. Resolution of closely arriving events is poor. Some events have distorted waveforms.

Results intermediate between those of Group I and IV are subdivided into Group II (records P32, P34, P35, P36, P39, P40, P41, P43, P45, and P50 corresponding to Figures 12, 14, 15, 16, 19, 20, 21, 22, 24, and 29, respectively) and Group III (records P38, P44, P47, and P51 corresponding to Figures 18, 23, 26, and 30, respectively). Group II records produce variable stacks but they all have better quality than Group III records.

The explanation of the wide range of quality in the velocity stacks is probably related to the distribution of the weight coefficients $\tilde{w}$ among the channels of a record. Figures 9(a) to 9(d) display the weight distribution curves for the records in Groups I to IV respectively. The weights correponding to each record are normalized to a common maximum of 5. Comparison of these curves and the corresponding plots of the stack traces leads to the following observations:

(a) When two records have the same number of good channels (those with weight two or greater) and similar values of θ (within about 20° of each other), the efficiency of WDS as a velocity filter is greater for the record whose good quality channels are most widely separated. For instance, compare the result from record P30 (good quality channels 1, 4, 9, and 12; Figures 9(a) and 10) with the result from record P32 (good quality channels 4, 5, 7, and 8; Figures 9(b) and 12).

(b) A very large value of θ (60° or greater) diminishes the otherwise good effect of a good weight distribution on the stack traces, as on records P43 and P50; see Figures 9(c), 22, and 29 .

(c) The general character of the weight distribution curves for records in the same group are similar; however, they differ from group to group. Starting from Group I, they change from having many widely separated peaks (or good channels, numbering to at least three) to the single peak type of curve of Group IV (see Figures 9(a) to 9(d)); Group IV velocity stacks are all single channel dominated. This change explains the progressive decrease in the quality of the velocity stack from Group I to Group IV as described earlier.

(d) The values of θ for records within a group may differ widely. For instance, θ varies from 36°(P37) to 67°(P48) in Group I. Since each group represents similar quality stacks, this means that the character of the weight distribution primarily determines the quality of the stack for any given record with the effect of θ secondary. However, the effect of θ becomes significant when the type of the weight distribution in a record is borderline between two groups and

when the deviation of the linear array from the shot-to-station direction is sufficiently large (e.g., record P50; Figures 9(a), 9(b), and 29).

(iii) An apparent early event (A_1) was obtained on record P35 (see Figure 16 and Table 6). This spurious event is the result of stacking at low apparent velocity (3.26 km/sec) and is not found on the analog playback of the same record.

(iv) All events interpreted as Pg, P*, PP, Pn, and PPPP by Hajnal (1970) are observed on the WDS traces. There is good station to station correlation for these events. This is clear from the X-T and X^2-T^2 plots in Figures 32 and 33. The straight lines on these Figures are linear least squares fit to the data.

(v) Two further events, referred to as X1 and X2, have been correlated on records P30 to P52. Event X1 is compared later in this study to the event X1 described by Hajnal.

(vi) A minor result is the possible identification of Pn on records P38, P39, and P40.

(vii) There are a large number of high amplitude events on most of the stacks that cannot be easily correlated across the survey. These events are probably the result of severe crustal scattering.

The arrival times of the events Pg, P*, PP, Pn, PPPP, X1 and X2 are shown in the tables following (Tables 1 to 22). These tables also give the times of the other events found on each record. The figures accompanying these tables show the WDS traces from which the arrivals were picked. The values obtained by Hajnal are given in the tables for comparison. The second number of each entry in

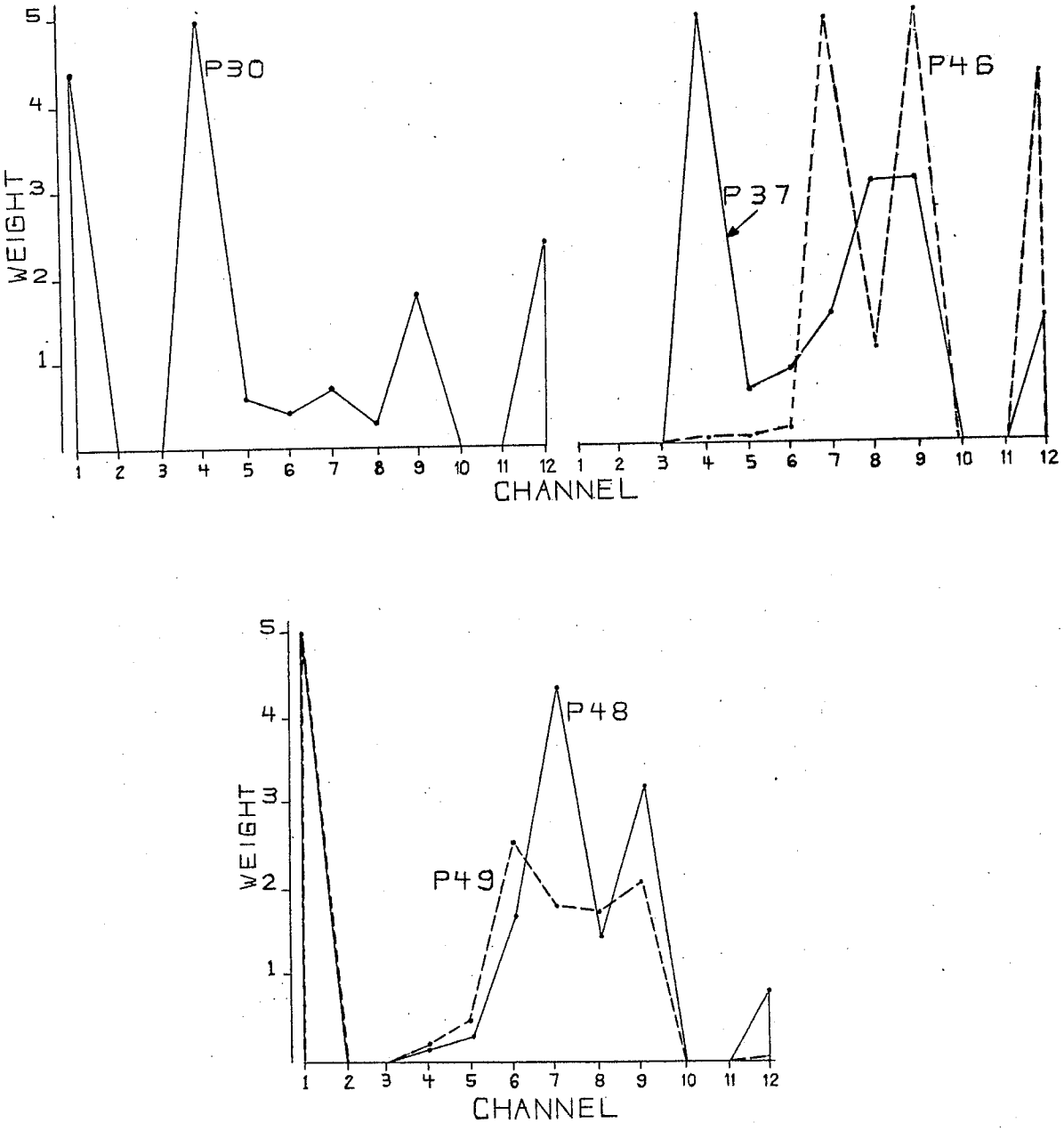

Figure 9(a). Weight distribution curves for records in Group I (includes P30, P37, P46, P48, and P49).

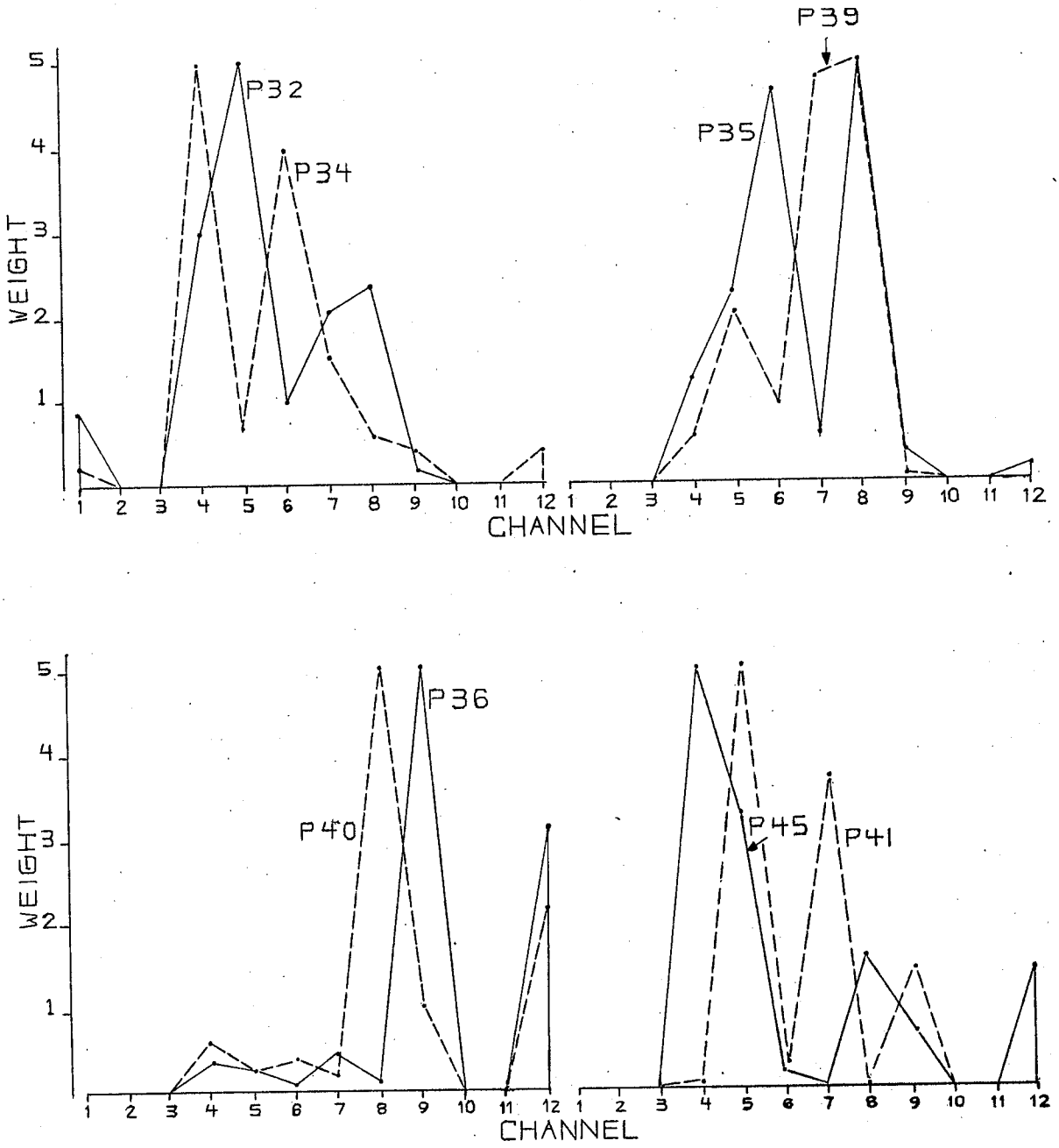

Figure 9(b). Weight distribution curves for records in Group II (includes P32, P34, P35, P36, P39, P40, P41, P43, P45, and P50).

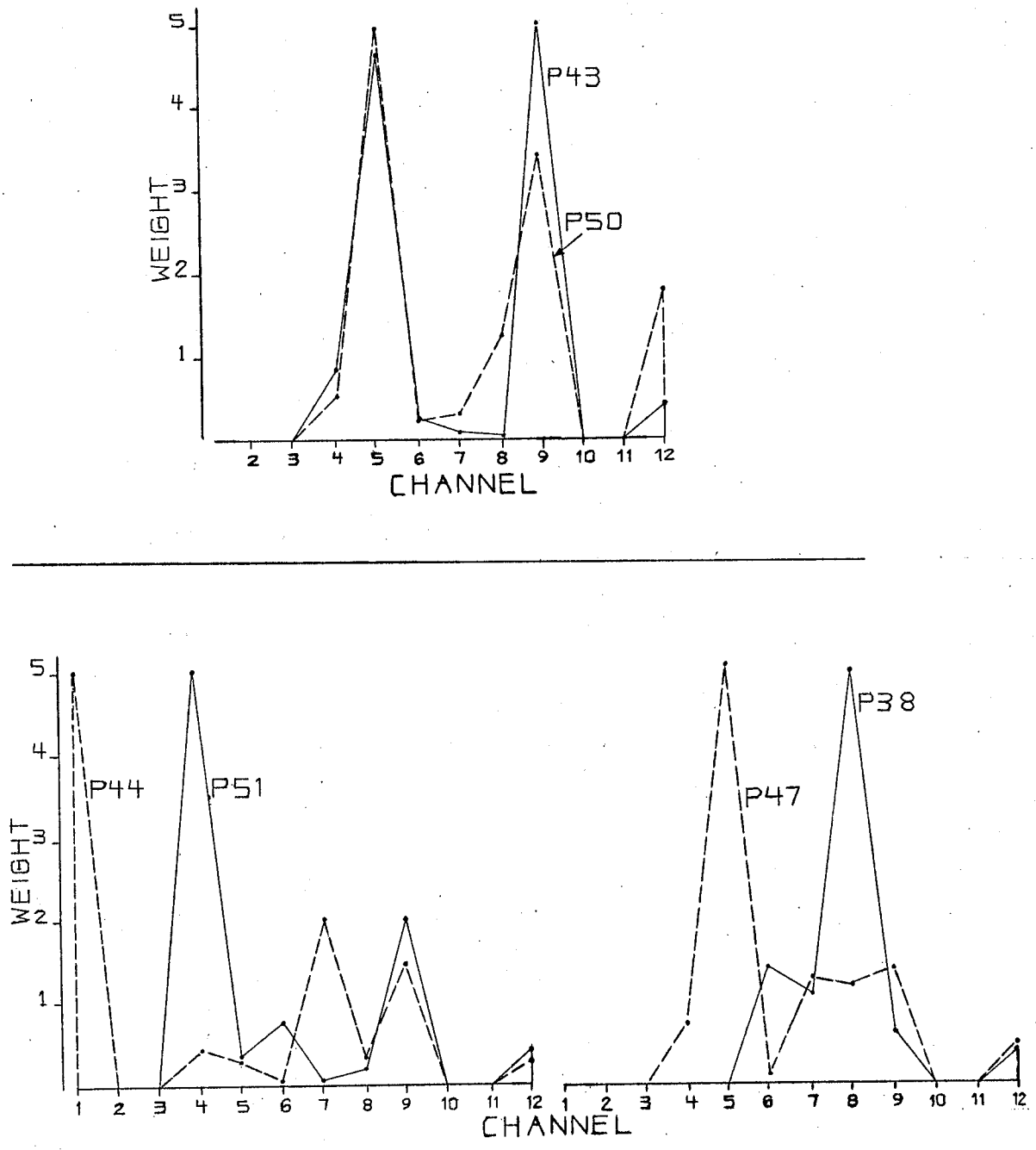

Figure 9(c). Weight distribution curves for records in Group III (includes P38, P44, P47, and P51).

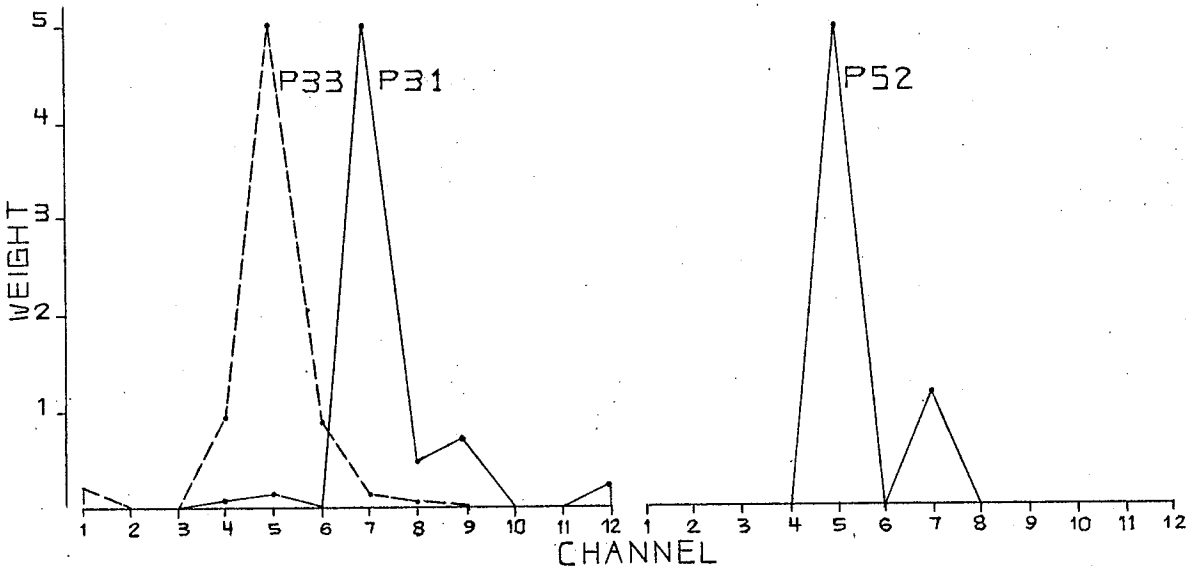

Figure 9(d). Weight distribution curves for records in Group IV (includes P31, P33, and P52).

the time column represents the error estimate. In the identification column, the symbols Pg, P*, PP, Pn, and PPPP are used to denote the WDS events which parallel Hajnal's Pg, P*, PP, Pn, and PPPP, respectively.

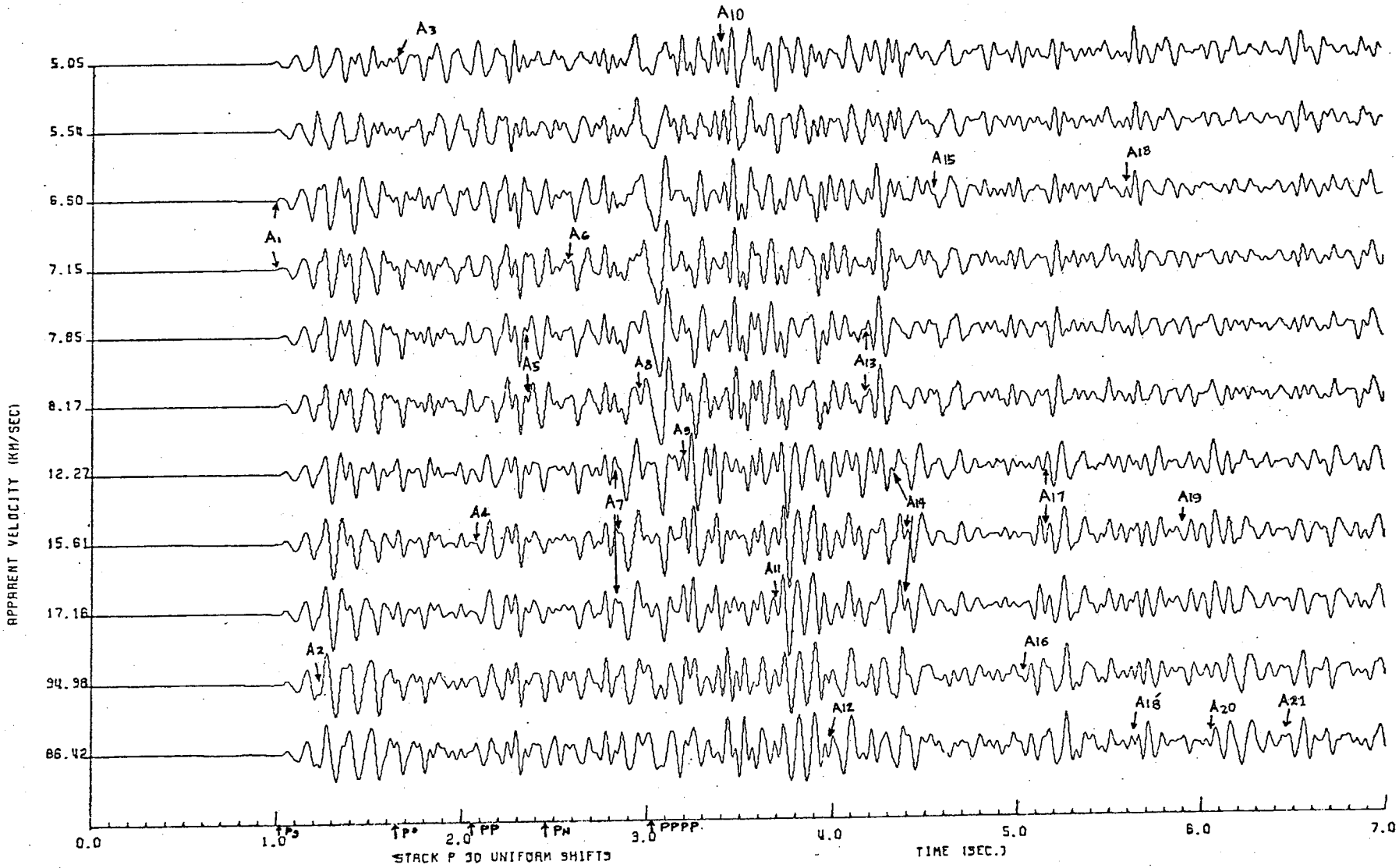

Figure 10 Plot for record P30 showing the arrivals.

TABLE 1

Record P30, $\theta = 42^{\circ}$, Distance = 128.84 km, Reference Time = 20.13 sec

Arrival	Time (sec)		Identification	Hajnal (1970)
A_1	21.13	.04	Pg	Pg : 21.14
A_2	21.38	.04	X1	
A_3	21.84	.04	P*	P* : 21.77
A_4	22.21	.04	PP	PP : 22.19
A_5	22.51	.04	Pn	Pn : 22.60
A_6	22.71	.05		
A_7	22.99	.05	X2	
A_8	23.11	.05	PPPP	PPPP : 23.14
A_9	23.34	.04		
A_{10}	23.56	.04		
A_{11}	23.84	.04		
A_{12}	24.10	.04		
A_{13}	24.33	.05		
A_{14}	24.53	.03		
A_{15}	24.71	.04		
A_{16}	25.16	.04		
A_{17}	25.28	.04		
A_{18}, A_{18}'	25.77	.05		
A_{19}	26.04	.05		
A_{20}	26.16	.04		
A_{21}	26.59	.04		

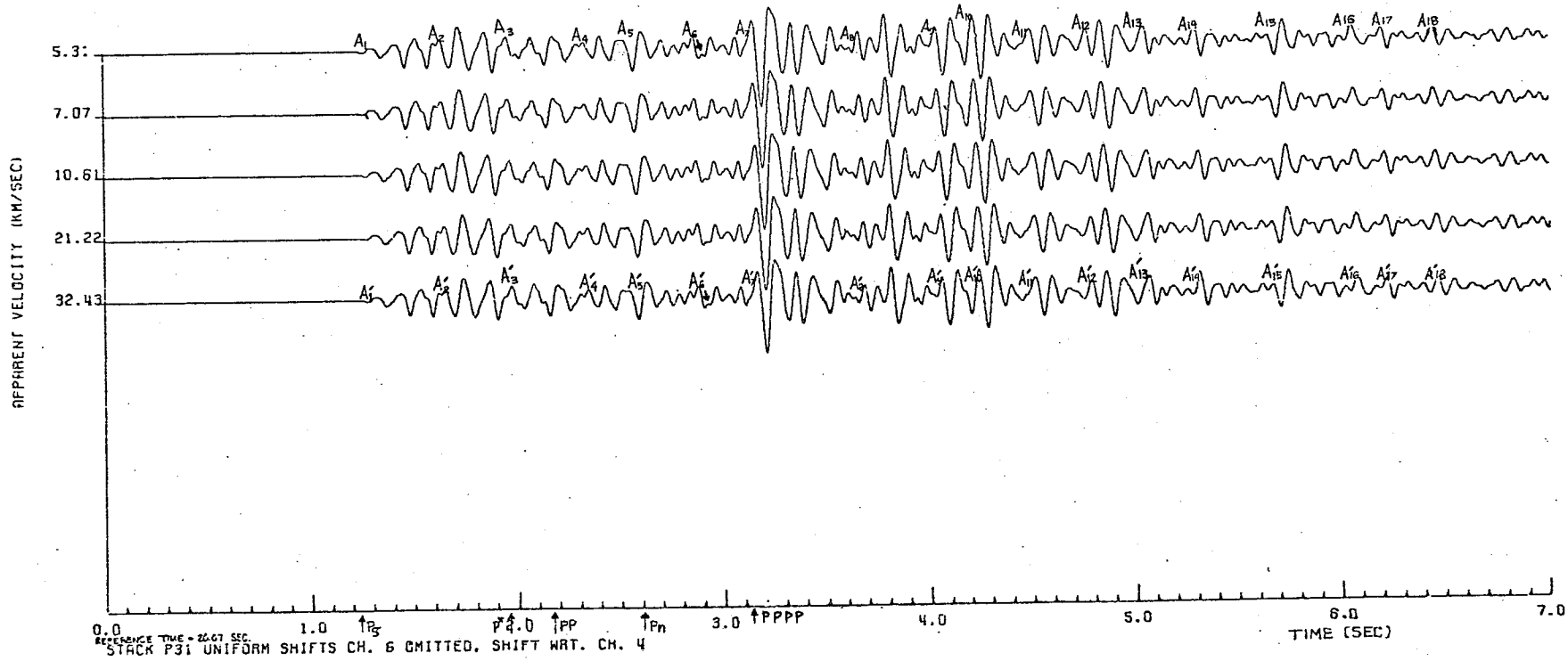

Figure 11. Plot for record P31 showing the arrivals.

TABLE 2

Record P31, $\theta = 74^{\circ}$, Distance = 129.20 km, Reference Time = 20.07 sec

Arrival	Time (sec)		Identification	Hajnal (1970)
A_1, A_1'	21.32	.05	Pg	Pg : 21.29
A_2, A_2'	21.71	.04	X1	
A_3, A_3'	22.03	.04	P*	P* : 22.01
A_4, A_4'	22.39	.04	PP	PP : 22.23
A_5, A_5'	22.62	.04	Pn	Pn : 22.65
A_6, A_6'	22.97	.04	X2	
A_7, A_7'	23.19	.04	PPPP	PPPP : 23.20
A_8, A_8'	23.70	.03		
A_9, A_9'	24.09	.04		
A_{10}, A_{10}'	24.24	.04		
A_{11}, A_{11}'	24.54	.04		
A_{12}, A_{12}'	24.83	.04		
A_{13}, A_{13}'	25.04	.05		
A_{14}, A_{14}'	25.28	.04		
A_{15}, A_{15}'	25.72	.04		
A_{16}, A_{16}'	26.09	.04		
A_{17}, A_{17}'	26.25	.05		
A_{18}, A_{18}'	26.47	.04		

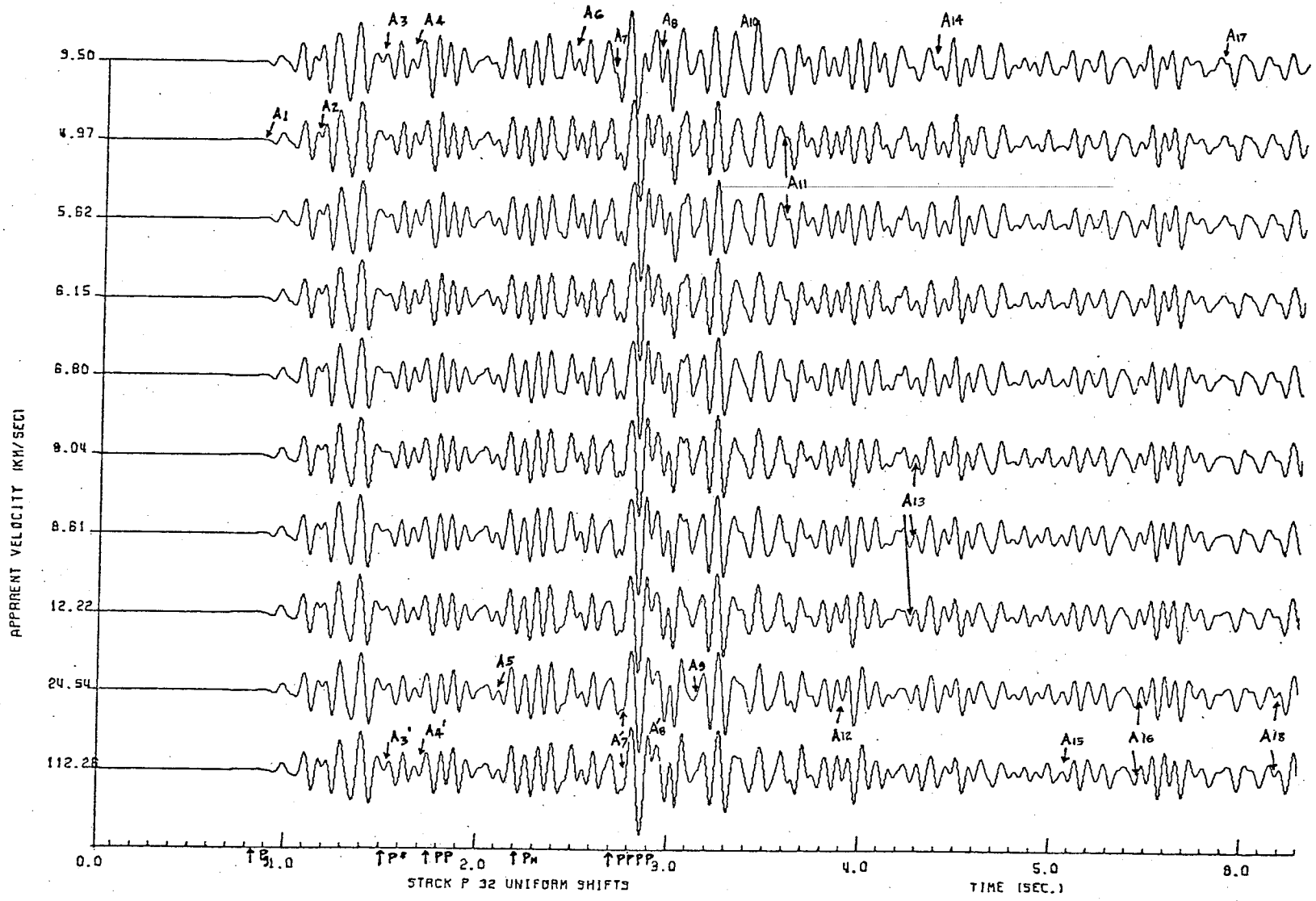

Figure 12. Plot for record P32 showing the arrivals.

TABLE 3

Record P32, $\theta = 56^{\circ}$, Distance = 129.80 km, Reference Time = 20.54 sec

Arrival	Time (sec)		Identification	Hajnal (1970)
A_1	21.40	.06	Pg	Pg : 21.38
A_2	21.69	.04	X1	
A_3, A_3'	22.05	.06	P*	P* : 22.06
A_4, A_4'	22.25	.05	PP	PP : 22.31
A_5	22.67	.04	Pn	Pn : 22.75
A_6	23.02	.06	X2	
A_7, A_7'	23.26	.06	PPPP	PPPP : 23.25
A_8, A_8'	23.47	.05		
A_9	23.66	.04		
A_{10}	23.91	.07		
A_{11}	24.13	.04		
A_{12}	24.45	.05		
A_{13}	24.82	.04		
A_{14}	24.94	.04		
A_{15}	25.62	.05		
A_{16}	26.02	.04		
A_{17}	26.44	.04		
A_{18}	26.74	.04		

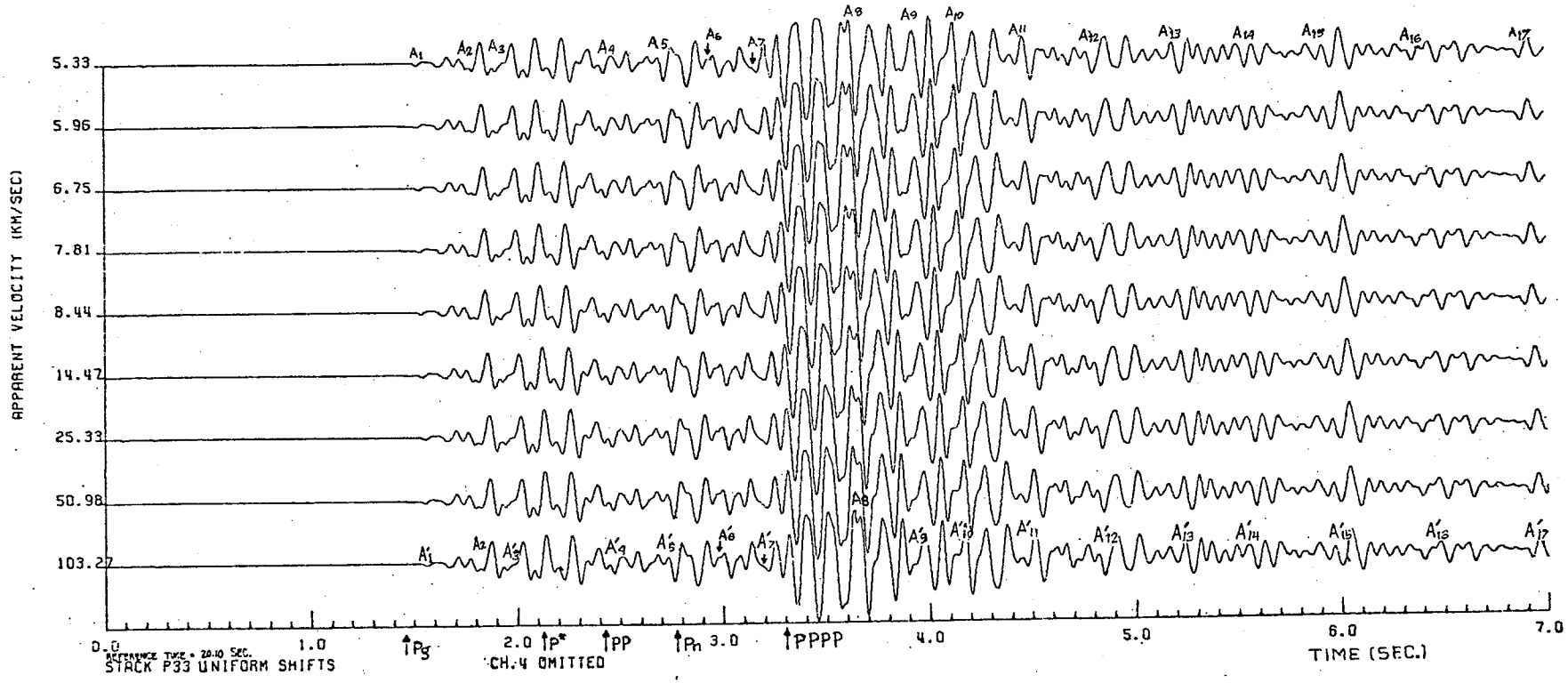

Figure 13. Plot for record P33 showing the arrivals.

TABLE 4

Record P33, $\theta = 64^{\circ}$, Distance = 130.90 km, Reference Time = 20.10 sec

Arrival	Time (sec)		Identification	Hajnal (1970)
A_1, A_1'	21.62	.06	Pg	Pg : 21.54
A_2, A_2'	21.79	.06	X1	
A_3, A_3'	22.08	.06	P*	P* : 22.22
A_4, A_4'	22.53	.08	PP	PP : 22.51
A_5, A_5'	22.80	.06	Pn	Pn : 22.87
A_6, A_6'	23.06	.04	X2	
A_7, A_7'	23.28	.06	PPPP	PPPP : 23.40
A_8, A_8'	23.75	.06		
A_9, A_9'	24.01	.06		
A_{10}, A_{10}'	24.21	.06		
A_{11}, A_{11}'	24.53	.06		
A_{12}, A_{12}'	24.91	.06		
A_{13}, A_{13}'	25.24	.03		
A_{14}, A_{14}'	25.64	.06		
A_{15}, A_{15}'	25.94	.06		
A_{16}, A_{16}'	26.53	.06		
A_{17}, A_{17}'	26.97	.06		

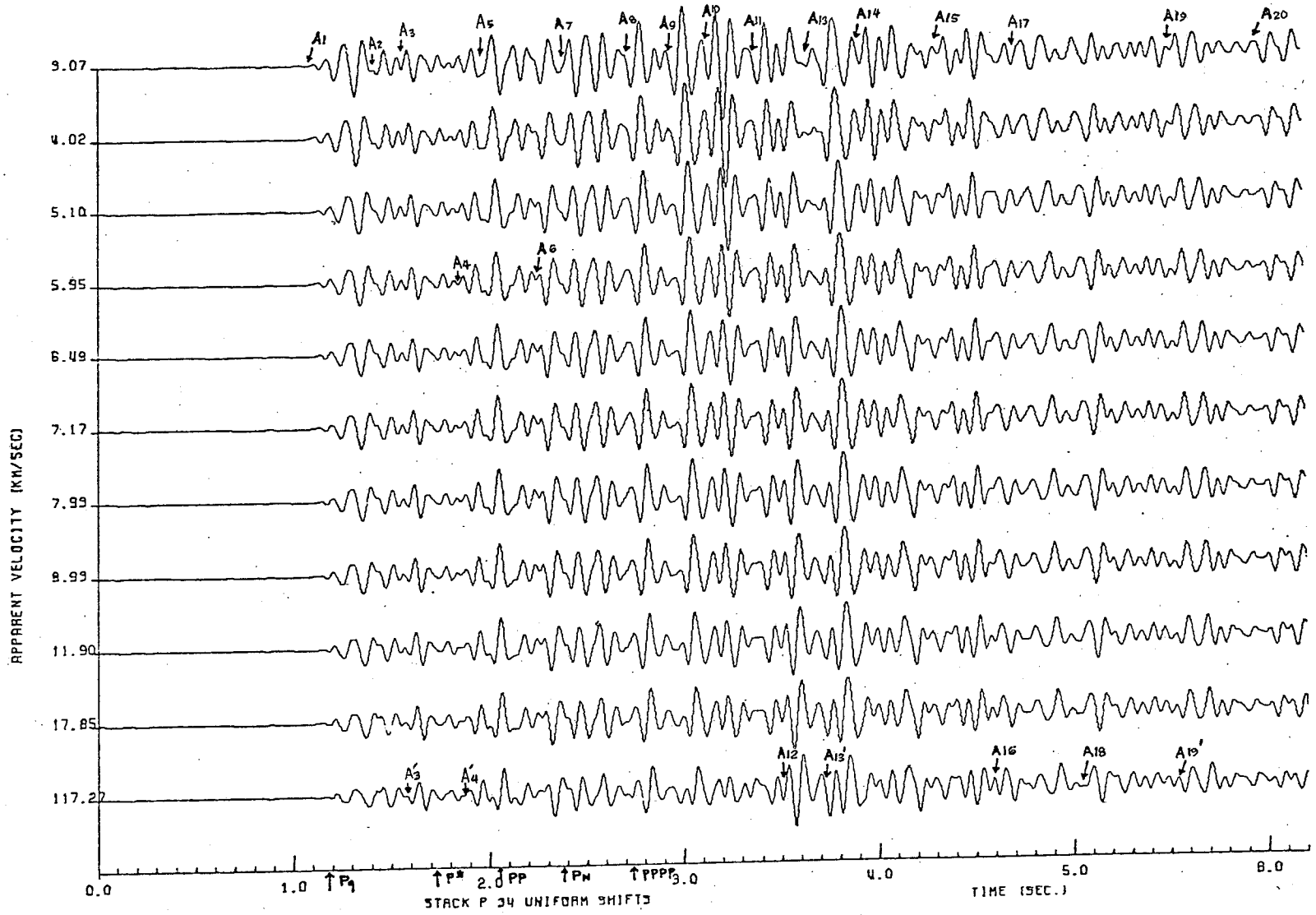

Figure 14. Plot for record P34 showing the arrivals.

TABLE 5

Record P34, $\theta = 72^{\circ}$, Distance = 132.69 km, Reference Time = 20.74 sec

Arrival	Time (sec)		Identification	Hajnal (1970)
A_1	21.85	.06	Pg	Pg : 21.92
A_2	22.21	.05	X1	
A_3, A_3'	22.34	.04	P*	P* : 22.47
A_4, A_4'	22.57	.06		
A_5	22.73	.06	PP	PP : 22.80
A_6	23.00	.04	Pn	
A_7	23.15	.06	X2	Pn : 23.12
A_8	23.50	.08	PPPP	PPPP : 23.48
A_9	23.67	.06		
A_{10}	23.90	.07		
A_{11}	24.13	.06		
A_{12}	24.25	.05		
A_{13}, A_{13}'	24.44	.08		
A_{14}	24.71	.06		
A_{15}	25.09	.06		
A_{16}	25.34	.06		
A_{17}	25.47	.06		
A_{18}	25.75	.09		
A_{19}, A_{19}'	26.26	.06		
A_{20}	26.75	.06		

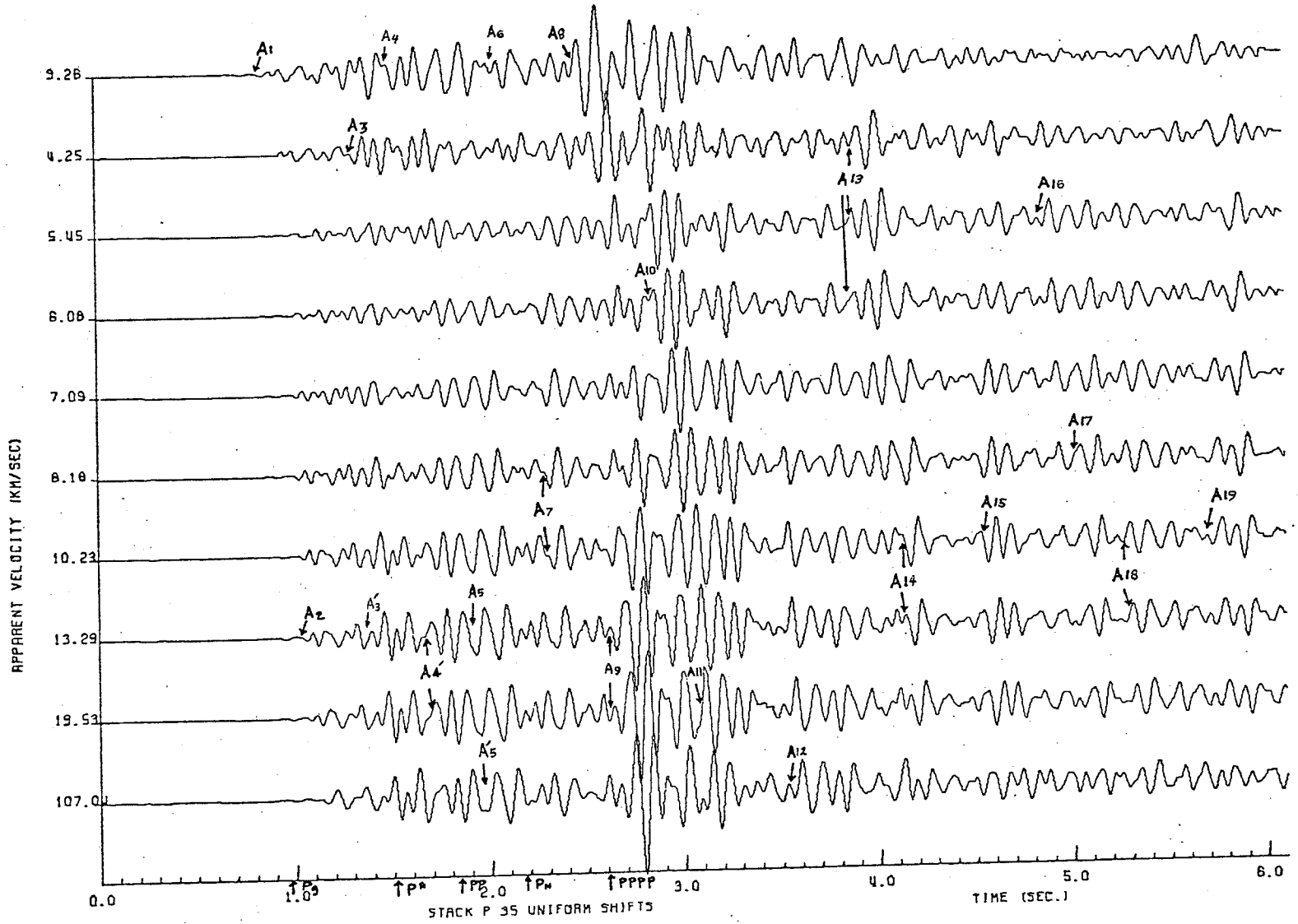

Figure 15. Plot for record P35 showing the arrivals.

TABLE 6

Record P35, $\theta = 23^{\circ}$, Distance = 133.40 km, Reference Time = 21.07 sec

Arrival	Time (sec)		Identification	Hajnal (1970)
A_1	21.86	.04	Spurious	
A_2	22.11	.05	Pg	Pg : 22.06
A_3, A_3'	22.42	.06	X1	
A_4, A_4'	22.67	.08	P*	P* : 22.58
A_5, A_5'	23.01	.08	PP	PP : 22.91
A_6	23.14	.03	Pn	Pn : 23.21
A_7	23.37	.05	X2	
A_8	23.54	.05		
A_9	23.70	.06	PPPP	PPPP : 23.68
A_{10}	23.92	.04		
A_{11}	24.15	.05		
A_{12}	24.61	.04		
A_{13}	24.94	.04		
A_{14}	25.19	.04		
A_{15}	25.61	.06		
A_{16}	25.91	.04		
A_{17}	26.08	.06		
A_{18}	26.32	.05		
A_{19}	26.77	.04		

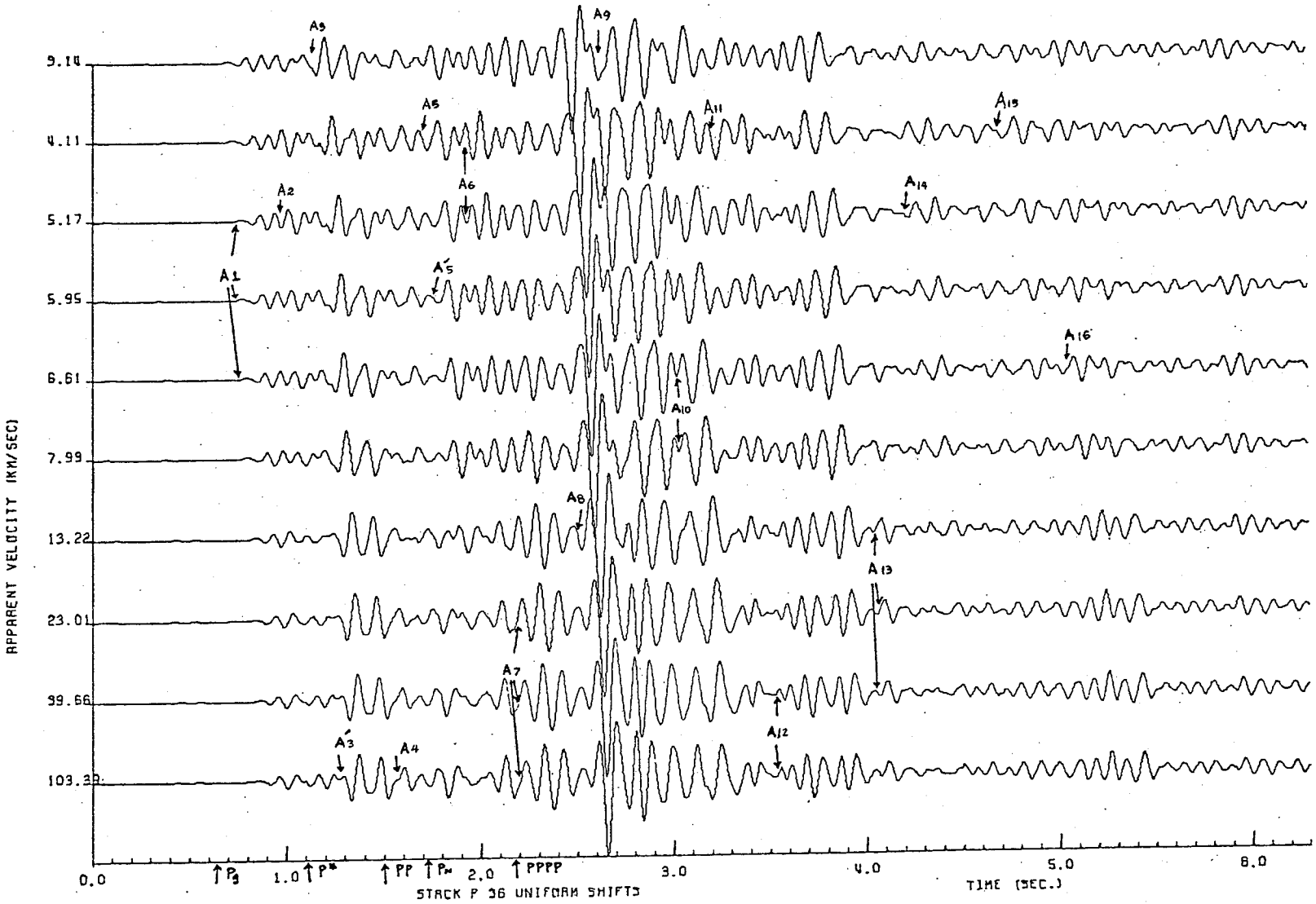

Figure 16. Plot for record P 36 showing the arrivals.

TABLE 7

Record P36, $\theta = 59^{\circ}$, Distance = 133.58 km, Reference Time = 21.51 sec

Arrival	Time (sec)		Identification	Hajnal (1970)
A_1	22.26	.04	Pg	Pg : 22.15
A_2	22.42	.05	X1	
A_3, A_3'	22.73	.04	P*	P* : 22.62
A_4	23.09	.05	PP	PP : 23.01
A_5, A_5'	23.25	.06	Pn	Pn : 23.24
A_6	23.47	.04	X2	
A_7	23.71	.07	PPPP	PPPP : 23.70
A_8	24.02	.07		
A_9	24.18	.05		
A_{10}	24.55	.06		
A_{11}	24.74	.06		
A_{12}	25.02	.05		
A_{13}	25.56	.05		
A_{14}	25.76	.04		
A_{15}	26.23	.04		
A_{16}	26.56	.04		

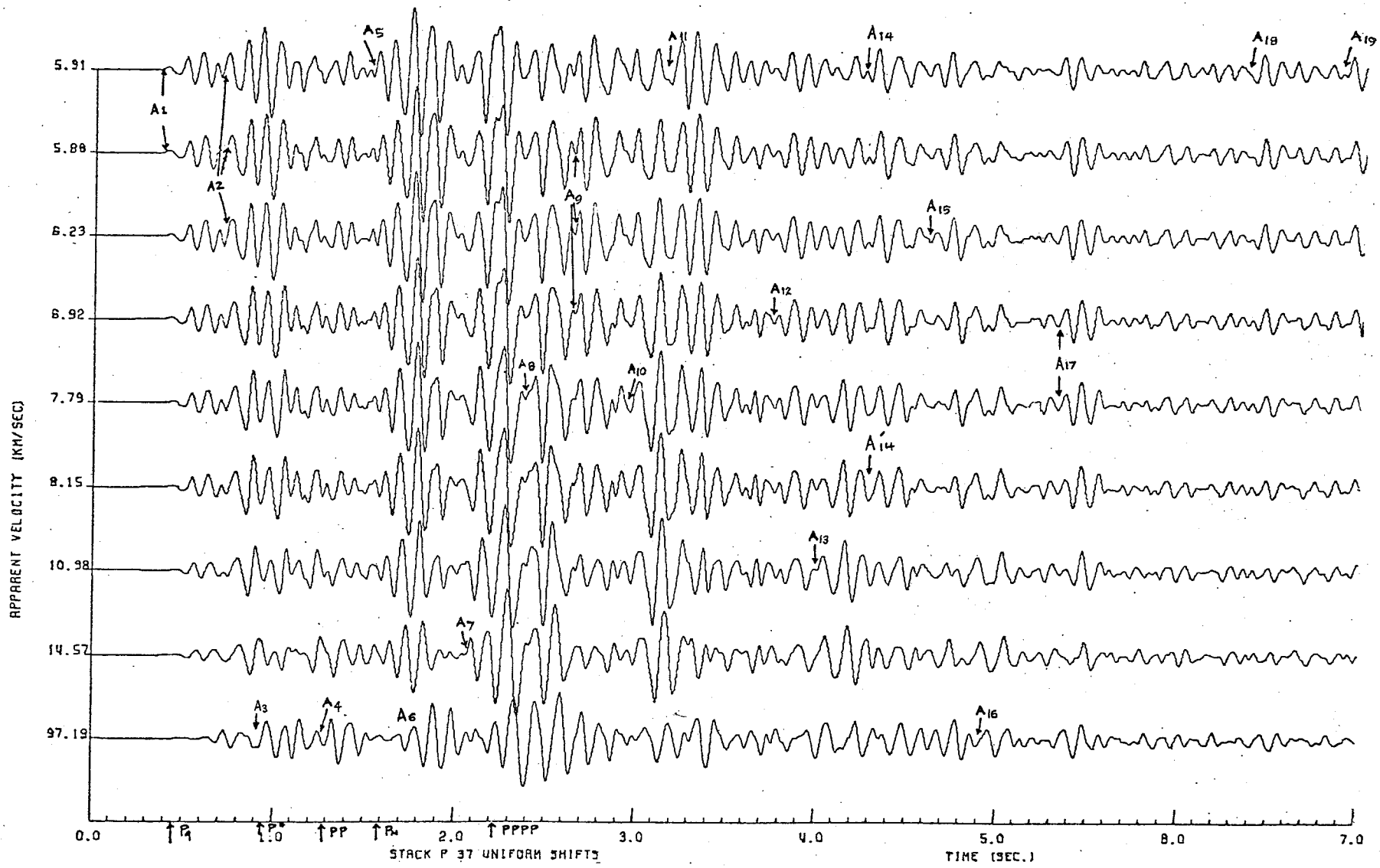

Figure 17. Plot for record P 37 showing the arrivals.

TABLE 8

Record P37, $\theta = 36^{\circ}$, Distance = 134.19 km, Reference Time = 21.76 sec

Arrival	Time (sec)		Identification	Hajnal (1970)
A_1	22.16	.03	Pg	Pg : 22.21
A_2	22.47	.05	X1	
A_3	22.69	.07	P*	P* : 22.70
A_4	23.03	.06	PP	PP : 23.05
A_5	23.31	.04	Pn	Pn : 23.35
A_6	23.51	.08	X2	
A_7	23.83	.04	PPPP	PPPP : 23.98
A_8	24.14	.05		
A_9	24.41	.04		
A_{10}	24.70	.08		
A_{11}	24.91	.08		
A_{12}	25.52	.05		
A_{13}	25.77	.04		
A_{14}, A_{14}'	26.06	.04		
A_{15}	26.39	.04		
A_{16}	26.66	.04		
A_{17}	27.08	.04		
A_{18}	28.16	.06		
A_{19}	28.68	.05		

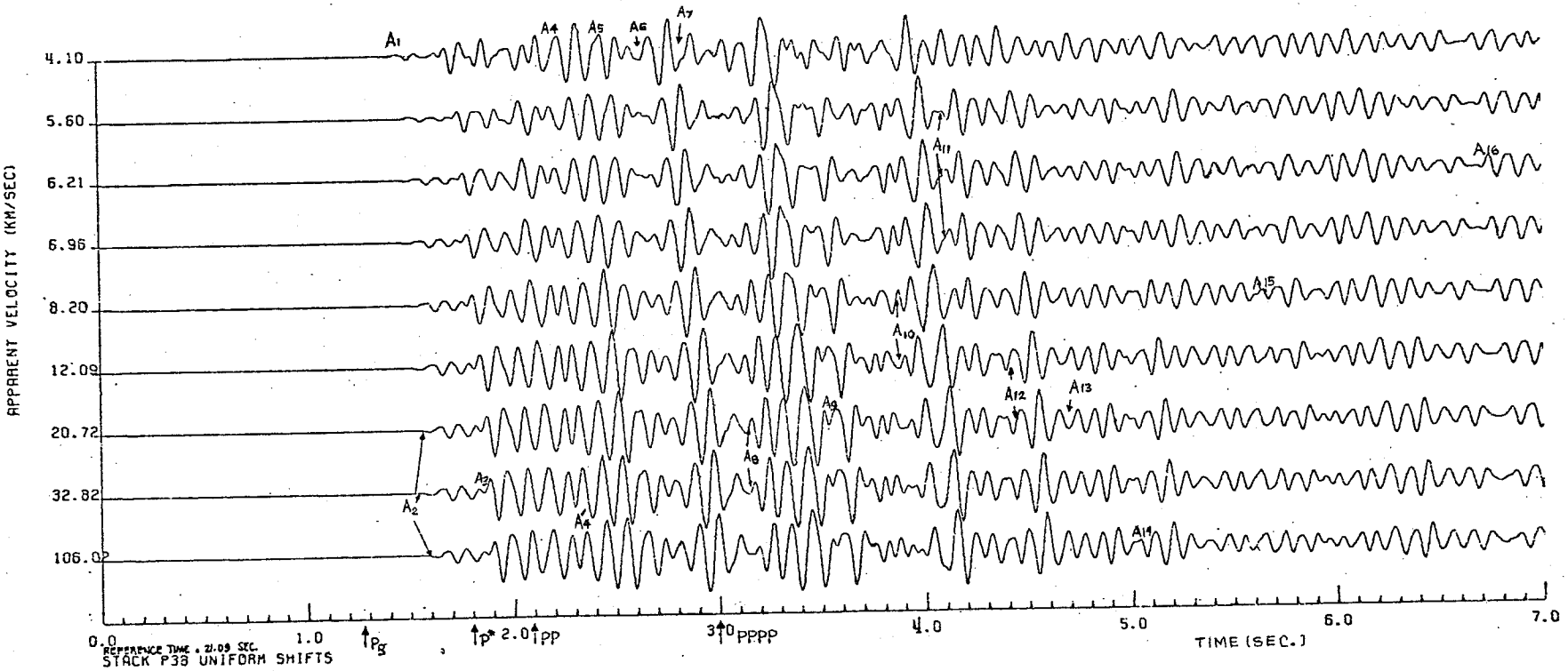

Figure 18. Plot for record P38 showing the arrivals.

TABLE 9

Record P38, $\theta = 6^{\circ}$, Distance = 135.40 km, Reference Time = 21.09 sec

Arrival	Time (sec)		Identification	Hajnal (1970)
A_1	22.49	.05	Pg	Pg : 22.36
A_2	22.67	.03	X1	
A_3	22.96	.06	P*	P* : 22.89
A_4, A_4'	23.34	.10	PP	PP : 23.18
A_5	23.51	.15	Pn	
A_6	23.70	.04	X2	
A_7	23.92	.04	PPPP	PPPP : 24.08
A_8	24.25	.06		
A_9	24.62	.07		
A_{10}	24.98	.09		
A_{11}	25.20	.06		
A_{12}	25.46	.07		
A_{13}	25.78	.06		
A_{14}	26.12	.04		
A_{15}	26.72	.07		
A_{16}	27.79	.07		

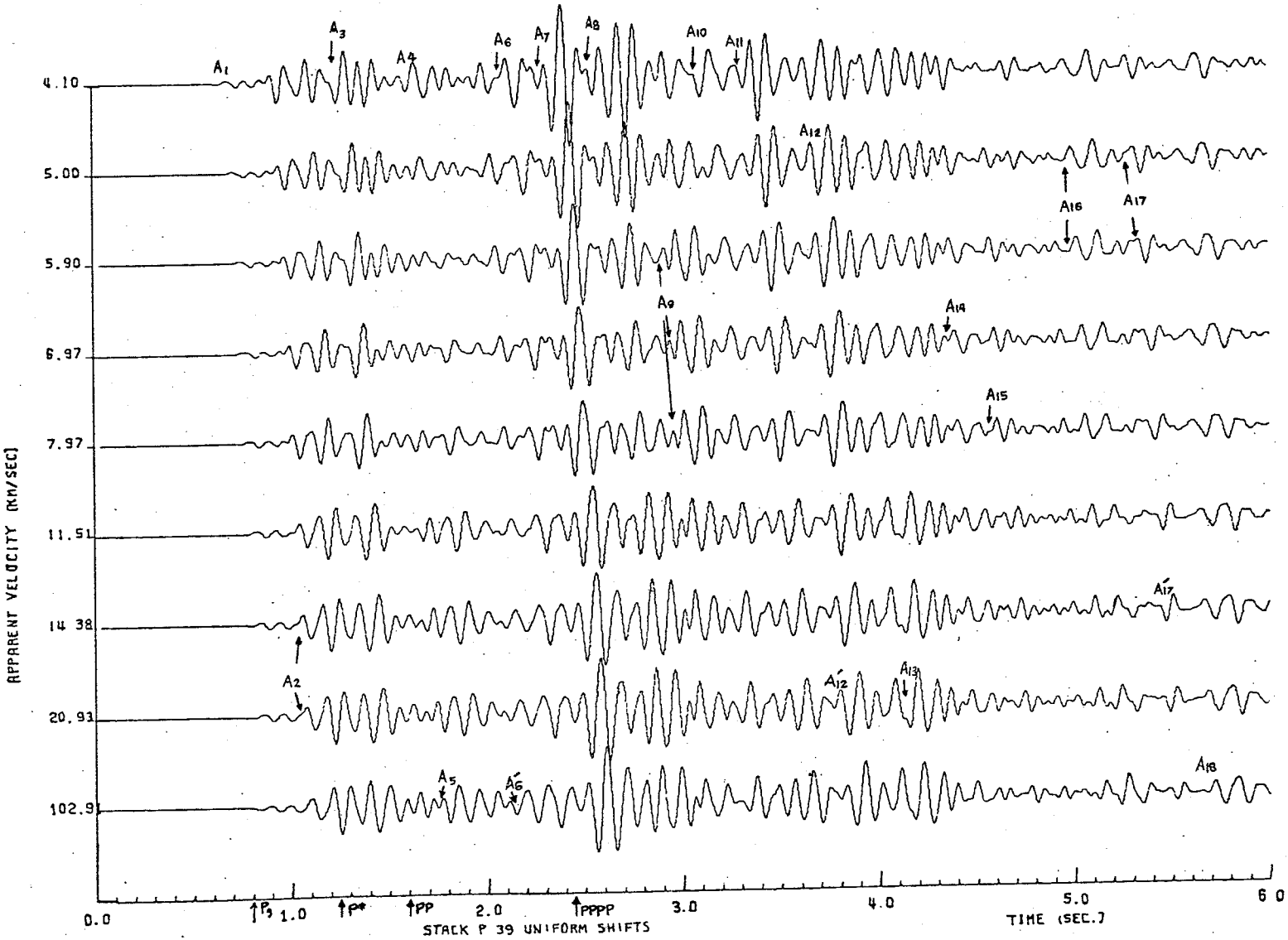

Figure 19. Plot for record P39 showing the arrivals.

TABLE 10

Record P39, $\theta = 5^{\circ}$, Distance = 137.09 km, Reference Time = 21.90 sec

Arrival	Time (sec)		Identification	Hajnal (1970)
A_1	22.64	.06	Pg	Pg : 22.70
A_2	23.00	.05	X1	
A_3	23.15	.05	P*	P* : 23.15
A_4	23.50	.07	PP	PP : 23.50
A_5	23.65	.07	Pn	
A_6, A_6'	24.00	.04	X2	
A_7	24.22	.04	PPPP	PPPP : 24.36
A_8	24.44	.04		
A_9	24.83	.04		
A_{10}	25.01	.04		
A_{11}	25.23	.08		
A_{12}, A_{12}'	25.61	.07		
A_{13}	26.03	.04		
A_{14}	26.30	.05		
A_{15}	26.50	.05		
A_{16}	26.90	.04		
A_{17}	27.30	.15		
A_{18}	27.57	.04		

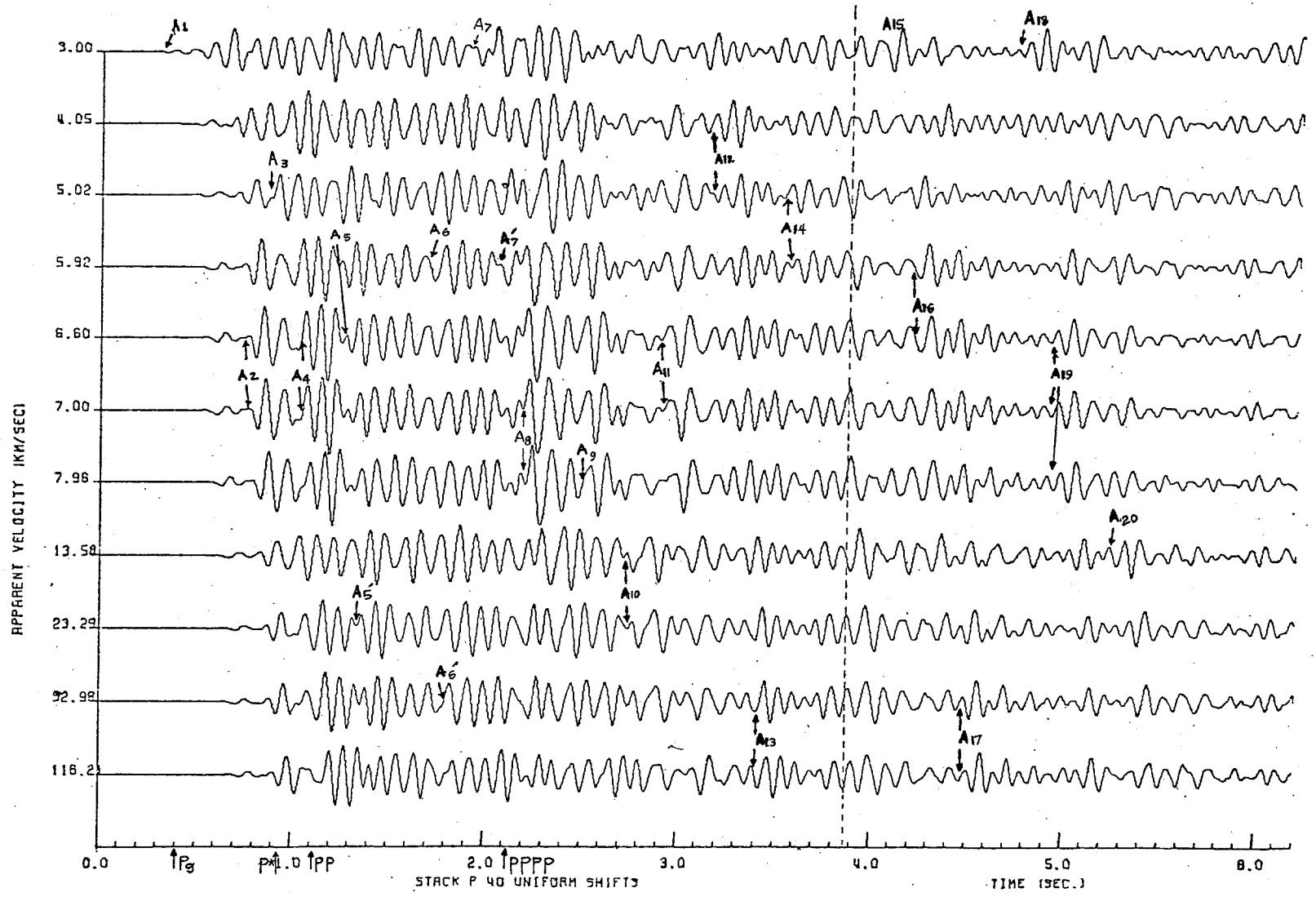

Figure 20. Plot for record P40 showing the arrivals. The broken line indicates the change to bigger plotting scale. S = 1.44

TABLE 11

Record P40, $\theta = 2^{\circ}$, Distance = 138.85 km, Reference Time = 22.53 sec

Arrival	Time (sec)		Identification	Hajnal (1970)
A_1	22.99	.07	Pg	Pg : 22.93
A_2	23.29	.08	X1	
A_3	23.45	.06	P*	P* : 23.47
A_4	23.73	.05	PP	PP : 23.70
A_5, A_5'	23.90	.08	Pn	
A_6, A_6'	24.27	.06	X2	
A_7, A_7'	24.59	.06		
A_8	24.73	.05	PPPP	PPPP : 24.64
A_9	25.04	.04		
A_{10}	25.28	.04		
A_{11}	25.46	.06		
A_{12}	25.70	.04		
A_{13}	25.94	.04		
A_{14}	26.08	.06		
A_{15}	26.61	.06		
A_{16}	26.75	.06		
A_{17}	26.99	.04		
A_{18}	27.33	.03		
A_{19}	27.46	.04		
A_{20}	27.74	.03		

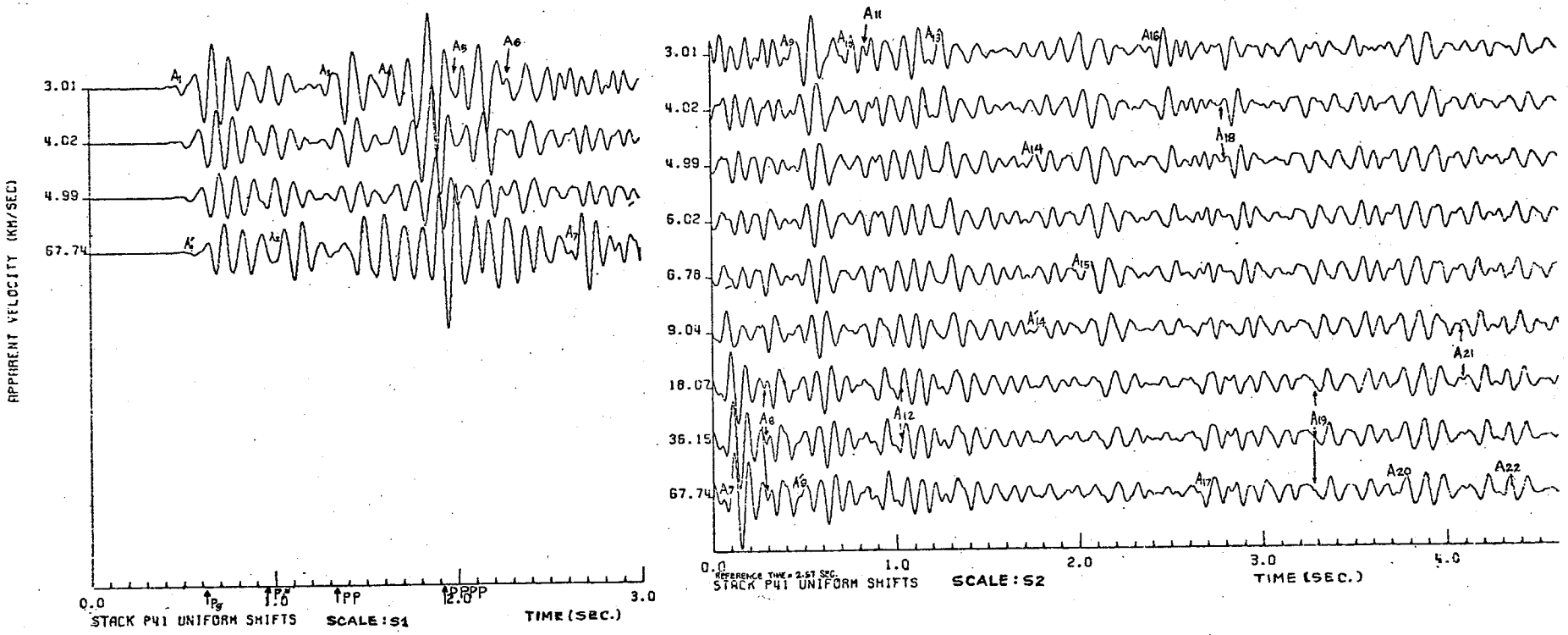

Figure 21. Plot for record P41 showing the arrivals. S = 1.27

TABLE 12

Record P41, $\theta = 62$, Distance = 149.62 km, Reference Time = 24.12 sec

Arrival	Time (sec)		Identification	Hajnal (1970)
A_1, A_1'	24.64	.05	Pg	Pg : 24.71
A_2	25.16	.05	P*	P* : 25.07
A_3	25.37	.04	X1	
A_4	25.73	.07	PP	PP : 25.45
A_5	26.12	.05	PPPP	PPPP : 26.03
A_6	26.39	.05		
A_7	26.73	.04		
A_8	26.93	.05		
A_9, A_9'	27.13	.06		
A_{10}	27.39	.04		
A_{11}	27.54	.04		
A_{12}	27.72	.04		
A_{13}	27.89	.09		
A_{14}, A_{14}'	28.43	.06		
A_{15}	28.65	.09		
A_{16}	29.07	.04		
A_{17}	29.35	.05		
A_{18}	29.49	.04		
A_{19}	29.99	.05		
A_{20}	30.44	.04		
A_{21}	30.77	.04		
A_{22}	30.97	.05		

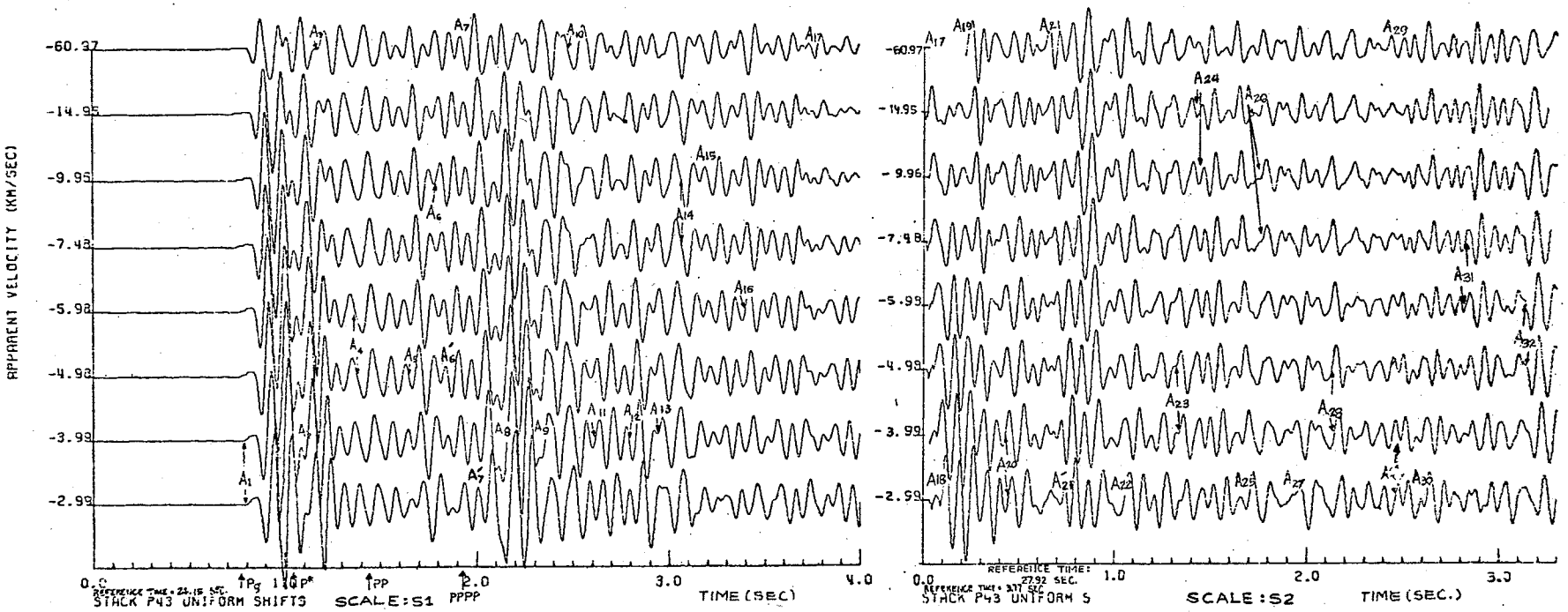

Figure 22. Plot for record P43 showing the arrivals. S = 2.46

TABLE 13

Record P43, $\theta = 105^{\circ}$, Distance = 150.16 km, Reference Time = 24.15 sec

Arrival	Time (sec)		Identification	Hajnal (1970)
A_1	24.94	.04	Pg	Pg : 24.92
A_2	25.21	.05	P*	P* : 25.16
A_3	25.33	.04	X1	
A_4	25.53	.06	PP	PP : 25.60
A_5	25.80	.05	X2	
A_6	25.92	.06	PPPP	PPPP : 26.08
A_7	26.12	.08		
A_8	26.27	.08		
A_9	26.48	.08		
A_{10}	26.60	.06	Uncertain	
A_{11}	26.77	.05		
A_{12}	26.95	.05		
A_{13}	27.08	.05		
A_{14}	27.22	.05		
A_{15}	27.32	.04		
A_{16}	27.55	.06		
A_{17}	27.87	.05		
A_{18}	27.93	.04		
A_{19}	28.12	.07		
A_{20}	28.25	.04		
A_{21}, A_{21}'	28.57	.05		
A_{22}	28.92	.05		
A_{23}	29.25	.04		
A_{24}	29.34	.04		
A_{25}	29.57	.05		
A_{26}	29.68	.06		
A_{27}	29.86	.05		
A_{28}	30.05	.04		
A_{29}, A_{29}'	30.40	.09		
A_{30}	30.52	.04		
A_{31}	30.75	.06		
A_{32}	31.05	.06		

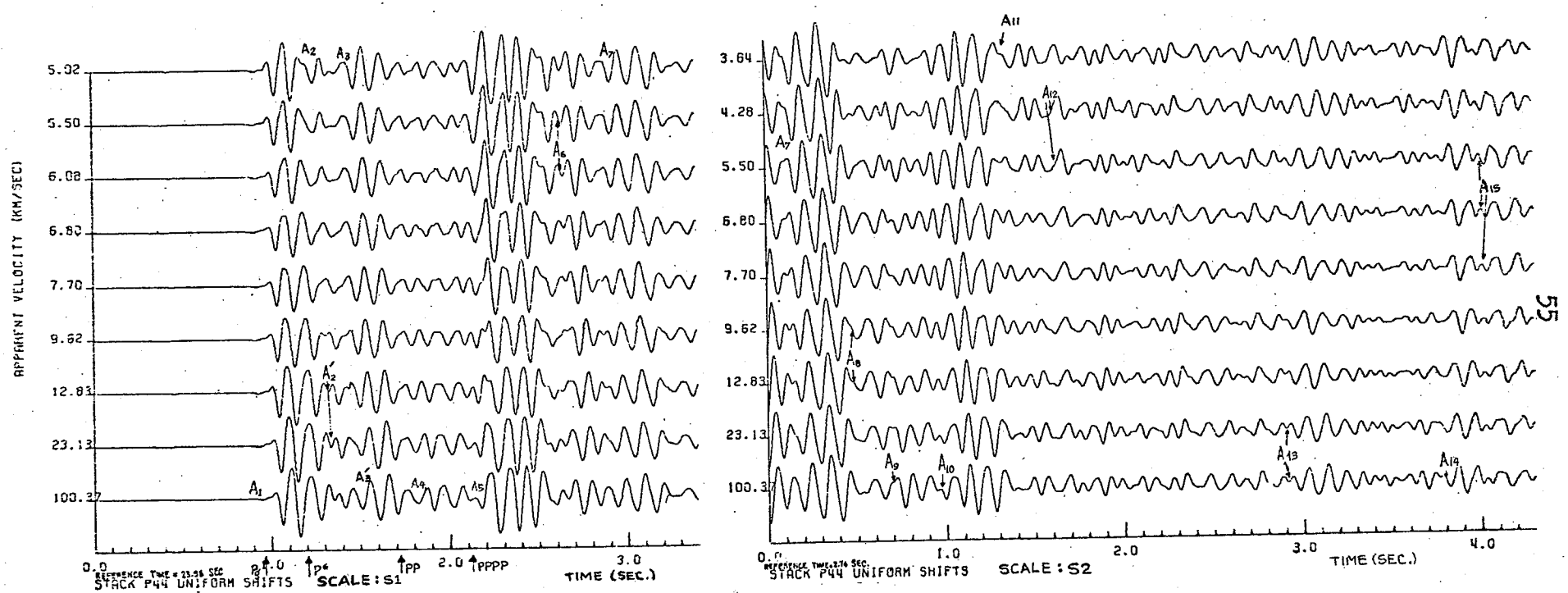

Figure 23. Plot for record P44 showing the arrivals. S = 1.68

TABLE 14

Record P44, $\theta = 60^{\circ}$, Distance = 150.95 km, Reference Time = 23.98 sec

Arrival	Time (sec)		Identification	Hajnal (1970)
A_1	24.95	.05	Pg	Pg : 24.95
A_2, A_2'	25.25	.08	P*	P* : 25.19
A_3, A_3'	25.40	.05	X1	
A_4	25.77	.05	PP	PP : 25.70
A_5	26.12	.04	PPPP	PPPP : 26.09
A_6	26.61	.05		
A_7	26.85	.09		
A_8	27.20	.09		
A_9	27.42	.04		
A_{10}	27.69	.04		
A_{11}	28.05	.04		
A_{12}	28.36	.04		
A_{13}	29.64	.06		
A_{14}	30.49	.05		
A_{15}	30.73	.04		

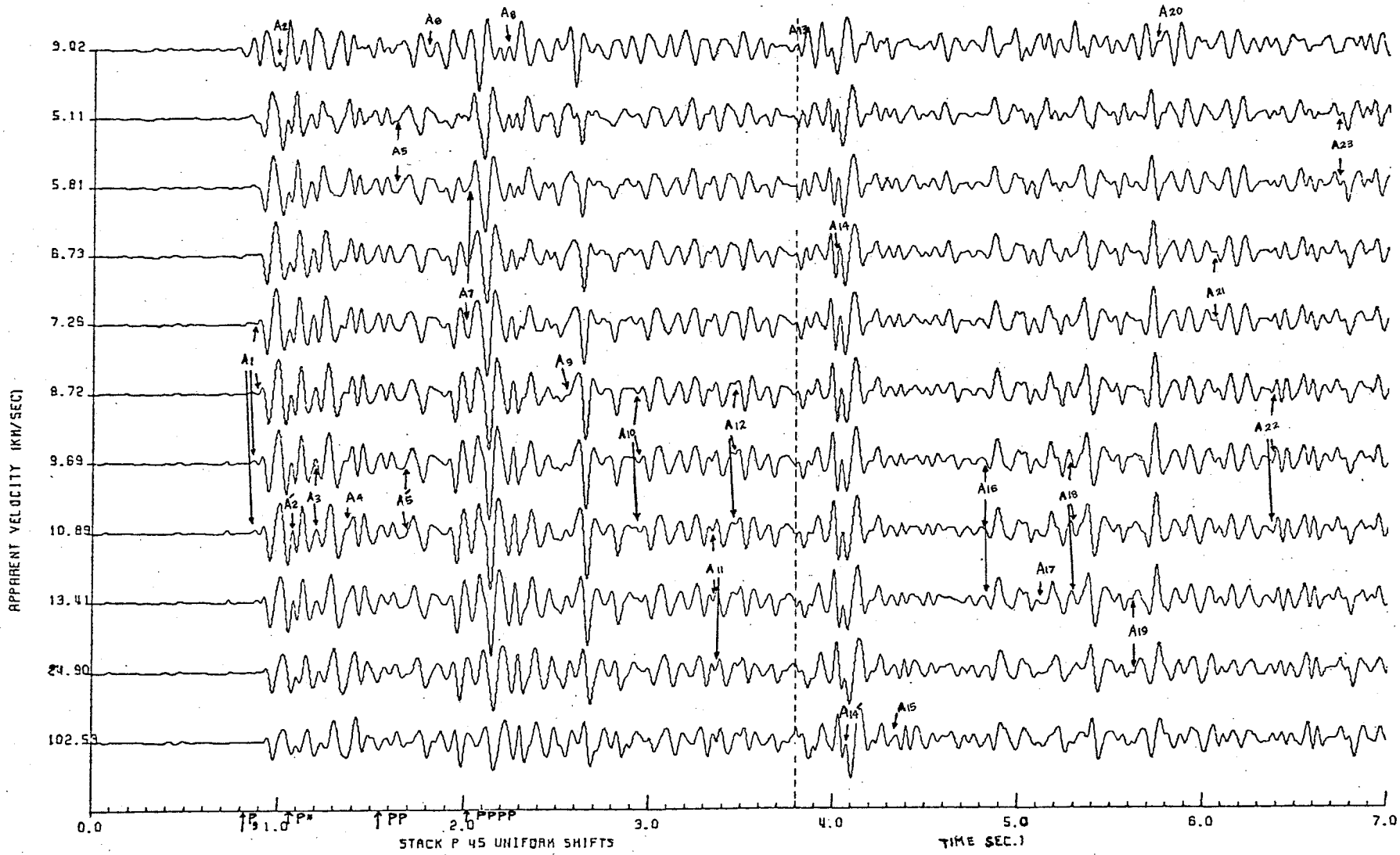

Figure 24. Plot for record P45 showing the arrivals. The broken line indicates a change to bigger plotting scale.
S = 2.38

TABLE 15

Record P45, $\theta = 41^{\circ}$, Distance = 151.10 km, Reference Time = 24.18 sec

Arrival	Time (sec)		Identification	Hajnal (1970)
A_1	25.05	.06	Pg	Pg : 25.00
A_2	25.24	.06	P*	P* : 25.24
A_3	25.40	.04	X1	
A_4	25.59	.04		
A_5, A_5'	25.87	.04	PP	PP : 25.73
A_6	26.00	.04	X2	
A_7	26.22	.04	PPPP	PPPP : 26.19
A_8	26.43	.04		
A_9	26.74	.05		
A_{10}	27.14	.05		
A_{11}	27.54	.04		
A_{12}	27.65	.04		
A_{13}	27.98	.04		
A_{14}, A_{14}'	28.21	.05	Uncertain	
A_{15}	28.54	.04		
A_{16}	29.00	.04		
A_{17}	29.30	.04		
A_{18}	29.48	.09		
A_{19}	29.80	.05		
A_{20}	29.87	.03		
A_{21}	30.25	.05		
A_{22}	30.54	.05		
A_{23}	30.92	.04		

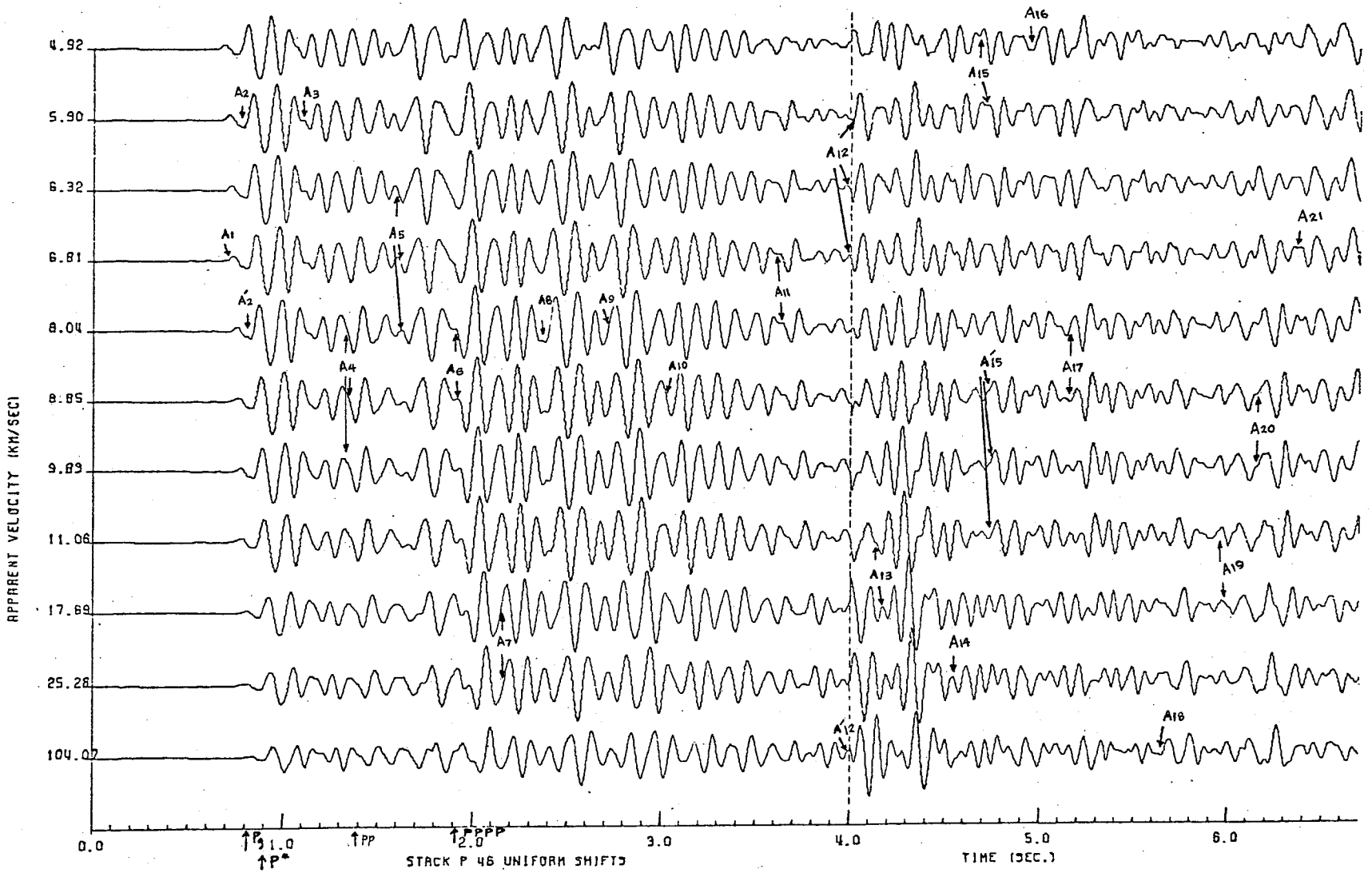

Figure 25. Plot for P46 showing the arrivals. The broken line indicates a change to a bigger scale.

S = 3.63

TABLE 16

Record P46, $\theta = 40^{\circ}$, Distance = 151.61 km, Reference Time = 24.38 sec

Arrival	Time (sec)		Identification	Hajnal (1970)
A_1	25.09	.04	Pg	Pg : 25.20
A_2, A_2'	25.25	.04	P*	P* : 25.28
A_3	25.49	.04	X1	
A_4	25.74	.05	PP	PP : 25.77
A_5	25.99	.06	X2	
A_6	26.30	.05	PPPP	PPPP : 26.31
A_7	26.53	.09		
A_8	26.78	.06		
A_9	27.12	.06		
A_{10}	27.42	.05		
A_{11}	28.03	.04		
A_{12}, A_{12}'	28.38	.08	Uncertain	
A_{13}	28.55	.07		
A_{14}	28.93	.04		
A_{15}, A_{15}'	29.08	.06		
A_{16}	29.35	.05		
A_{17}	29.53	.04		
A_{18}	30.02	.05		
A_{19}	30.36	.05		
A_{20}	30.56	.04		
A_{21}	30.78	.04		

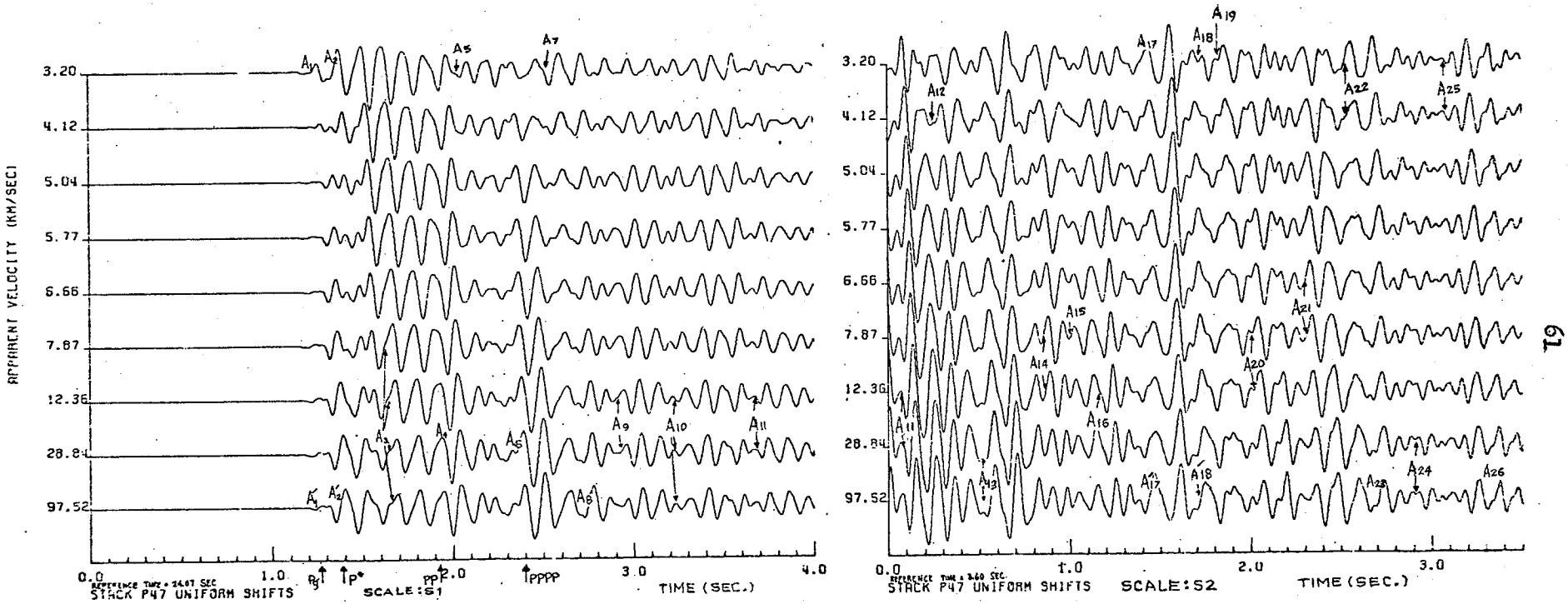

Figure 26. Plot for record P47 showing the arrivals. S = 3.71

TABLE 17

Record P47, $\theta = 68^{\circ}$, Distance = 152.46 km, Reference Time = 24.07 sec

Arrival	Time (sec)		Identification	Hajnal (1970)
A_1, A_1'	25.27	.03	Pg	Pg : 25.31
A_2, A_2'	25.40	.04	P*	P* : 25.42
A_3	25.72	.04	X1	
A_4	25.97	.06	PP	PP : 25.95
A_5	26.12	.04	X2	
A_6	26.42	.04	PPPP	PPPP : 26.45
A_7	26.57	.04		
A_8	26.79	.05		
A_9	27.00	.06		
A_{10}	27.30	.04		
A_{11}	27.75	.03		
A_{12}	27.90	.05		
A_{13}	28.19	.05		
A_{14}	28.53	.04		
A_{15}	28.66	.03		
A_{16}	28.85	.05		
A_{17}, A_{17}'	29.07	.10		
A_{18}, A_{18}'	29.37	.08		
A_{19}	29.49	.04		
A_{20}	29.80	.04		
A_{21}	29.98	.05		
A_{22}	30.18	.05		
A_{23}	30.35	.04		
A_{24}	30.59	.04		
A_{25}	30.76	.04		
A_{26}	31.17	.03		

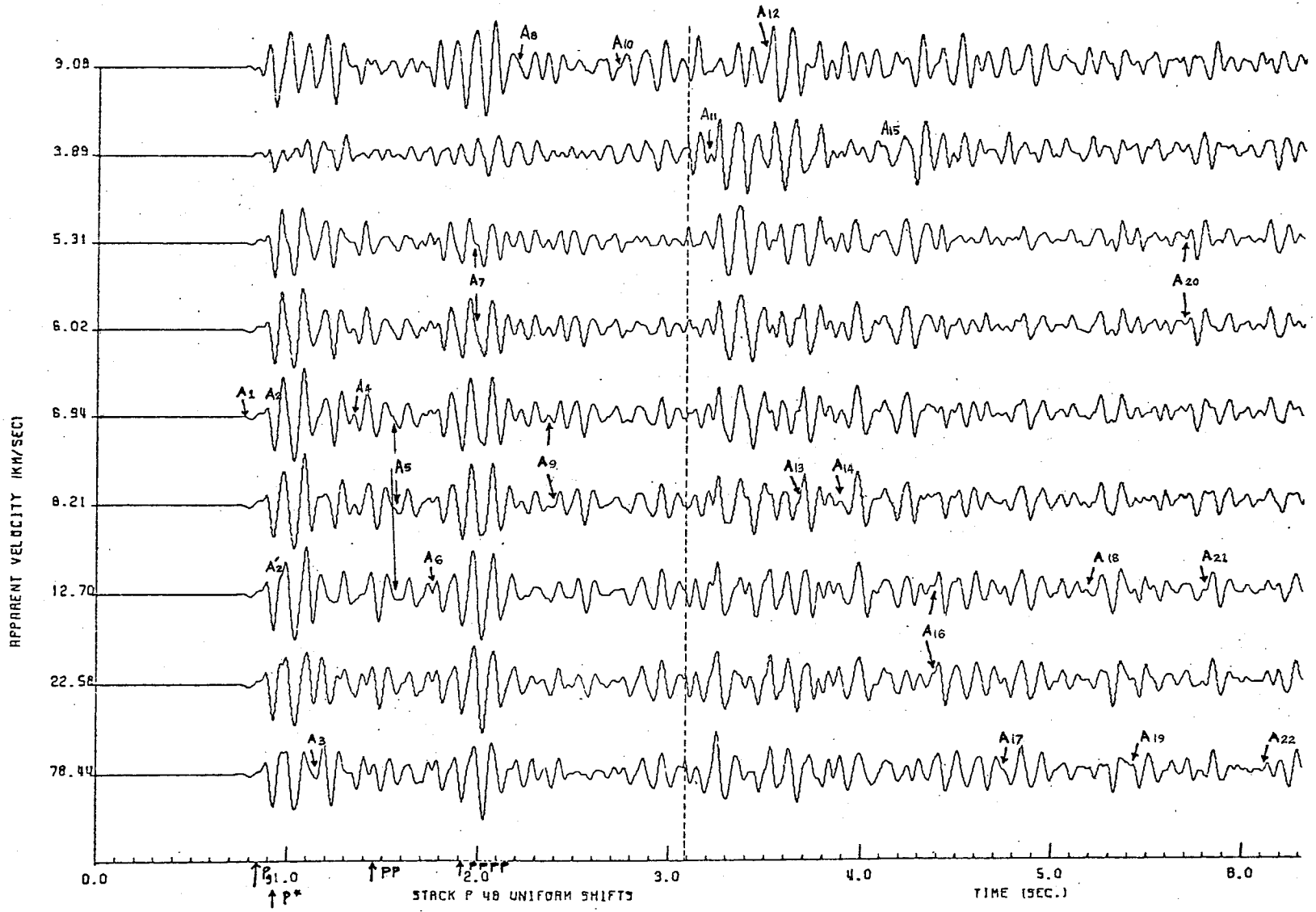

Figure 27. Plot for P48 showing the arrivals. The broken line marks a change to a bigger plotting scale. S = 3.07

TABLE 18

Record P48, $\theta = 67^{\circ}$, Distance = 153.06 km, Reference Time = 24.57 sec

Arrival	Time (sec)		Identification	Hajnal (1970)
A_1	25.36	.03	Pg	Pg : 25.41
A_2, A_2'	25.54	.06	P*	P* : 25.49
A_3	25.73	.06	X1	
A_4	25.95	.07	PP	PP : 26.05
A_5	26.14	.04	X2	
A_6	26.34	.03	PPPP	PPPP : 26.49
A_7	26.57	.05		
A_8	26.80	.04		
A_9	26.96	.04		
A_{10}	27.32	.04		
A_{11}	27.80	.03		
A_{12}	28.07	.04		
A_{13}	28.25	.03		
A_{14}	28.45	.04		
A_{15}	28.67	.03		
A_{16}	28.93	.05		
A_{17}	29.34	.05		
A_{18}	29.76	.04		
A_{19}	30.01	.04		
A_{20}	30.28	.04		
A_{21}	30.39	.04		
A_{22}	30.70	.05		

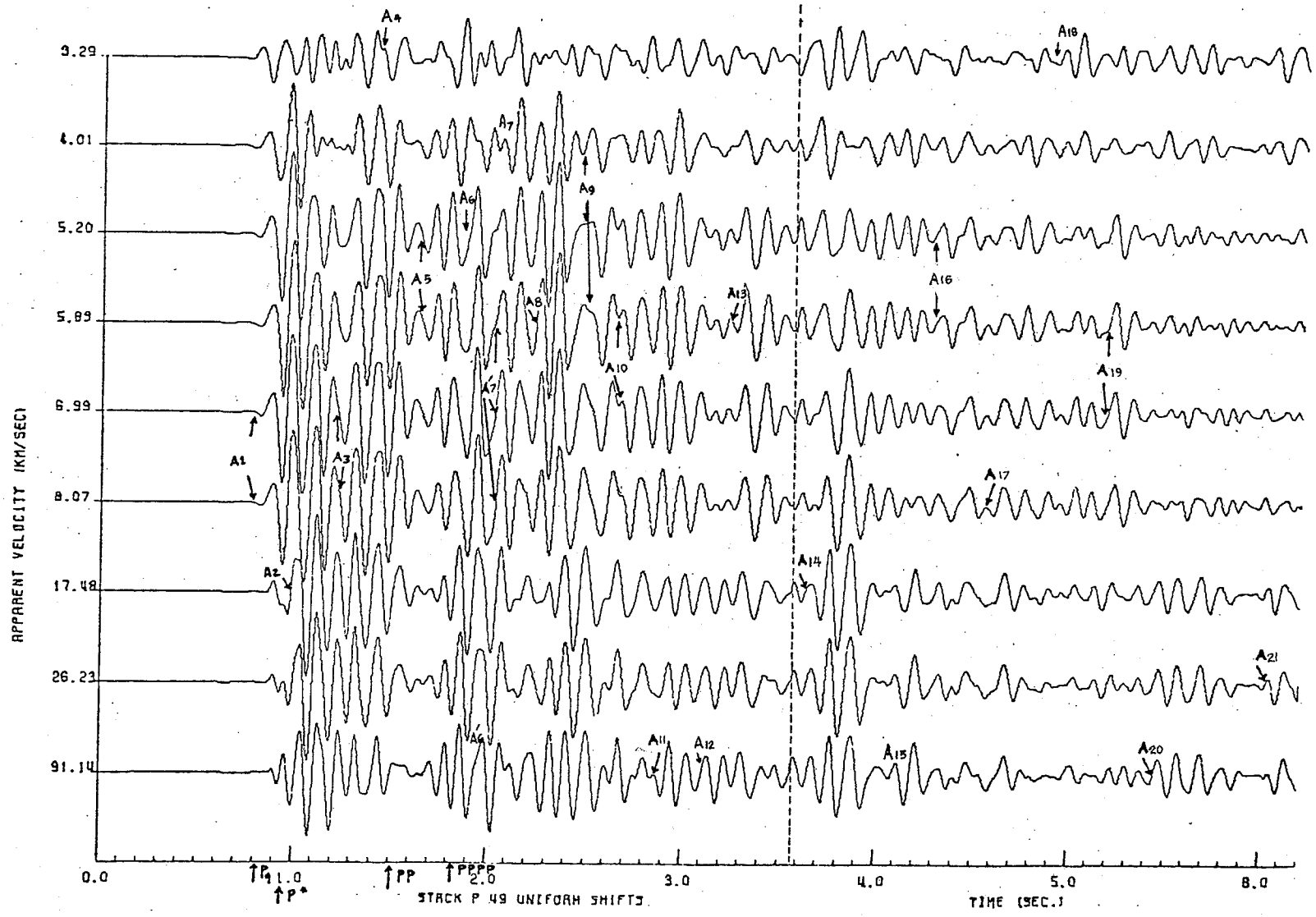

Figure 28. Plot for P49 showing the arrivals. The broken line indicates a change to a bigger plotting scale. S = 2.36

TABLE 19

Record P49, $\theta = 63^{\circ}$, Distance = 154.16 km, Reference Time = 24.71 sec

Arrival	Time (sec)		Identification	Hajnal (1970)
A_1	25.50	.03	Pg	Pg : 25.53
A_2	25.69	.05	P*	P* : 25.65
A_3	25.93	.07	X1	
A_4	26.17	.04	PP	PP : 26.23
A_5	26.34	.04	X2	PPPP : 26.55
A_6, A_6'	26.61	.05	PPPP	
A_7, A_7'	26.74	.06		
A_8	26.94	.05		
A_9	27.20	.05		
A_{10}	27.37	.04		
A_{11}	27.57	.04		
A_{12}	27.82	.05		
A_{13}	27.95	.05		
A_{14}	28.34	.05		
A_{15}	28.79	.04		
A_{16}	29.01	.04		
A_{17}	29.26	.04		
A_{18}	29.66	.04		
A_{19}	29.89	.07		
A_{20}	30.15	.04		
A_{21}	30.73	.05		

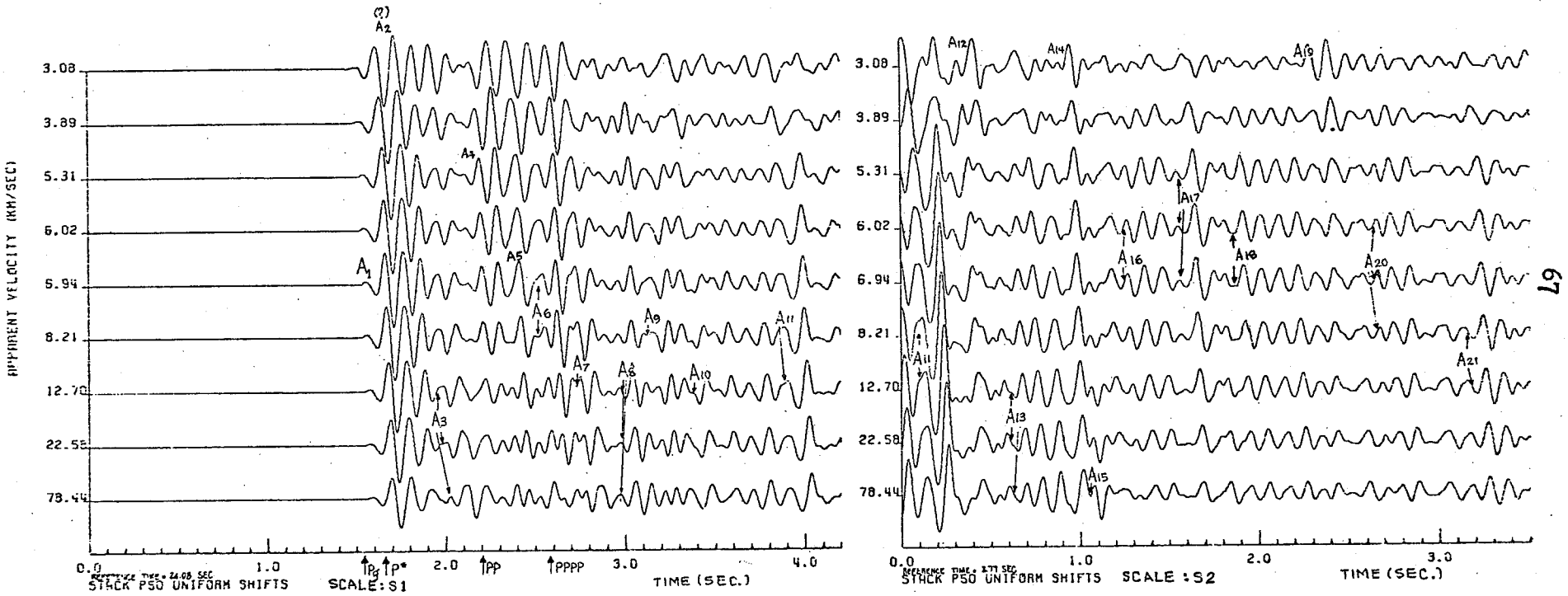

Figure 29. Plot for record P50 showing the arrivals. S = 2.34

TABLE 20

Record P50, $\theta = 67^{\circ}$, Distance = 154.60 km, Reference Time = 24.08 sec

Arrival	Time (sec)		Identification	Hajnal (1970)
A_1	25.62	.04	Pg	Pg : 25.62
A_2	- - - - - -		P*	P* : 25.75
A_3	26.05	.05	X1	
A_4	26.17	.05	PP	PP : 26.28
A_5	26.43	.05	X2	
A_6	26.61	.04	PPPP	PPPP : 26.65
A_7	26.82	.04		
A_8	27.06	.06		
A_9	27.21	.05		
A_{10}	27.47	.04		
A_{11}	27.96	.06		
A_{12}	28.12	.04		
A_{13}	28.48	.06		
A_{14}	28.73	.04		
A_{15}	28.91	.05		
A_{16}	29.10	.08		
A_{17}	29.41	.05		
A_{18}	29.70	.05		
A_{19}	30.08	.04		
A_{20}	30.49	.04		
A_{21}	31.02	.05		

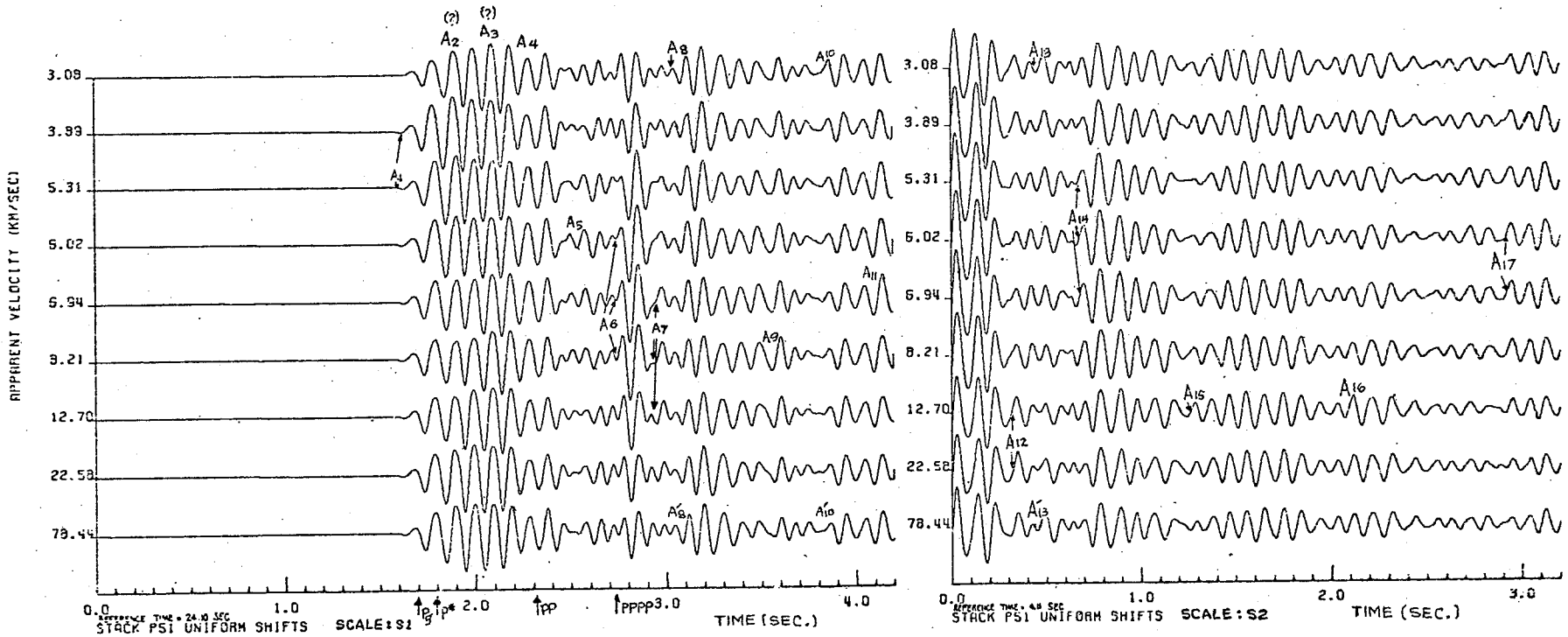

Figure 30. Plot for record P51 showing the arrivals. S = 2.35

TABLE 21

Record P51, $\theta = 67^{\circ}$, Distance = 155.64 km, Reference Time = 24.10 sec

Arrival	Time (sec)	Identification	Hajnal (1970)
A_1	25.70 .03	Pg	Pg : 25.81
A_2	- - - - - -	P*	P* : 25.89
A_3	- - - - - -	X1	
A_4	26.40 .06	PP	PP : 26.42
A_5	26.59 .04	X2	
A_6	26.85 .04	PPPP	PPPP : 26.83
A_7	27.02 .04		
A_8, A_8'	27.13 .05		
A_9	27.63 .04		
A_{10}	27.92 .05		
A_{11}	28.18 .04		
A_{12}	28.52 .04		
A_{13}, A_{13}'	28.66 .05		
A_{14}	28.87 .05		
A_{15}	29.49 .04		
A_{16}	30.27 .05		
A_{17}	31.12 .06		

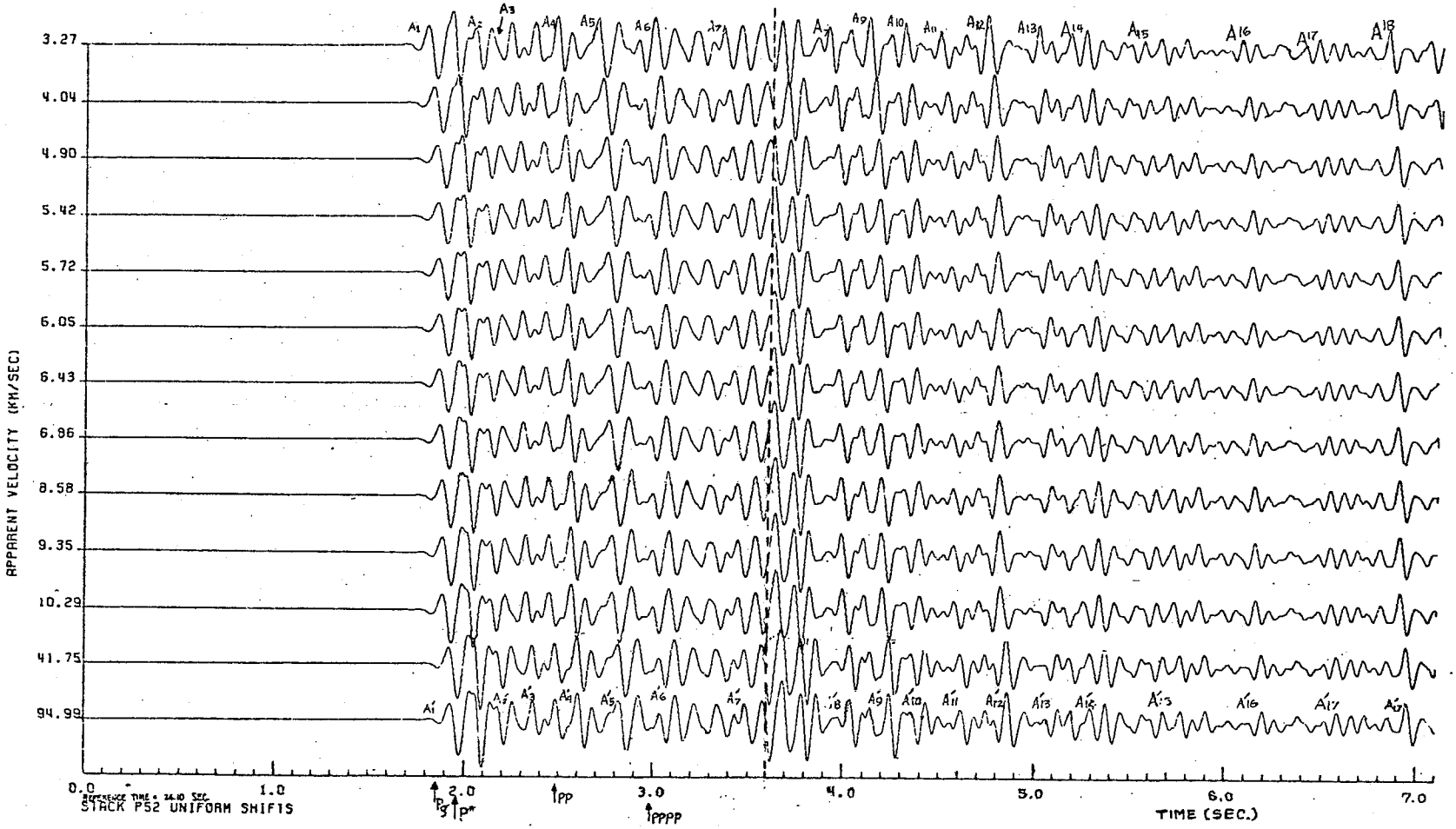

Figure 31. Plot for record P52 showing the arrivals. The broken line indicates the change to bigger plotting scale. S = 1.89

TABLE 22

Record P52, $\theta = 27^{\circ}$, Distance = 156.63 km, Reference Time = 24.10 sec

Arrival	Time (sec)		Identification	Hajnal (1970)
A_1, A_1'	25.88	.09	Pg	Pg : 25.95
A_2, A_2'	26.19	.10	P*	P* : 26.05
A_3, A_3'	26.31	.15	X1	
A_4, A_4'	26.58	.10	PP	PP : 26.58
A_5, A_5'	26.82	.10	X2	
A_6, A_6'	27.05	.09	PPPP	PPPP : 27.09
A_7, A_7'	27.50	.09		
A_8, A_8'	28.03	.09		
A_9, A_9'	28.24	.08		
A_{10}, A_{10}'	28.36	.07		
A_{11}, A_{11}'	28.59	.07		
A_{12}, A_{12}'	28.81	.07		
A_{13}, A_{13}'	29.10	.07		
A_{14}, A_{14}'	29.30	.07		
A_{15}, A_{15}'	29.65	.07		
A_{16}, A_{16}'	30.16	.07		
A_{17}, A_{17}'	30.53	.07		
A_{18}, A_{18}'	30.96	.08		

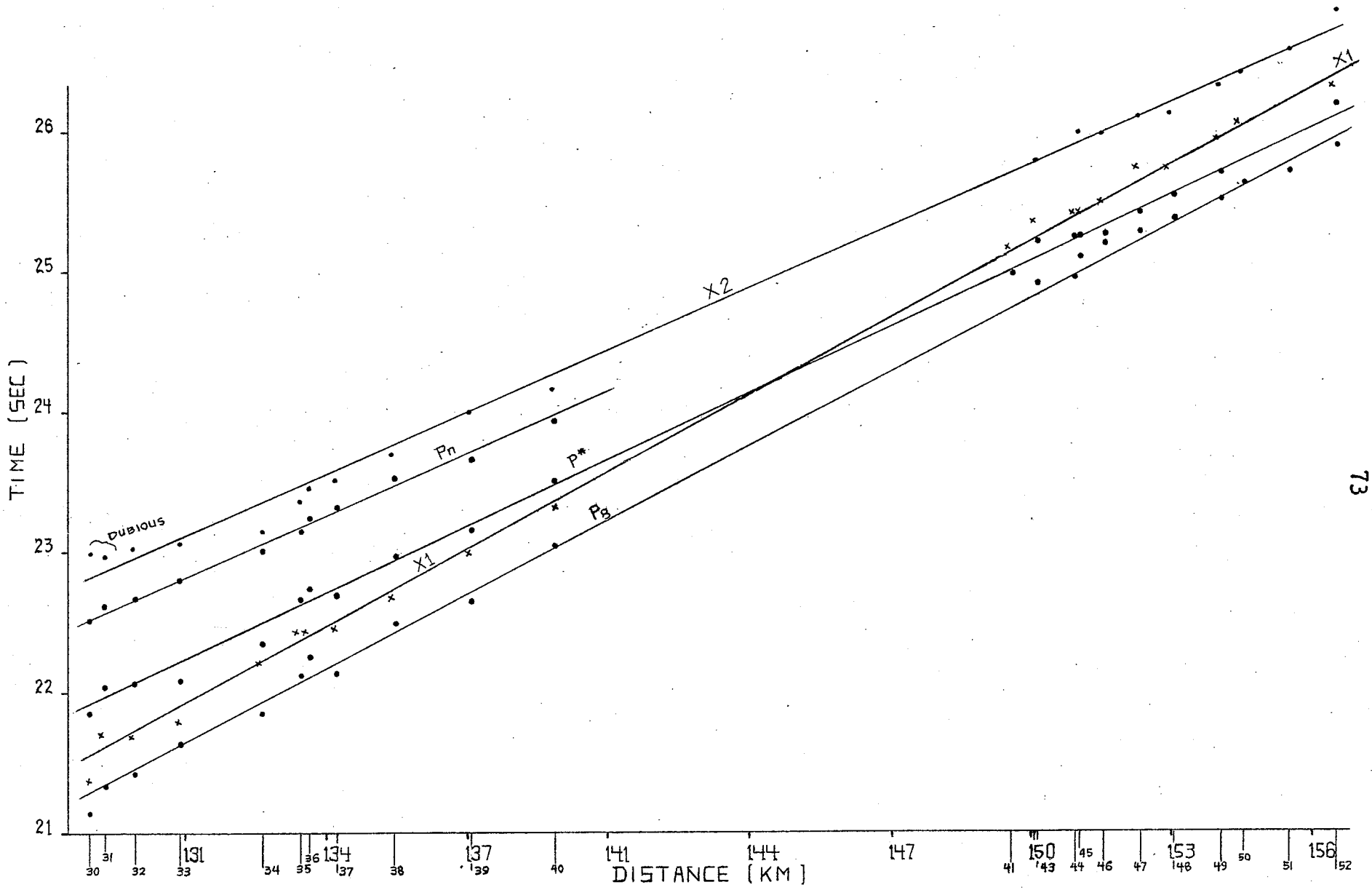

Figure 32. X-T plots for the events Pg, P*, X1, X2, and Pn.

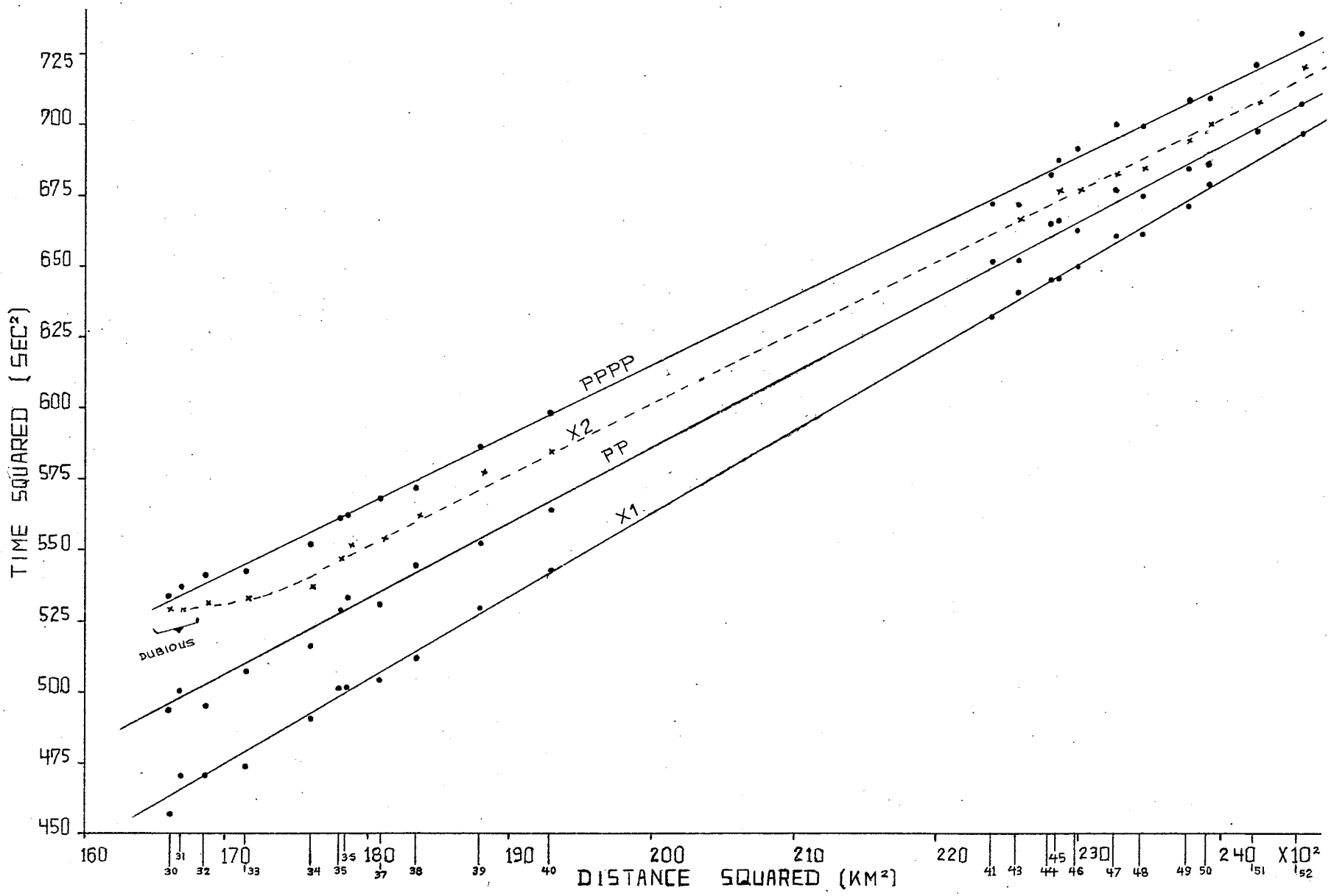

Figure 33. $X^2 - T^2$ plots for the events X1, PP, X2, and PPPP.

3.3 Comparison with the Results of Hajnal (1970)

Apart from the comparison of travel times in Tables 1 to 22, the velocity calculations from the present results can be compared with those of Hajnal. Hajnal computes velocity values for the events Pg, Xl, and PP. Similar calculations in this section are compared to Hajnal's results. Velocity values for P* and Pn estimated from the X-T plots on Figure 16 of Hajnal (1970, pp.111-112) are compared with the velocities obtained from the present P* and Pn observations in section 3.4.

Pg

Linear regression on the direct wave arrivals leads to the following equation:

(13) $t = (-0.29385 \pm 0.00282) + (0.16751 \pm 0.00138) x$

where t is travel time and x is shot-to-recorder distance. The slope gives the near-surface velocity $v_1 = (5.97 \pm 0.05)$ km/sec. Hajnal (1970, p.82) reports $v_1 = (5.98 \pm 0.06)$ km/sec and slope equal to (0.1671 $\pm$ 0.0055) with 90% confidence on the error estimate.

Equation (13) is obtained using only 21 records compared to the 59 records used by Hajnal.

The intercept is non-zero but negative. Only a small part of this (approximately -0.04 to -0.05 sec) can be attributed to the use of shot to recorder distances which are arclengths, s, rather than chords, c.* Contribution to the negative value of the intercept from possible

---

* $s = \bar{R}b$, $c = 2\bar{R}\sin b/2$ where $\bar{R}$ = mean radius of the earth in the neaighborhood of the shot point and the recording stations, and where b = shot to recorder epicentral distance. Pg travels along c, if Fermat's principle applies and the near surface velocity is constant. The values of s used in this study were calculated using the program DISTAN (Hajnal, 1970, pp.265-267).

difference in elevation between the shot point and the recording stations (whether the shot point is higher or lower in elevation than the stations) is also ruled out. The travel time for the direct wave in this case is

(14) $$t = \left(h^2/x^2 + 1 \right)^{\frac{1}{2}} \frac{x}{v_1}$$

To a first order approximation, this can be rewritten as

(15) $$t = \frac{x}{v_1} + \frac{h^2}{2x v_1} = \frac{x}{v_1} + c(x)$$

where $0 \leq c(x) < 1$, $|h| \ll x$. A least squares fit of the form $y = ax + b$ to the Pg data will give an intercept which is an average value of $c(x)$, $x_{P30} \leq x \leq x_{P52}$. Since this average is necessarily positive, the negative value of the intercept has to be attributed to other factors. For instance, overdetermination of shot to recorder distances by 1.73km is sufficient. There is also the possibility of missing the first arrival on the farthest records by a few milliseconds due to low amplitudes.

PP

Hajnal (1970) interprets PP as wide-angled reflection from the Intermediate discontinuity (believed to be the same as the Conrad discontinuity (Hall and Hajnal, 1969)). Hajnal fitted a straight line to the 59 data points and obtained a velocity $\bar{v}_1 = (6.03 \pm 0.05)$ km/sec (Hajnal, 1970, p.80). A straight line fit to the present 21 data points gives the equation

(16) $$t^2 = (0.02671 \pm 0.00048) x^2 + (51.11383 \pm 0.75028)$$

and the values $\bar{v}_1 = (6.12 \pm 0.05)$ km/sec and $h = (21.88 \pm 0.52)$ km. No value of h from the PP data is reported by Hajnal.

X1

This event arrives immediately after Pg on records P30 to P40; on the further records, it comes after P*. It is clear from Figures 32 and 33 that both the X-T and the X^2-T^2 plots of the X1 data show good linear trends. The linear least squares fit to the X-T plot (Figure 32) has the equation

(17) $t = (0.17460 \pm 0.00114) x - (0.96347 \pm 0.00764)$

while the linear least squares fit to the X^2-T^2 plot (Figure 33) has the equation

(18) $t^2 = (0.02929 \pm 0.00046) x^2 - (22.56656 \pm 0.33374)$

The negative intercepts of both equations (17) and (18) are incompatible with X1 originating from either a simple plane horizontal/dipping refractor or a simple plane horizontal reflector (Dobrin, 1960, pp.70-106). For a reflector dipping with angle ϕ, the travel time equation is

(19) $t^2 = \frac{x^2}{\bar{U}_1^2} + \frac{2xh \sin \phi}{\bar{U}_1} + \frac{4h^2}{\bar{U}_1^2}$ (Hajnal, 1970, p.71)

To calculate a least squares fit of the form (19), define $x_i^2 = p_i$, $t_i^2 = q_i$, and $H = \sum_{i=1}^{21} (q_i - ap_i - bp_i^{\frac{1}{2}} - c)^2$. The conditions for minimum deviation of the points (x_i^2, t_i^2) from the curve $q = ap + bp^{\frac{1}{2}} + c$ are $\frac{\partial H}{\partial a} = \frac{\partial H}{\partial b} = \frac{\partial H}{\partial c} = 0$. These three conditions will give three equations which can be transformed using Cramer's rule into three matrix equations for a, b, and c. The desired equation is

(20) $t^2 = (0.01419) x^2 + (4.29841) x - (327.15037)$

where error estimates have been omitted. The coefficients of x^2 and the intercepts of equations (18) and (20) are expectedly different since two different curves are being fitted to the same data (hence

different expressions for the coefficients and the intercepts are obtained) and the actual subsurface deviates from the idealized conditions assumed in either equation. The sign of the third term in equations (19) and (20) are opposite. It appears, therefore, that X1 is neither a refraction nor a reflection from either a plane horizontal or dipping interface.

On the basis of the sections and the tables of arrival times given by Hajnal (1970; sections on pp.113-117; Table VI on pp. 109-110), and the WDS traces and arrival times obtained in this study (Figures 10 to 31, Tables 1 to 22), it is probable that X1(WDS) and X1(Hajnal) are the same event. Assuming X1 is a reflection, Hajnal (personal communication) reports a velocity of 5.84 km/sec from the slope of the X^2-T^2 straight line fit to the data (Hajnal, 1970, p.148). This is in excellent agreement with the 5.84 km/sec obtained from the X^2-T^2 plot of Figure 33. However, the negative intercept of the X^2-T^2 line in both studies (-10.72 ± 7.44 sec^2, Hajnal, 1970; -22.57 ± 0.33 sec^2, this study) demonstrates that a complex situation exists. Figure 19 of Hajnal (1970, p.127) shows one possibility. The calculated depths to the X1 reflector shown in Hajnal's Figure 19 vary from 1.5 km to 5.0 km in the distance range 95 km to 128 km. If X1(Hajnal) and X1(WDS) are indeed the same event, the lower intercept of X1(WDS) indicates a shallower reflector between 128 km and 156 km. For a complex reflector, the true X-T and X^2-T^2 plots of the arrival times will be non-linear. To reconcile this with the observed linearity of the X-T and X^2-T^2 plots for the X1(Hajnal) and X1(WDS), it would be necessary to interpret these

observed curves merely as approximately linear segments of the basically non-linear, true X-T and X^2-T^2 curves for the event.

3.4 Additional Results

P*

This is interpreted by Hall and Hajnal (1969) and Hajnal (1970) as the refraction from the Intermediate discontinuity. A linear least squares fit to the data points shown in Figure 32 gives

(21) $t = (0.15071 \pm 0.00135) x + (2.48567 \pm 0.02576)$

The slope gives $U_2 = (6.64 \pm 0.05)$ km/sec. The velocity estimated from Hajnal's X-T plot for this event (Figure 16, pp.111-112, Hajnal, 1970) is (6.15 ± 0.45) km/sec. Hall and Hajnal (1969) and Hajnal (1970, pp.81,84) report the velocity (6.85 ± 0.04) km/sec. The estimate of the depth h calculated from equation (21) is (19.61 ± 0.52) km. This value is lower than the (21.88 ± 0.52) km obtained from the PP data.

Pn

This is interpreted by Hall and Hajnal (1969) and Hajnal (1970) as the refraction from the Mohorovičic discontinuity. Linear regression on the 11 data points (including the three additional arrival times determined in this study for P38, P39, and P40) gives

(22) $t = (0.13970 \pm 0.00135) x + (4.54000 \pm 0.03946)$

Applying the travel time equation for refraction from a horizontal interface beneath two layers (Dobrin, 1960, p.74),

(23) $$t = \frac{x}{U_a} + \frac{2h\sqrt{U_a^2 - U_1^2}}{U_a U_1} + \frac{2H\sqrt{U_a^2 - U_2^2}}{U_a U_2}$$

where $\bar{v}_1$ = (6.12 ± 0.05) km/sec, v_2 = (6.64 ± 0.05) km/sec, h = thickness of the first layer, and H = thickness of the second layer. The slope gives the velocity v_a = (7.16 ± 0.06) km/sec. The value obtained from Figure 16 of Hajnal is (7.02 ± 0.50) km/sec. Both are lower than (7.92 ± 0.06) km/sec reported by Hall and Hajnal (1969) and Hajnal (1970) for the upper mantle velocity. This latter estimate is based on significantly more data than are used in the present study.

If the Moho dips away from the source, v_a is only an apparent velocity along the surface and is lower than the true upper mantle velocity. To account for this, a dip angle of 11° 4' (assuming a smooth plane interface) suffices. No further information can be obtained from the Pn travel time curve without making unreasonable assumptions about the geometry of the Moho between the shot point and receivers. For example, a simple plane boundary dipping away from the shot point at 11° 4' would be 22.20 km beneath the shot point and between 47.38 km and 52.82 km beneath the receivers. Clearly, this extrapolation is unrealistic. Therefore, Hajnal's depth estimate at 128 km is used for the model in Figure 34.

X2

The travel times for this event are shown on X-T and X^2-T^2 plots in Figures 32 and 33. The straight line fit to the X-T plot has the equation

(24) $t = (0.14040 \pm 0.00113) x + (4.72203 \pm 0.04462)$

This equation gives an apparent velocity of 7.12 km/sec which probably indicates the existence of a dipping boundary below the Mohorovicic

discontinuity. Without either a reversed profile or additional velocity information, the velocity beneath, and depth to this boundary are indeterminate.

3.5 A Simple Model

Collecting the results, a simple model of the crust with uniform-velocity layers is constructed in Figure 34. Like Hajnal's model, it has three layers. The depth to the top interface (X1 reflector) is not well defined in the region of this study but is shallower than that at shorter distances. The depth to the Intermediate discontinuity is the average value of the estimates from the PP and P* data and is less than the (22.85 ± 1.43) km value shown on Figure 19 of Hajnal. The dip of 11° 4' away from the shot point found for the Moho is the opposite of the gentle slope toward the shot point between the distances 85 km and 156 km given by Hajnal. The average velocity of the top layer is the same, within error limits, as Hajnal(s value. However, the velocity beneath the Intermediate discontinuity is lower.

3.6 Conclusion

This study has shown that at its present stage of development, the new processing technique involving a weighted differential stack provides a useful tool for enhancing seismic events in addition to those that can be identified using the digital processing techniques employed by Hajnal.

Using the times from the new data, a simple three layer crustal model is derived. It is basically the same as that obtained by Hajnal with only minor differences.

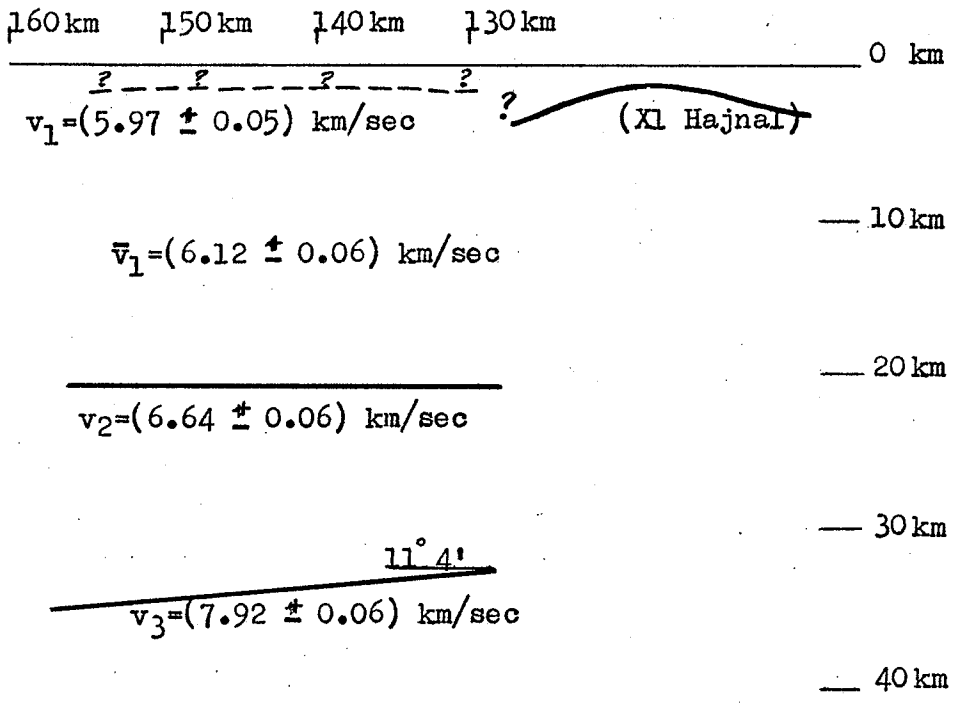

Figure 34. A simple crustal model

APPENDIX A

Summary of Relevant Information

Field Book No.	*Tape 1 Index No.	Hajnal's Notation	@Reference Time (sec)	Tape 1
P30	30	A-30	19.96	VOL=SER=HA9018
P31	31	A-31	20.07	Bin=925
P32	32	A-32	20.03	RECFM=F
P33	33	A-33	20.10	LRECL=2404
P34	34	A-34	19.88	BLKSIZE=2404
P35	35	A-35	20.04	DSN=GEOG.HAJNEL.A0001
P36	36	A-36	20.14	DENSITY=2
P37	37	A-37	21.76	Digital interval = 0.0017143 sec
P38	38	A-38	20.06	No. of logical records per recording station = 120
P39	39	A-39	20.03	No. of samples per logical record per channel = 100
P40	40	A-40	20.13	

Field Book No.	*Tape 2 Index No.	Hajnal's Notation	@Reference Time (sec)	Tape 2
P48	41	A-48	24.12	VOL=SER=HA9019
P49	42	A-49	23.97	Bin=927
P50	43	A-50	24.15	RECFM=F
P51	44	A-51	23.98	LRECL=2404
P52	45	A-52	24.18	BLKSIZE=2404
P53	46	A-53	24.04	DSN=GEOG.HAJNEL.A0001
P54	47	A-54	24.07	DENSITY=2
P55	48	A-55	24.06	Digital interval = 0.0017143 sec
P56	49	A-56	24.02	No. of logical records per recording station = 120
P57	50	A-57	24.08	No. of samples per logical record per channel = 100
P58	51	A-58	24.10	
P59	52	A-59	24.10	

*Notation used in this thesis with 'P' written before each record number.

@Time of the beginning of a tape record from shot time.

APPENDIX B

Program MVSTACK

This program is a modification of the program NSTACK.

NOREC	Number of records for which stacking will be done
LAB	Label for the x-axis
LABEL	Label for the y-axis
W1	Start of noise window (in seconds)
W1L	Length of noise window (in seconds)
W2	Start of signal window (in seconds)
W2L	Length of signal window (in seconds)
NOVEL	Number of traces (or stacks) per job
ISHIFT	Array containing the relative shifts of channels 2 to 12 with respect to channel 1
DI	Digital sampling interval = .0017143 (in seconds)
IR	Record number
IB	Logical record number
IS	Sample number
RTIME	Time at the origin of the plot
DALEN	Length of record to be stacked (in seconds)
NULL (I)	I=0, trace of channel I is to be ignored I=1, trace of channel I is to be added in stack
D	Geophone separation
A1	Angle θ

```
      INTEGER NULL(12),LABEL(20),LAB(10),RTIME
      DIMENSION IBUF(4000),ISHIFT(12,12),WT(12)
      INTEGER*2 TRACE (4100),IS,A,B,DATA(12, 800),IDELT(12),TRACE1(600)
      DEFINE FILE 13 (192,2004,L,INT)
      CALL PLOTS(IBUF,4000)
      READ (5,5) NOREC
      DO 2121 ICOUN = 1,NOREC
      REWIND 8
      READ (5,1) IREC,IPHASE,IJOB
    1 FORMAT (3I4)
      WRITE (6,222) IREC,IPHASE,IJOB
  222 FORMAT (////,' ','STACK OF RECORD',I4,3X,',PHASE',I4,3X,',JOB',
     CI4//)
      READ(5,9) (LAB(K),K=1,10)
      READ(5,5) NOVEL
    5 FORMAT(I4,F3.1)
C
C     DI = DIGITAL INTERVAL
C
      DI=.0017143
      READ(5,13) W1,W1L,W2,W2L
   13 FORMAT(4F8.3)
      DO 141 ICI = 1,NOVEL
      READ (5,6) (ISHIFT(ICI,KKK),KKK=1,12)
    6 FORMAT (12I6)
  141 WRITE (6,2)(ISHIFT(ICI,KKK),KKK=2,12),ICI
    2 FORMAT(/' ','CHANNELS 2 TO 12 ARE SHIFTED',/ ,' ',11I10,/ ,' ',
     C'SAMPLES WITH RESPECT TO CHANNEL 1, RESPECTIVELY, IN STACK',I4 )
      READ(5,4) IR,IB,IS,RTIME,DALEN,(NULL(I),I=1,12),D,A1
    4 FORMAT (4I4,2X,F6.2,2X,12I1,2X,2F5.1 )
      READ(5,9) (LABEL(K),K=1,20)
    9 FORMAT(20A4)
C
      READ (5,62) (WT(I),I=1,12)
   62 FORMAT (12F6.4)
      CALL SEARCH (IR,IB)
C
C     II = NUMBER OF SAMPLES TO PROCESS
      II = DALEN/DI + .5
      NBLKS = II/600 + 1
C
C     THIS PORTION READS THE DATA FROM THE INPUT TAPE
C
      WRITE (6,55)
   55 FORMAT (' ', 10X, 'PLOT COVERS BLOCKS BETWEEN AND INCLUDING' )
      DO 60 M=1,NBLKS
      IX=1
      DO 10 L = 1,6
      IZ=IX+99
      READ(8,30) A,B,((DATA(I,K),I=1,12),K=IX,IZ)
      IF(M.EQ.1 .AND. L .EQ.1) WRITE (6,7) A,B
   30 FORMAT ( 2A2,250A2, 250A2, 250A2, 250A2, 250A2)
   10 IX=IX+100
      IF(M.EQ.NBLKS ) WRITE (6,7) A,B
    7 FORMAT (' ', 13X, 'RECORD NO.', I5, 6X, ' LREC.NO.', I5 )
C
C     THIS PORTION APPLIES WEIGHTING FACTORS TO THE TRACES
C
      DO 60 K=1,12
      IF(NULL(K).EQ.0) GO TO 60
      INT=15*(K-1)+M
      DO 50 KD = 1,600
   50 DATA(K,KD)=WT(K)*DATA(K,KD)
      WRITE(13' INT) (DATA(K,J),J=1,600)
   60 CONTINUE
C
C     THE '3' IN THE FOLLOWING STATEMENT DETERMINES THE TIME SCALE OF
C     THE PLOT ( = 3 INCHES/SECOND)
```

```
C
      XSL=3*DI
      YAXIS = 12.3
      ALLOW=1.4
      DIST = 12.3/9
      ITEST = 1
      CALL PLOT (0., -11., -3)
      CALL PLOT (0.,ALLOW,-3)
      CALL FACTOR (.62)
      CALL PLOT (0.,YAXIS,-2)
      CALL SYMBOL(-1.2,-9.0,.14,LAB,90.,40)
      CALL PLOT(0.,0.,3)
C
      DO 900 KA=1,NOVEL
      IX=1
C
C     THIS PORTION DETERMINES THE FIRST TRACE TO BE STACKED AND READS
C     IT FROM THE DISK
C
      IKC=1
90    IF(NULL(IKC)) 110,100,110
100   IKC=IKC+1
      GO TO 90
110   INT=15*(IKC-1)+1
      DO 250 KE=1,NBLKS
      IZ = IX + 599
      READ(13' INT) (TRACE(NY),NY=IX,IZ)
 250  IX = IX + 600
C
C      THIS PORTION READS NEW TRACES FROM THE DISK, SHIFTS THEM
C      RELATIVE TO THE FIRST TRACE AND ADDS THEM TO IT. THE TIME
C      SHIFTS ARE NOT NECESSARILY UNIFORM.
C
      DO 400 KF=1,12
      IH=0
      IF(NULL(KF).EQ.0) GO TO 400
      IF(KF.EQ.IKC) GO TO 400
      IF (ISHIFT(KA,KF)-0) 320,330,310
 310  IW = ISHIFT (KA,KF)
      GO TO 340
 320  IH = IABS(ISHIFT(KA,KF))-1
330   IW=1
340   INT=15*(KF-1)+1
      DO 300 KG=1,NBLKS
      READ(13' INT) (TRACE1(I),I=1,600)
      DO 350 KH=IW,600
      IH=IH+1
350   TRACE(IH)=TRACE(IH)+TRACE1(KH)
300   IW=1
400   CONTINUE
C
C     THIS PORTION NORMALIZES AND PLOTS THE DATA VALUES.
C
C       SCALE OF THE PLOT
C
      IF(KA.GT.1) GO TO 440
      READ (5,430) TMAX, YSL
 430  FORMAT (2F15.7)
      TMAXTE = 2.
      WRITE (6,444) TMAX, YSL
 444  FORMAT (' ','MAXIMUM VALUE', F12.3,6X,'NORM',2X,F10.7)
 440  CONTINUE
C
C
      SUM = 0.
      P = 0*COS(A1*0.0174533)
      P=ABS(P)
      V4 = P/ISHIFT(KA,4)/DI*3
      V5 = P/ISHIFT(KA,5) /DI*4
      V6 = P/ISHIFT(KA,6)/DI*5
      V7 = P/ISHIFT(KA,7)/DI *6
      V8 = P/ISHIFT(KA,8)/DI *7
      V9 = P/ISHIFT(KA,9)/DI*8
      V12= P/ISHIFT(KA,12)/DI*11
```

```
      V = (V4+V5+V6+V7+V8+V9+V12)/7.
      W=V
C
      IF (ITEST) 666,666,550
  550 CALL NUMBER(-.7 ,0.,.14,W,0.,2)
      CALL PLOT(0.,0.,3)
      CALL PLOT(-.1,0.,2)
      CALL PLOT(0.,0.,3)
      DO 500 LA=1,II
      XDL=(LA-1)*XSL
      TR = TRACE (LA)
      YDL=YSL*TR
      ISWIT = 0
      IF (ABS(TR).NE.TR) ISWIT = 1
      TR = YDL
      IF (ABS(TR).GE.TMAXTE) TR=TMAXTE
      IF(ABS(TR).GE.TMAXTE .AND. ISWIT.EQ.1) TR=-TR
      YDL = TR
  500 CALL PLOT(XDL,YDL,2)
      CALL PLOT (XDL,0.,-3)
      CALL PLOT (0.,-DIST,-3)
      GO TO 900
  666 DO 580 LA = 1,II
      XDL = (LA-1)*XSL
      TR = TRACE (II+1-LA)
      YDL=YSL*TR
      ISWIT = 0
      IF (ABS(TR).NE.TR) ISWIT = 1
      TR = YDL
      IF (ABS(TR).GE.TMAXTE) TR=TMAXTE
      IF(ABS(TR).GE.TMAXTE.AND.ISWIT.EQ.1) TR=-TR
      YDL = TR
  580 CALL PLOT (-XDL,YDL,2)
      CALL PLOT (-XDL,0.,-3)
      CALL NUMBER(-.7 ,0.,.14,W,0.,2)
      CALL PLOT(0.,0.,3)
      CALL PLOT (-.1,0.,2)
      CALL PLOT(0.,0.,3)
      CALL PLOT (0.,-DIST,-3)
  900 ITEST =-ITEST
      IF (NOVEL/2*2 .EQ. NOVEL) GO TO 760
      CALL PLOT (-XDL,0.,-3)
  760 YLEFT = YAXIS -NOVEL*DIST
      CALL PLOT (0.,-YLEFT,-3)
      YSL = .01
C
C     THIS PORTION PLOTS THE TIME SCALE.
      CALL TIME (TRACE,II)
      DO 800 LA=1,II
      XDL=(LA-1)*XSL
      YDL=TRACE(LA)*YSL
  800 CALL PLOT (XDL,YDL,2)
      CALL SYMBOL(5.,-.6,.14,LABEL,0.,80)
      CALL PLOT (-.2,-.3,-3)
C
C     THIS PORTION LABELS THE TIME SCALE.
C
      XPAGE=0.
      ISECS=DALEN+1.5+RTIME
      JL=1+RTIME
      DO 1010  I=JL,ISECS
      FPN=FLOAT(I-1)
      CALL NUMBER (XPAGE,0.,.14,FPN,0.,1)
 1010 XPAGE=XPAGE+3.
      XPAGE=XPAGE+6.
      CALL PLOT (XPAGE,0.,-3)
 2121 CONTINUE
      CALL PLOT(0.,0.,999)
      STOP
      END
```

```
      SUBROUTINE WEIGHT (IR,IB,IS,W1,W1L,W2,W2L,WT,DATA,NULL,IS1,IS2,
     CIP,I9)
      INTEGER NULL(12)
      INTEGER*2 DATA(12, 800),A,B,IS
      REAL WT(12)
      DI=.0017143
C
C     CALCULATION OF PARAMETERS
C
      IIONE=W1/DI+.5
      IF(W1.LT.0.) IIONE=ABS(W1/DI-.5)
      IITWO=W2/DI+.5
      IF (W1.GE.0.) GO TO 666
      IBW1 = IB - (IIONE + IS )/100
      GO TO 777
  666 IBW1 = IB + (IIONE + IS )/100
  777 IBW2 = IB + (IITWO + IS )/100
      IW1L=(W1L/DI)/100 + 2
      IW2L=(W2L/DI)/100 + 2
      IS1=IIONE-100*(IBW1-IB) + IS
      IF(W1.LT.0.) IS1 =  100*(IB-IBW1)-IIONE + IS
      IS2=IITWO-100*(IBW2-IB) + IS
      WRITE (6,888)IW1L,IW2L,IBW1,IBW2,IIONE,IITWO
  888 FORMAT(/ ' ',' PARAMETERS: IW1L',I4,5X,'IW2L',I4,5X,'IBW1',I4,5X,
     X'IBW2',I4,5X,'IIONE',I4,5X,'IITWO',I4/ )
C
C     READS THE DATA VALUES OF THE NOISE WINDOW AND DETERMINES THE POWER
C     IN THAT WINDOW
C
      CALL SEARCH(IR,IBW1)
      IW=1
      DO 10 J=1,IW1L
      IWW=IW+99
      READ(8,30) A,B,((DATA(I,K),I=1,12),K=IW,IWW)
   30 FORMAT ( 2A2,250A2, 250A2, 250A2, 250A2, 250A2)
   10 IW=IW+100
      I8=IS1+W1L/DI+.5
      DO 40 I=1,12
      IF(NULL(I).EQ.0) GO TO 40
      SUM=0.
      DO 20 K=IS1,I8
   20 SUM=SUM+DATA(I,K)*DATA(I,K)
      WT(I)=SUM/(I8-IS1)
   40 CONTINUE
C
C     READS THE DATA VALUES OF THE SIGNAL WINDOW AND DETERMINES THE
C     POWER IN THAT WINDOW
C
      DO 21 J = 1,3
   21 BACKSPACE 8
      CALL SEARCH(IR,IBW2)
      IW=1
      DO 50 J=1,IW2L
      IWW=IW+99
      READ(8,30) A,B,((DATA(I,K),I=1,12),K=IW,IWW)
   50 IW=IW+100
      I9=IS2+W2L/DI+.5
      DO 70 I=1,12
      SUM=0.
      IF(NULL(I)) 55,55,58
   55 WT(I)=0.
      WRITE(6,56) I
   56 FORMAT (' ', 10X, 'CHANNEL',I4,5X,'          SIGNAL TO NOISE RATIO
     XNOT CALCULATED' )
      GO TO 70
   58 DO 60 K=IS2,I9
   60 SUM=SUM+DATA(I,K)*DATA(I,K)
      SUM=SUM/(I9-IS2)
C
C     CALCULATES THE STATISTICAL SIGNAL TO NOISE RATIO
C
   69 SNRAT = SQRT(SUM/WT(I) - 1.)
```

```
C
C       CALCULATES A WEIGHTING FACTOR DIRECTLY PROPORTIONAL TO THE S/N
C       RATIO AND INVERSLY PROPORTIONAL TO THE AMPLITUDE OF THE NOISE
C
        WT(I)=SNRAT/SQRT(WT(I))
        WRITE(6,71) I,SNRAT
  71    FORMAT (' ',10X,'CHANNEL',I4,5X,'SIGNAL TO NOISE RATIO',F12.4 )
        WRITE(6,72) WT(I)
  72    FORMAT (' ','WEIGHT IS',F12.3)
70      CONTINUE
        SUM=0.
C
C       NORMALIZES THE WEIGHTING FACTORS
C
        DO 80 J=1,12
  80    SUM = SUM + WT(J)
        SUM = 3./SUM
        WTMAX = 0.
        DO 90 J=1,12
        WT(J) = WT(J)/SUM
        IF(WT(J).GT.WTMAX) WTMAX=WT(J)
  90    CONTINUE
        DO 91 I=1,12
        IF(WTMAX.LE.5.) GO TO 91
        WT(I) = WT(I)/WTMAX*5.
  91    WRITE (6,100) I,WT(I)
  100   FORMAT (' ',10X,'CHANNEL',I4,5X,'WEIGHTING FACTOR',F8.4 )
        REWIND 8
        RETURN
        END

        SUBROUTINE SEARCH (IR,IB)
        INTEGER*2 A,B
        DO 100 I=1,7000
        READ(8,30) A,B
30      FORMAT(2A2)
        IF(A.EQ.IR.AND.B.EQ.IB) GO TO 15
100     CONTINUE
15      BACKSPACE 8
        RETURN
        END
        SUBROUTINE TIME (TRACE,II)
        INTEGER*2 TRACE (4100)
        DI=.0017143
        DO 510 JJ = 1,II
510     TRACE(JJ)=0
        N45=II*DI*10
        N46=II*DI+1
        DO 370 I=1,N45
        K=(.1/DI)*I+.5
370     TRACE(K)= 10
        DO 380 I=1,N46
        K=(1./DI)*I+.5
380     TRACE(K)= 25
        RETURN
        END
```

APPENDIX C

Sample Calculation of Relative Shifts

```
      $JOB   WATFIV     R. SANTOS
 1           DIMENSION V(12),NULL(12),ID(12),VR(12),RR(12)
 2           READ 10, D,A,(NULL(I),I=1,12)
 3        10 FORMAT (2F6.3,2X,12I1)
 4           DO 1 I = 1,99
 5           DO 2 IK=4,12
 6           IF(NULL(IK).EQ.0) GO TO 2
 7           P=A*.0174533
 8           ID(IK)=I
 9           V(IK) = D*(IK-1)*COS(P)/ID(IK)/.0017143
10           RR(IK) = (IK-1)/12. *.0017143 + I
11           VR(IK) = (IK-1)*D*COS(P)/RR(IK)/.0017143
12        2  CONTINUE
13           PRINT 11, ID(4),V(4),VR(4),ID(5),V(5),VR(5),ID(6),V(6),VR(6),
            CID(7),V(7),VR(7),ID(8),V(8),VR(8),ID(9),V(9),VR(9),
            CID(12),V(12),VR(12)
14        11 FORMAT (' ',7(1X,I2,2(F7.2)))
15        1  CONTINUE
16           STOP
17           END
```

$\theta = 6^\circ$

$k(9)$ v $\bar{v}_g$

AVERAGE EFFECTIVE APPARENT VELOCITY

70.69 KM/SEC

$ENTRY

	Ch. 4		Ch. 5		Ch. 6		Ch. 7		Ch. 8		Ch. 9		Ch. 12	
1	229.73	183.79	306.31	229.73	382.89	270.27	459.47	306.31	536.04	338.55	612.62	367.57	842.35	439.49
2	114.87	102.10	153.16	131.28	191.44	158.44	229.73	183.79	268.02	207.50	306.31	229.73	421.18	288.81
3	76.58	70.69	102.10	91.89	127.63	112.06	153.16	131.28	178.68	149.59	204.21	167.08	280.78	215.07
4	57.43	54.05	76.58	70.69	95.72	86.69	114.87	102.10	134.01	116.95	153.16	131.28	210.59	171.33
5	45.95	43.76	61.26	57.43	76.58	70.69	91.89	83.54	107.21	96.01	122.52	108.11	168.47	142.37
6	38.29	36.76	51.05	48.36	63.81	59.67	76.58	70.69	89.34	81.42	102.10	91.89	140.39	121.79
7	32.82	31.69	43.76	41.77	54.70	51.63	65.64	61.26	76.58	70.69	87.52	79.91	120.34	106.40
8	28.72	27.85	38.29	36.76	47.86	45.49	57.43	54.05	67.01	62.45	76.58	70.69	105.29	94.47
9	25.53	24.84	34.03	32.82	42.54	40.66	51.05	48.36	59.56	55.93	66.07	63.37	93.59	84.64
10	22.97	22.41	30.63	29.64	38.29	36.76	45.95	43.76	53.60	50.65	61.26	57.43	84.24	77.16
11	20.88	20.42	27.85	27.03	34.81	33.54	41.77	39.95	48.73	46.28	55.69	52.51	76.58	70.49
12	19.14	18.75	25.53	24.84	31.91	30.84	38.29	36.76	44.67	42.60	51.05	48.36	70.20	65.21
13	17.67	17.34	23.56	22.97	29.45	28.54	35.34	34.03	41.23	39.46	47.12	44.83	64.80	60.53
14	16.41	16.12	21.88	21.37	27.35	26.56	32.82	31.69	38.29	36.76	43.76	41.77	60.17	56.47
15	15.32	15.06	20.42	19.98	25.53	24.84	30.63	29.64	35.74	34.40	40.84	39.10	56.16	52.92
16	14.36	14.14	19.14	18.75	23.93	23.32	28.72	27.85	33.50	32.32	38.29	36.76	52.65	49.79
17	13.51	13.32	18.02	17.67	22.52	21.98	27.03	26.26	31.53	30.49	36.04	34.68	49.55	47.02
18	12.76	12.59	17.02	16.71	21.27	20.79	25.53	24.84	29.78	28.85	34.03	32.82	46.80	44.53
19	12.09	11.93	16.12	15.84	20.15	19.72	24.18	23.56	28.21	27.37	32.24	31.15	44.33	42.29
20	11.49	11.34	15.32	15.06	19.14	18.75	22.97	22.41	26.80	26.04	30.63	29.64	42.12	40.27
21	10.94	10.81	14.59	14.36	18.23	17.88	21.88	21.37	25.53	24.84	29.17	28.27	40.11	38.43
22	10.44	10.33	13.92	13.72	17.40	17.08	20.88	20.42	24.37	23.74	27.85	27.03	38.29	36.76
23	9.99	9.88	13.32	13.13	16.65	16.35	19.98	19.55	23.31	22.77	26.64	25.89	36.62	35.22
24	9.57	9.47	12.76	12.59	15.95	15.68	19.14	18.75	22.34	21.81	25.53	24.84	35.10	33.81
25	9.19	9.10	12.25	12.09	15.32	15.06	18.38	18.02	21.44	20.95	24.50	23.87	33.69	32.50
26	8.84	8.75	11.78	11.63	14.73	14.49	17.67	17.34	20.62	20.16	23.56	22.97	32.40	31.29
27	8.51	8.43	11.34	11.21	14.18	13.97	17.02	16.71	19.85	19.43	22.69	22.14	31.20	30.17
28	8.20	8.13	10.94	10.81	13.67	13.47	16.41	16.12	19.14	18.75	21.88	21.37	30.08	29.13
29	7.92	7.85	10.56	10.44	13.20	13.02	15.84	15.58	18.48	18.12	21.12	20.65	29.05	28.16
30	7.66	7.59	10.21	10.10	12.76	12.59	15.32	15.06	17.87	17.53	20.42	19.98	28.08	27.25
31	7.41	7.35	9.88	9.78	12.35	12.19	14.82	14.59	17.29	16.97	19.76	19.35	27.17	26.39
32	7.18	7.12	9.57	9.47	11.97	11.81	14.36	14.14	16.75	16.45	19.14	18.75	26.32	25.59
33	6.96	6.91	9.28	9.19	11.60	11.46	13.92	13.72	16.24	15.96	18.56	18.20	25.53	24.84
34	6.76	6.71	9.01	8.92	11.26	11.13	13.51	13.32	15.77	15.50	18.02	17.67	24.78	24.12
35	6.56	6.52	8.75	8.67	10.94	10.81	13.13	12.94	15.32	15.06	17.50	17.18	24.07	23.45
36	6.38	6.34	8.51	8.43	10.64	10.51	12.76	12.59	14.89	14.65	17.02	16.71	23.40	22.82
37	6.21	6.17	8.28	8.20	10.35	10.23	12.42	12.25	14.49	14.26	16.56	16.26	22.77	22.22
38	6.05	6.01	8.06	7.99	10.08	9.97	12.09	11.93	14.11	13.89	16.12	15.84	22.17	21.65
39	5.89	5.85	7.85	7.79	9.82	9.71	11.78	11.63	13.74	13.54	15.71	15.44	21.60	21.10
40	5.74	5.71	7.66	7.59	9.57	9.47	11.49	11.34	13.40	13.21	15.32	15.06	21.06	20.59
41	5.60	5.57	7.47	7.41	9.34	9.24	11.21	11.07	13.07	12.89	14.94	14.70	20.55	20.10
42	5.47	5.44	7.29	7.24	9.12	9.03	10.94	10.81	12.76	12.59	14.59	14.36	20.06	19.63
43	5.34	5.31	7.12	7.07	8.90	8.82	10.69	10.56	12.47	12.30	14.25	14.03	19.59	19.18
44	5.22	5.19	6.96	6.91	8.70	8.62	10.44	10.33	12.18	12.02	13.92	13.72	19.14	18.75

45	5.11	5.08	45	6.81	6.76	45	8.51	8.43	45	10.21	10.10	45	11.91	11.76	45	13.61	13.42	45	18.72	18.35
46	4.99	4.97	46	6.66	6.61	46	8.32	8.25	46	9.99	9.88	46	11.65	11.51	46	13.32	13.13	46	18.31	17.95
47	4.89	4.86	47	6.52	6.47	47	8.15	8.07	47	9.78	9.67	47	11.41	11.27	47	13.03	12.85	47	17.92	17.58
48	4.79	4.76	48	6.38	6.34	48	7.98	7.91	48	9.57	9.47	48	11.17	11.03	48	12.76	12.59	48	17.55	17.22
49	4.69	4.66	49	6.25	6.21	49	7.81	7.75	49	9.38	9.28	49	10.94	10.81	49	12.50	12.33	49	17.19	16.88
50	4.59	4.57	50	6.13	6.09	50	7.66	7.59	50	9.19	9.10	50	10.72	10.60	50	12.25	12.09	50	16.85	16.54
51	4.50	4.48	51	6.01	5.97	51	7.51	7.45	51	9.01	8.92	51	10.51	10.39	51	12.01	11.86	51	16.52	16.23
52	4.42	4.40	52	5.89	5.85	52	7.36	7.30	52	8.84	8.75	52	10.31	10.19	52	11.78	11.63	52	16.20	15.92
53	4.33	4.31	53	5.78	5.74	53	7.22	7.17	53	8.67	8.59	53	10.11	10.00	53	11.56	11.42	53	15.89	15.62
54	4.25	4.23	54	5.67	5.64	54	7.09	7.04	54	8.51	8.43	54	9.93	9.82	54	11.34	11.21	54	15.60	15.34
55	4.18	4.16	55	5.57	5.54	55	6.96	6.91	55	8.35	8.28	55	9.75	9.64	55	11.14	11.01	55	15.32	15.06
56	4.10	4.08	56	5.47	5.44	56	6.84	6.79	56	8.20	8.13	56	9.57	9.47	56	10.94	10.81	56	15.04	14.80
57	4.03	4.01	57	5.37	5.34	57	6.72	6.67	57	8.06	7.99	57	9.40	9.31	57	10.75	10.62	57	14.78	14.54
58	3.96	3.94	58	5.28	5.25	58	6.60	6.55	58	7.92	7.85	58	9.24	9.15	58	10.56	10.44	58	14.52	14.30
59	3.89	3.88	59	5.19	5.16	59	6.49	6.44	59	7.79	7.72	59	9.09	9.00	59	10.38	10.27	59	14.28	14.06
60	3.83	3.81	60	5.11	5.08	60	6.38	6.34	60	7.66	7.59	60	8.93	8.85	60	10.21	10.10	60	14.04	13.83
61	3.77	3.75	61	5.02	4.99	61	6.28	6.23	61	7.53	7.47	61	8.79	8.70	61	10.04	9.93	61	13.81	13.60
62	3.71	3.69	62	4.94	4.91	62	6.18	6.13	62	7.41	7.35	62	8.65	8.57	62	9.88	9.78	62	13.59	13.39
63	3.65	3.63	63	4.86	4.84	63	6.08	6.04	63	7.29	7.24	63	8.51	8.43	63	9.72	9.62	63	13.37	13.18
64	3.59	3.58	64	4.79	4.76	64	5.98	5.94	64	7.18	7.12	64	8.38	8.30	64	9.57	9.47	64	13.16	12.98
65	3.53	3.52	65	4.71	4.69	65	5.89	5.85	65	7.07	7.01	65	8.25	8.17	65	9.42	9.33	65	12.96	12.78
66	3.48	3.47	66	4.64	4.62	66	5.80	5.76	66	6.96	6.91	66	8.12	8.05	66	9.28	9.19	66	12.76	12.59
67	3.43	3.42	67	4.57	4.55	67	5.71	5.68	67	6.86	6.81	67	8.00	7.93	67	9.14	9.05	67	12.57	12.40
68	3.38	3.37	68	4.50	4.48	68	5.63	5.60	68	6.76	6.71	68	7.88	7.82	68	9.01	8.92	68	12.39	12.22
69	3.33	3.32	69	4.44	4.42	69	5.55	5.52	69	6.66	6.61	69	7.77	7.70	69	8.88	8.79	69	12.21	12.05
70	3.28	3.27	70	4.38	4.36	70	5.47	5.44	70	6.56	6.52	70	7.66	7.59	70	8.75	8.67	70	12.03	11.88
71	3.24	3.22	71	4.31	4.29	71	5.39	5.36	71	6.47	6.43	71	7.55	7.49	71	8.63	8.55	71	11.86	11.71
72	3.19	3.18	72	4.25	4.23	72	5.32	5.29	72	6.38	6.34	72	7.45	7.39	72	8.51	8.43	72	11.70	11.55
73	3.15	3.14	73	4.20	4.18	73	5.25	5.22	73	6.29	6.25	73	7.34	7.28	73	8.39	8.32	73	11.54	11.40
74	3.10	3.09	74	4.14	4.12	74	5.17	5.15	74	6.21	6.17	74	7.24	7.19	74	8.28	8.20	74	11.38	11.24
75	3.06	3.05	75	4.08	4.07	75	5.11	5.08	75	6.13	6.09	75	7.15	7.09	75	8.17	8.10	75	11.23	11.10
76	3.02	3.01	76	4.03	4.01	76	5.04	5.01	76	6.05	6.01	76	7.05	7.00	76	8.06	7.99	76	11.08	10.95
77	2.98	2.97	77	3.98	3.96	77	4.97	4.95	77	5.97	5.93	77	6.96	6.91	77	7.96	7.89	77	10.94	10.81
78	2.95	2.94	78	3.93	3.91	78	4.91	4.88	78	5.89	5.85	78	6.87	6.82	78	7.85	7.79	78	10.80	10.67
79	2.91	2.90	79	3.88	3.86	79	4.85	4.82	79	5.82	5.78	79	6.79	6.74	79	7.75	7.69	79	10.66	10.54
80	2.87	2.86	80	3.83	3.81	80	4.79	4.76	80	5.74	5.71	80	6.70	6.65	80	7.66	7.59	80	10.53	10.41
81	2.84	2.83	81	3.78	3.77	81	4.73	4.70	81	5.67	5.64	81	6.62	6.57	81	7.56	7.50	81	10.40	10.28
82	2.80	2.79	82	3.74	3.72	82	4.67	4.65	82	5.60	5.57	82	6.54	6.49	82	7.47	7.41	82	10.27	10.16
83	2.77	2.76	83	3.69	3.68	83	4.61	4.59	83	5.54	5.50	83	6.46	6.41	83	7.38	7.32	83	10.15	10.04
84	2.73	2.73	84	3.65	3.63	84	4.56	4.54	84	5.47	5.44	84	6.38	6.34	84	7.29	7.24	84	10.03	9.92
85	2.70	2.69	85	3.60	3.59	85	4.50	4.48	85	5.41	5.37	85	6.31	6.26	85	7.21	7.15	85	9.91	9.80
86	2.67	2.66	86	3.56	3.55	86	4.45	4.43	86	5.34	5.31	86	6.23	6.19	86	7.12	7.07	86	9.79	9.69
87	2.64	2.63	87	3.52	3.51	87	4.40	4.38	87	5.28	5.25	87	6.16	6.12	87	7.04	6.99	87	9.68	9.58
88	2.61	2.60	88	3.48	3.47	88	4.35	4.33	88	5.22	5.19	88	6.09	6.05	88	6.96	6.91	88	9.57	9.47
89	2.58	2.57	89	3.44	3.43	89	4.30	4.28	89	5.16	5.13	89	6.02	5.98	89	6.88	6.83	89	9.46	9.37
90	2.55	2.55	90	3.40	3.39	90	4.25	4.23	90	5.11	5.08	90	5.96	5.92	90	6.81	6.76	90	9.36	9.27
91	2.52	2.52	91	3.37	3.35	91	4.21	4.19	91	5.05	5.02	91	5.89	5.85	91	6.73	6.68	91	9.26	9.16
92	2.50	2.49	92	3.33	3.32	92	4.16	4.14	92	4.99	4.97	92	5.83	5.79	92	6.66	6.61	92	9.16	9.07
93	2.47	2.46	93	3.29	3.28	93	4.12	4.10	93	4.94	4.91	93	5.76	5.73	93	6.59	6.54	93	9.06	8.97
94	2.44	2.44	94	3.26	3.25	94	4.07	4.06	94	4.89	4.86	94	5.70	5.67	94	6.52	6.47	94	8.96	8.87
95	2.42	2.41	95	3.22	3.21	95	4.03	4.01	95	4.84	4.81	95	5.64	5.61	95	6.45	6.40	95	8.87	8.78
96	2.39	2.39	96	3.19	3.18	96	3.99	3.97	96	4.79	4.76	96	5.58	5.55	96	6.38	6.34	96	8.77	8.69
97	2.37	2.36	97	3.16	3.15	97	3.95	3.93	97	4.74	4.71	97	5.53	5.49	97	6.32	6.27	97	8.68	8.60
98	2.34	2.34	98	3.13	3.12	98	3.91	3.89	98	4.69	4.66	98	5.47	5.44	98	6.25	6.21	98	8.60	8.52
99	2.32	2.31	99	3.09	3.08	99	3.87	3.85	99	4.64	4.62	99	5.41	5.38	99	6.19	6.15	99	8.51	8.43

$\theta = 6°$

15.06 KM/SEC

8.43 KM/SEC

CORE USAGE OBJECT CODE= 1312 BYTES, ARRAY AREA= 240 BYTES, TOTAL AREA AVAILABLE= 102400 BYTES

DIAGNOSTICS NUMBER OF ERRORS= 0, NUMBER OF WARNINGS= 0, NUMBER OF EXTENSIONS= 0

COMPILE TIME= 0.14 SEC, EXECUTION TIME= 1.34 SEC, WATFIV - JUL 1973 V1L4 13.53.44 MONDAY 3 NOV 75

```
      $JOB  WATFIV    R. SANTOS
 1          DIMENSION V(12),NULL(12),ID(12),VR(12),RR(12)
 2          READ 10, D,A,(NULL(I),I=1,12)
 3       10 FORMAT (2F6.3,2X,12I1)
 4          DO 1 I = 1,99
 5          DO 2 IK=4,12
 6          IF(NULL(IK).EQ.0) GO TO 2
 7          P=A*.0174533
 8          ID(IK)=I
 9          V(IK) = D*(IK-1)*COS(P)/ID(IK)/.0017143
10          RR(IK) = (IK-1)/12. * .0017143 +
11          VR(IK) = (IK-1)*D*COS(P)/RR(IK)/.0017143
12       2  CONTINUE
13          PRINT 11, ID(4),V(4),VR(4),ID(5),V(5),VR(5),ID(6),V(6),VR(6),
           CID(7),V(7),VR(7),ID(8),V(8),VR(8),ID(9),V(9),VR(9),
           CID(12),V(12),VR(12)
14       11 FORMAT (' ',7(1X,I2,2(F7.2)))
15       1  CONTINUE
16          STOP
17          END
```

$\theta = 23°$

$ENTRY

1	212.63	170.11	1	283.51	212.63	1	354.39	250.16	1	425.27	283.51	1	496.15	313.36	1	567.03	340.22	1	779.66	406.78			
2	106.32	94.50	2	141.76	121.51	2	177.20	146.64	2	212.63	170.11	2	248.07	192.06	2	283.51	212.63	2	389.83	267.31			
3	70.88	65.43	3	94.50	85.05	3	118.13	103.72	3	141.76	121.51	3	165.38	138.46	3	189.01	154.64	3	259.89	199.06			
4	53.16	50.03	4	70.88	65.43	4	88.60	80.24	4	106.32	94.50	4	124.04	108.25	4	141.76	121.51	4	194.92	158.57			
5	42.53	40.50	5	56.70	53.16	5	70.88	65.43	5	85.05	77.32	5	99.23	88.86	5	113.41	100.06	5	155.93	131.77			
6	35.44	34.02	6	47.25	44.77	6	59.07	55.23	6	70.88	66.43	6	82.69	75.36	6	94.50	85.05	6	129.94	112.72			
7	30.38	29.33	7	40.50	38.66	7	50.63	47.78	7	60.75	56.70	7	70.88	65.43	7	81.00	73.96	7	111.38	96.48			
8	26.58	25.77	8	35.44	34.02	8	44.30	42.11	8	53.16	50.03	8	62.02	57.80	8	70.88	65.43	8	97.46	87.44			
9	23.63	22.99	9	31.50	30.38	9	39.38	37.63	9	47.25	44.77	9	55.13	51.77	9	63.00	58.66	9	86.63	78.62			
10	21.26	20.74	10	28.35	27.44	10	35.44	34.02	10	42.53	40.50	10	49.61	46.88	10	56.70	53.16	10	77.97	71.42			
11	19.33	18.90	11	25.77	25.02	11	32.22	31.04	11	38.66	36.98	11	45.10	42.83	11	51.55	48.60	11	70.88	65.43			
12	17.72	17.36	12	23.63	22.99	12	29.53	28.54	12	35.44	34.02	12	41.35	39.43	12	47.25	44.77	12	64.97	60.36			
13	16.36	16.05	13	21.81	21.26	13	27.26	26.41	13	32.71	31.50	13	38.17	36.53	13	43.62	41.49	13	59.97	56.02			
14	15.19	14.92	14	20.25	19.78	14	25.31	24.58	14	30.38	29.33	14	35.44	34.02	14	40.50	38.66	14	55.69	52.27			
15	14.18	13.44	15	18.90	18.49	15	23.63	22.99	15	28.35	27.44	15	33.08	31.64	15	37.80	36.19	15	51.98	48.98			
16	13.29	13.09	16	17.72	17.36	16	22.15	21.59	16	26.58	25.77	16	31.01	29.92	16	35.44	34.02	16	48.73	46.09			
17	12.51	12.33	17	16.68	16.36	17	20.85	20.35	17	25.02	24.30	17	29.19	28.22	17	33.35	32.10	17	45.86	43.52			
18	11.81	11.65	18	15.75	15.46	18	19.69	19.24	18	23.63	22.99	18	27.56	26.70	18	31.50	30.38	18	43.31	41.22			
19	11.19	11.05	19	14.92	14.66	19	18.65	18.25	19	22.38	21.81	19	26.11	25.34	19	29.84	28.83	19	41.03	39.15			
20	10.63	10.50	20	14.18	13.94	20	17.72	17.36	20	21.26	20.74	20	24.81	24.10	20	28.35	27.44	20	38.98	37.27			
21	10.13	10.01	21	13.50	13.29	21	16.88	16.55	21	20.25	19.78	21	23.63	22.99	21	27.00	26.17	21	37.13	35.57			
22	9.67	9.56	22	12.89	12.69	22	16.11	15.81	22	19.33	18.90	22	22.55	21.97	22	25.77	25.02	22	35.44	34.02			
23	9.24	9.15	23	12.33	12.15	23	15.41	15.13	23	18.49	18.10	23	21.57	21.04	23	24.65	23.96	23	33.90	32.60			
24	8.86	8.77	24	11.81	11.65	24	14.77	14.51	24	17.72	17.36	24	20.67	20.18	24	23.63	22.99	24	32.49	31.29			
25	8.51	8.42	25	11.34	11.19	25	14.18	13.94	25	17.01	16.68	25	19.85	19.39	25	22.68	22.09	25	31.19	30.08			
26	8.18	8.10	26	10.90	10.77	26	13.63	13.42	26	16.36	16.05	26	19.08	18.66	26	21.81	21.26	26	29.99	28.97			
27	7.88	7.80	27	10.50	10.37	27	13.13	12.93	27	15.75	15.46	27	18.38	17.99	27	21.00	20.49	27	28.88	27.93			
28	7.59	7.53	28	10.13	10.01	28	12.66	12.47	28	15.19	14.92	28	17.72	17.36	28	20.25	19.78	28	27.85	26.96			
29	7.33	7.27	29	9.78	9.67	29	12.22	12.05	29	14.66	14.42	29	17.11	16.77	29	19.55	19.11	29	26.88	26.06			
30	7.09	7.03	30	9.45	9.35	30	11.81	11.65	30	14.18	13.94	30	16.54	16.22	30	18.90	18.49	30	25.99	25.22			
31	6.86	6.80	31	9.15	9.05	31	11.43	11.28	31	13.72	13.50	31	16.00	15.71	31	18.29	17.91	31	25.15	24.43			
32	6.64	6.59	32	8.86	8.77	32	11.07	10.93	32	13.29	13.09	32	15.50	15.23	32	17.72	17.36	32	24.36	23.69			
33	6.44	6.40	33	8.59	8.51	33	10.74	10.61	33	12.89	12.69	33	15.03	14.77	33	17.18	16.84	33	23.63	22.99			
34	6.25	6.21	34	8.34	8.26	34	10.42	10.30	34	12.51	12.33	34	14.59	14.35	34	16.68	16.36	34	22.93	22.33			
35	6.08	6.03	35	8.10	8.02	35	10.13	10.01	35	12.15	11.98	35	14.18	13.94	35	16.20	15.90	35	22.28	21.71			
36	5.91	5.87	36	7.88	7.80	36	9.84	9.73	36	11.81	11.65	36	13.78	13.56	36	15.75	15.46	36	21.66	21.12			
37	5.75	5.71	37	7.66	7.59	37	9.58	9.47	37	11.49	11.34	37	13.41	13.20	37	15.33	15.05	37	21.07	20.56			
38	5.60	5.56	38	7.46	7.40	38	9.33	9.22	38	11.19	11.05	38	13.06	12.86	38	14.92	14.66	38	20.52	20.03			
39	5.45	5.42	39	7.27	7.21	39	9.09	8.99	39	10.90	10.77	39	12.72	12.53	39	14.54	14.29	39	19.99	19.53			
40	5.32	5.28	40	7.09	7.03	40	8.86	8.77	40	10.63	10.50	40	12.40	12.23	40	14.18	13.94	40	19.49	19.05			
41	5.19	5.15	41	6.91	6.86	41	8.64	8.56	41	10.37	10.25	41	12.10	11.93	41	13.83	13.61	41	19.02	18.60			
42	5.06	5.03	42	6.75	6.70	42	8.44	8.36	42	10.13	10.01	42	11.81	11.65	42	13.50	13.29	42	18.56	18.17			
43	4.94	4.92	43	6.59	6.54	43	8.24	8.16	43	9.89	9.78	43	11.54	11.38	43	13.19	12.99	43	18.13	17.75			
44	4.83	4.81	44	6.44	6.40	44	8.05	7.98	44	9.67	9.56	44	11.28	11.13	44	12.89	12.69	44	17.72	17.36			

68.92 KM/SEC

45	4.73	4.70	45	6.30	6.25	45	7.88	7.80	45	9.45	9.35	45	11.03	10.88	45	12.60	12.42	45	17.33	16.98
46	4.62	4.60	46	6.16	6.12	46	7.70	7.64	46	9.24	9.15	46	10.79	10.65	46	12.33	12.15	46	16.95	16.62
47	4.52	4.50	47	6.03	5.99	47	7.54	7.47	47	9.05	8.95	47	10.56	10.43	47	12.06	11.90	47	16.59	16.27
48	4.43	4.41	48	5.91	5.87	48	7.38	7.32	48	8.86	8.77	48	10.34	10.21	48	11.81	11.65	48	16.24	15.94
49	4.34	4.32	49	5.79	5.75	49	7.23	7.17	49	8.68	8.59	49	10.13	10.01	49	11.57	11.42	49	15.91	15.62
50	4.25	4.23	50	5.67	5.63	50	7.09	7.03	50	8.51	8.42	50	9.92	9.81	50	11.34	11.19	50	15.59	15.31
51	4.17	4.15	51	5.56	5.52	51	6.95	6.89	51	8.34	8.26	51	9.73	9.62	51	11.12	10.97	51	15.29	15.02
52	4.09	4.07	52	5.46	5.42	52	6.82	6.76	52	8.18	8.10	52	9.54	9.44	52	10.90	10.77	52	14.99	14.73
53	4.01	3.99	53	5.35	5.32	53	6.69	6.63	53	8.02	7.95	53	9.36	9.26	53	10.70	10.57	53	14.71	14.46
54	3.94	3.92	54	5.25	5.22	54	6.56	6.51	54	7.88	7.80	54	9.19	9.09	54	10.50	10.37	54	14.44	14.20
55	3.87	3.85	55	5.15	5.12	55	6.44	6.40	55	7.73	7.66	55	9.02	8.93	55	10.31	10.19	55	14.18	13.94
56	3.80	3.78	56	5.06	5.03	56	6.33	6.28	56	7.59	7.53	56	8.86	8.77	56	10.13	10.01	56	13.92	13.70
57	3.73	3.71	57	4.97	4.94	57	6.22	6.17	57	7.46	7.40	57	8.70	8.62	57	9.95	9.83	57	13.68	13.46
58	3.67	3.65	58	4.89	4.86	58	6.11	6.07	58	7.33	7.27	58	8.55	8.47	58	9.78	9.67	58	13.44	13.23
59	3.60	3.59	59	4.81	4.78	59	6.01	5.96	59	7.21	7.15	59	8.41	8.33	59	9.61	9.50	59	13.21	13.01
60	3.54	3.53	60	4.73	4.70	60	5.91	5.87	60	7.09	7.03	60	8.27	8.19	60	9.45	9.35	60	12.99	12.80
61	3.49	3.47	61	4.65	4.62	61	5.81	5.77	61	6.97	6.91	61	8.13	8.06	61	9.30	9.20	61	12.78	12.59
62	3.43	3.42	62	4.57	4.55	62	5.72	5.68	62	6.86	6.80	62	8.00	7.93	62	9.15	9.05	62	12.58	12.39
63	3.38	3.36	63	4.50	4.48	63	5.63	5.59	63	6.75	6.70	63	7.88	7.80	63	9.00	8.91	63	12.38	12.20
64	3.32	3.31	64	4.43	4.41	64	5.54	5.50	64	6.64	6.59	64	7.75	7.68	64	8.86	8.77	64	12.18	12.01
65	3.27	3.26	65	4.36	4.34	65	5.45	5.42	65	6.54	6.49	65	7.63	7.57	65	8.72	8.63	65	11.99	11.83
66	3.22	3.21	66	4.30	4.27	66	5.37	5.34	66	6.44	6.40	66	7.52	7.45	66	8.59	8.51	66	11.81	11.65
67	3.17	3.16	67	4.23	4.21	67	5.29	5.26	67	6.35	6.30	67	7.41	7.34	67	8.46	8.38	67	11.64	11.48
68	3.13	3.12	68	4.17	4.15	68	5.21	5.18	68	6.25	6.21	68	7.30	7.23	68	8.34	8.26	68	11.47	11.31
69	3.08	3.07	69	4.11	4.09	69	5.14	5.11	69	6.16	6.12	69	7.19	7.13	69	8.22	8.14	69	11.30	11.15
70	3.04	3.03	70	4.05	4.03	70	5.06	5.03	70	6.08	6.03	70	7.09	7.03	70	8.10	8.02	70	11.14	10.99
71	2.99	2.98	71	3.99	3.97	71	4.99	4.96	71	5.99	5.95	71	6.99	6.93	71	7.99	7.91	71	10.98	10.84
72	2.95	2.94	72	3.94	3.92	72	4.92	4.89	72	5.91	5.87	72	6.89	6.84	72	7.88	7.80	72	10.83	10.69
73	2.91	2.90	73	3.88	3.87	73	4.85	4.83	73	5.83	5.79	73	6.80	6.74	73	7.77	7.70	73	10.68	10.55
74	2.87	2.86	74	3.83	3.81	74	4.79	4.76	74	5.75	5.71	74	6.70	6.65	74	7.66	7.59	74	10.54	10.41
75	2.84	2.83	75	3.78	3.76	75	4.73	4.70	75	5.67	5.63	75	6.62	6.56	75	7.56	7.49	75	10.40	10.27
76	2.80	2.79	76	3.73	3.71	76	4.66	4.64	76	5.60	5.56	76	6.53	6.48	76	7.46	7.40	76	10.26	10.14
77	2.76	2.75	77	3.68	3.67	77	4.60	4.58	77	5.52	5.49	77	6.44	6.40	77	7.36	7.30	77	10.13	10.01
78	2.73	2.72	78	3.63	3.62	78	4.54	4.52	78	5.45	5.42	78	6.36	6.31	78	7.27	7.21	78	10.00	9.88
79	2.69	2.68	79	3.59	3.57	79	4.49	4.46	79	5.38	5.35	79	6.28	6.23	79	7.18	7.12	79	9.87	9.76
80	2.66	2.65	80	3.54	3.53	80	4.43	4.41	80	5.32	5.28	80	6.20	6.16	80	7.09	7.03	80	9.75	9.64
81	2.63	2.62	81	3.50	3.49	81	4.38	4.35	81	5.25	5.22	81	6.13	6.08	81	7.00	6.94	81	9.63	9.52
82	2.59	2.59	82	3.46	3.44	82	4.32	4.30	82	5.19	5.15	82	6.05	6.01	82	6.91	6.86	82	9.51	9.40
83	2.56	2.55	83	3.42	3.40	83	4.27	4.25	83	5.12	5.09	83	5.98	5.94	83	6.83	6.78	83	9.39	9.29
84	2.53	2.52	84	3.38	3.36	84	4.22	4.20	84	5.06	5.03	84	5.91	5.87	84	6.75	6.70	84	9.28	9.18
85	2.50	2.49	85	3.34	3.32	85	4.17	4.15	85	5.00	4.97	85	5.84	5.80	85	6.67	6.62	85	9.17	9.07
86	2.47	2.47	86	3.30	3.28	86	4.12	4.10	86	4.94	4.92	86	5.77	5.73	86	6.59	6.54	86	9.07	8.97
87	2.44	2.44	87	3.26	3.25	87	4.07	4.05	87	4.89	4.86	87	5.70	5.66	87	6.52	6.47	87	8.96	8.87
88	2.42	2.41	88	3.22	3.21	88	4.03	4.01	88	4.83	4.81	88	5.64	5.60	88	6.44	6.40	88	8.86	8.77
89	2.39	.38	89	3.19	3.17	89	3.98	3.96	89	4.78	4.75	89	5.57	5.54	89	6.37	6.32	89	8.76	8.67
90	2.36	.36	90	3.15	3.14	90	3.94	3.92	90	4.73	4.70	90	5.51	5.48	90	6.30	6.25	90	8.66	8.58
91	2.34	2.33	91	3.12	3.10	91	3.89	3.88	91	4.67	4.65	91	5.45	5.42	91	6.23	6.19	91	8.57	8.48
92	2.31	2.30	92	3.08	3.07	92	3.85	3.83	92	4.62	4.60	92	5.39	5.36	92	6.16	6.12	92	8.47	8.39
93	2.29	2.28	93	3.05	3.04	93	3.81	3.79	93	4.57	4.55	93	5.33	5.30	93	6.10	6.05	93	8.38	8.30
94	2.26	2.26	94	3.02	3.01	94	3.77	3.75	94	4.52	4.50	94	5.28	5.25	94	6.03	5.99	94	8.29	8.21
95	2.24	2.23	95	2.98	2.97	95	3.73	3.71	95	4.48	4.45	95	5.22	5.19	95	5.97	5.93	95	8.21	8.13
96	2.21	2.21	96	2.95	2.94	96	3.69	3.68	96	4.43	4.41	96	5.17	5.14	96	5.91	5.87	96	8.12	8.04
97	2.19	2.19	97	2.92	2.91	97	3.65	3.64	97	4.38	4.36	97	5.11	5.08	97	5.85	5.81	97	8.04	7.96
98	2.17	2.16	98	2.89	2.88	98	3.62	3.60	98	4.34	4.32	98	5.06	5.03	98	5.79	5.75	98	7.96	7.88
99	2.15	2.14	99	2.86	2.85	99	3.58	3.56	99	4.30	4.27	99	5.01	4.98	99	5.73	5.69	99	7.88	7.80

$\theta = 23^\circ$

15.10 KM/SEC

8.42 KM/SEC

CORE USAGE OBJECT CODE= 1312 BYTES, ARRAY AREA= 240 BYTES, TOTAL AREA AVAILABLE= 102400 BYTES

DIAGNOSTICS NUMBER OF ERRORS= 0, NUMBER OF WARNINGS= 0, NUMBER OF EXTENSIONS= 0

COMPILE TIME= 0.14 SEC, EXECUTION TIME= 1.28 SEC, WATFIV - JUL 1973 V1L4 13.56.13 MONDAY 3 NOV 75

```
      $JOB  WATFIV    R. SANTOS
 1          DIMENSION V(12),NULL(12),ID(12),VR(12),RR(12)
 2          READ 10, D,A,(NULL(I),I=1,12)
 3       10 FORMAT (2F6.3,2X,12I1)
 4          DO 1 I = 1,99
 5          DO 2 IK=4,12
 6          IF(NULL(IK).EQ.0) GO TO 2
 7          P=A*.0174533
 8          ID(IK)=I
 9          V(IK) = D*(IK-1)*COS(P)/ID(IK)/.0017143
10          RR(IK) = (IK-1)/12. *.0017143 + I
11          VR(IK) = (IK-1)*D*COS(P)/RR(IK)/.0017143
12       2  CONTINUE
13          PRINT 11, ID(4),V(4),VR(4),ID(5),V(5),VR(5),ID(6),V(6),VR(6),
           CID(7),V(7),VR(7),ID(8),V(8),VR(8),ID(9),V(9),VR(9),
           CID(12),V(12),VR(12)
14       11 FORMAT (' ',7(1X,I2,2(F7.2)))
15       1  CONTINUE
16          STOP
17          END
```

$\theta = 72^\circ$

$ENTRY

1	71.38	67.11	1	95.18	71.38	1	118.97	83.98	1	142.76	95.18	1	166.56	105.10	1	190.35	114.21	1	261.73	136.56		
2	35.69	31.73	2	47.59	40.79	2	59.49	49.23	2	71.38	57.11	2	83.28	64.47	2	95.18	71.38	2	130.87	89.74		
3	23.79	21.96	3	31.73	28.55	3	39.66	34.82	3	47.59	40.79	3	55.52	46.48	3	63.45	51.91	3	87.24	66.83		67.46 KM/SEC
4	17.85	16.80	4	23.79	21.96	4	29.74	26.94	4	35.69	31.73	4	41.64	36.34	4	47.59	40.79	4	65.43	53.23		
5	14.28	13.60	5	19.04	17.65	5	23.79	21.96	5	28.55	25.96	5	33.31	29.83	5	38.07	33.59	5	52.35	44.24		
6	11.90	11.42	6	15.86	15.03	6	19.82	18.54	6	23.79	21.96	6	27.76	25.30	6	31.73	28.55	6	43.62	37.84		
7	10.20	9.85	7	13.60	12.98	7	17.00	16.04	7	20.39	19.04	7	23.79	21.96	7	27.19	24.83	7	37.39	33.06		
8	8.92	8.65	8	11.90	11.42	8	14.87	14.14	8	17.85	16.80	8	20.82	19.40	8	23.79	21.96	8	32.72	29.35		
9	7.93	7.72	9	10.58	10.20	9	13.22	12.63	9	15.86	15.03	9	18.51	17.38	9	21.15	19.69	9	29.08	26.39		
10	7.14	6.96	10	9.52	9.21	10	11.90	11.42	10	14.28	13.60	10	16.66	15.74	10	19.04	17.85	10	26.17	23.98		
11	6.49	6.35	11	8.65	8.40	11	10.82	10.42	11	12.98	12.41	11	15.14	14.38	11	17.30	16.32	11	23.79	21.96		
12	5.95	5.83	12	7.93	7.72	12	9.91	9.58	12	11.90	11.42	12	13.88	13.24	12	15.86	15.03	12	21.81	20.26		
13	5.49	5.39	13	7.32	7.14	13	9.15	8.87	13	10.98	10.58	13	12.81	12.26	13	14.64	13.93	13	20.13	18.81		
14	5.10	5.01	14	6.80	6.64	14	8.50	8.25	14	10.20	9.85	14	11.90	11.42	14	13.60	12.98	14	18.70	17.55		
15	4.76	4.68	15	6.35	6.21	15	7.93	7.72	15	9.52	9.21	15	11.10	10.69	15	12.69	12.15	15	17.45	16.44		14.86 KM/SEC
16	4.46	4.39	16	5.95	5.83	16	7.44	7.25	16	8.92	8.65	16	10.41	10.04	16	11.90	11.42	16	16.36	15.47		
17	4.20	4.14	17	5.60	5.49	17	7.00	6.83	17	8.40	8.16	17	9.80	9.47	17	11.20	10.77	17	15.40	14.61		
18	3.97	3.91	18	5.29	5.19	18	6.61	6.46	18	7.93	7.72	18	9.25	8.96	18	10.58	10.20	18	14.54	13.94		
19	3.76	3.71	19	5.01	4.92	19	6.26	6.13	19	7.51	7.32	19	8.77	8.51	19	10.02	9.68	19	13.78	13.14		
20	3.57	3.53	20	4.76	4.69	20	5.95	5.83	20	7.14	6.96	20	8.33	8.09	20	9.52	9.21	20	13.09	12.51		
21	3.40	3.36	21	4.53	4.46	21	5.67	5.56	21	6.80	6.64	21	7.93	7.72	21	9.06	8.79	21	12.46	11.94		
22	3.24	3.21	22	4.33	4.26	22	5.41	5.31	22	6.49	6.35	22	7.57	7.38	22	8.65	8.40	22	11.90	11.42		
23	3.10	3.07	23	4.14	4.08	23	5.17	5.08	23	6.21	6.08	23	7.24	7.06	23	8.28	8.04	23	11.38	10.94		
24	2.97	2.94	24	3.97	3.91	24	4.96	4.87	24	5.95	5.83	24	6.94	6.78	24	7.93	7.72	24	10.91	10.50		
25	2.86	2.83	25	3.81	3.76	25	4.76	4.68	25	5.71	5.60	25	6.66	6.51	25	7.61	7.42	25	10.47	10.10		
26	2.75	2.72	26	3.66	3.61	26	4.58	4.50	26	5.49	5.39	26	6.41	6.27	26	7.32	7.14	26	10.07	9.72		
27	2.64	2.62	27	3.53	3.48	27	4.41	4.34	27	5.29	5.19	27	6.17	6.04	27	7.05	6.88	27	9.69	9.38		
28	2.55	2.53	28	3.40	3.36	28	4.25	4.19	28	5.10	5.01	28	5.95	5.83	28	6.80	6.64	28	9.35	9.05		
29	2.46	2.44	29	3.28	3.24	29	4.10	4.04	29	4.92	4.84	29	5.74	5.63	29	6.56	6.42	29	9.03	8.75		
30	2.38	2.36	30	3.17	3.14	30	3.97	3.91	30	4.76	4.68	30	5.55	5.45	30	6.35	6.21	30	8.72	8.47		8.51 KM/SEC
31	2.30	2.28	31	3.07	3.04	31	3.84	3.79	31	4.61	4.53	31	5.37	5.27	31	6.14	6.01	31	8.44	8.20		
32	2.23	2.21	32	2.97	2.94	32	3.72	3.67	32	4.46	4.39	32	5.20	5.11	32	5.95	5.83	32	8.18	7.95		
33	2.16	2.15	33	2.88	2.86	33	3.61	3.56	33	4.33	4.26	33	5.05	4.96	33	5.77	5.65	33	7.93	7.72		
34	2.10	2.08	34	2.80	2.77	34	3.50	3.46	34	4.20	4.14	34	4.90	4.82	34	5.60	5.49	34	7.70	7.50		
35	2.04	2.03	35	2.72	2.69	35	3.40	3.36	35	4.08	4.02	35	4.76	4.68	35	5.44	5.34	35	7.48	7.29		
36	1.98	1.97	36	2.64	2.62	36	3.30	3.27	36	3.97	3.91	36	4.63	4.56	36	5.29	5.19	36	7.27	7.09		
37	1.93	1.92	37	2.57	2.55	37	3.22	3.18	37	3.86	3.81	37	4.50	4.43	37	5.14	5.05	37	7.07	6.90		
38	1.88	1.87	38	2.50	2.48	38	3.13	3.10	38	3.76	3.71	38	4.38	4.32	38	5.01	4.92	38	6.89	6.73		
39	1.83	1.82	39	2.44	2.42	39	3.05	3.02	39	3.66	3.61	39	4.27	4.21	39	4.88	4.80	39	6.71	6.56		
40	1.78	1.77	40	2.38	2.36	40	2.97	2.94	40	3.57	3.53	40	4.16	4.10	40	4.76	4.68	40	6.54	6.40		
41	1.74	1.73	41	2.32	2.30	41	2.90	2.87	41	3.48	3.44	41	4.06	4.01	41	4.64	4.57	41	6.38	6.24		
42	1.70	1.69	42	2.27	2.25	42	2.83	2.80	42	3.40	3.36	42	3.97	3.91	42	4.53	4.46	42	6.23	6.10		
43	1.66	1.65	43	2.21	2.20	43	2.77	2.74	43	3.32	3.28	43	3.87	3.82	43	4.43	4.36	43	6.09	5.96		
44	1.62	1.61	44	2.16	2.15	44	2.70	2.68	44	3.24	3.21	44	3.79	3.74	44	4.33	4.26	44	5.95	5.83		

APPENDIX D

Combination of Errors

Let p and q be two measurable quantities and δp and δq their errors, respectively; n the number of samples; $\delta p/p \ll 1$; $\delta q/q \ll 1$.

1. Simple rules

   a. Addition: $r = p + q$ $\quad \delta r = \delta p + \delta q$

   b. Subtraction: $r = p - q$ $\quad \delta r = \delta p + \delta q$

   c. Multiplication: $r = pq$ $\quad \delta r/r = \delta p/p + \delta q/q$

   d. Division: $r = p/q$ $\quad \delta r/r = \delta p/p + \delta q/q$

2. Error estimates in slope and intercept

For least squares fit of straight line $q = \alpha p + \beta$ to data,

$$\alpha = \frac{\begin{pmatrix} \sum p_i^2 & \sum p_i q_i \\ \sum p_i & \sum q_i \end{pmatrix}}{D} \qquad \beta = \frac{\begin{pmatrix} \sum p_i q_i & \sum p_i \\ \sum q_i & n \end{pmatrix}}{D}$$

where $D = \begin{pmatrix} \sum p_i^2 & \sum p_i \\ \sum p_i & n \end{pmatrix}$

a. X-T plot:

Replace p_i with x_i and q_i with t_i. Apply simple rules above directly to and to obtain

$$\delta\alpha = \frac{\sum (\delta x_i)t_i + (\delta t_i)x_i}{\sum x_i t_i} + 3\frac{\sum \delta x_i}{\sum x_i} + \frac{\sum \delta t_i}{\sum t_i} + 2\frac{\sum (\delta x_i)x_i}{\sum x_i^2}$$

$$\delta\beta = \delta\alpha + \frac{\sum (\delta x_i)x_i}{\sum x_i^2}$$

b. $X^2 - T^2$ plot:

Replace p_i with x_i^2 and q_i with t_i^2.

$$\delta\alpha = 2\frac{\sum (\delta x_i)x_i t_i^2 + (\delta t_i)t_i x_i^2}{\sum x_i^2 t_i^2} + 6\frac{\sum (\delta x_i)x_i}{\sum x_i^2}$$

$$+ \; 2\,\frac{\sum (\delta t_i)t_i}{\sum t_i^{\,2}} \; + \; 4\,\frac{\sum (\delta x_i)x_i^{\,3}}{\sum x_i^{\,4}}$$

$$\delta\beta = \delta\alpha + 4\,\frac{\sum (\delta x_i)x_i^{\,3}}{\sum x_i^{\,4}} - \frac{\sum (\delta x_i)x_i t_i^{\,2} + (\delta t_i)t_i x_i^{\,2}}{\sum x_i^{\,2}t_i^{\,2}}$$

Note: the error estimate for the shot to recorder distances is ± .1 km (Hajnal, 1970, p.93)

LIST OF REFERENCES

1. Baer, D.W., A Developmental near-vertical reflection seismic study of the upper crust in the Canadian Shield near Kenora, Unpublished M. Sc. Thesis, University of Manitoba, Winnipeg, Canada (1972).

2. Dorn, T.F., The development and testing of a portable single trace seismic recording system for crustal studies, M. Sc. Thesis, University of Manitoba, Winnipeg, Canada (1974)

3. Friesen, G.H., Development of the processing capability for crustal exploration on the Canadian Shield by the near vertical reflection technique, Unpublished M. Sc. Thesis, University of Manitoba, Winnipeg, Canada (1974).

4. Hajnal, Z., A continuous deep-crustal seismic refraction and near-vertical reflection profile in the Canadian Shield interpreted by digital processing techniques, Unpublished Ph. D. Thesis, University of Manitoba, Winnipeg, Canada (1970).

5. Hall, D.H. and Hajnal, Z., Crustal structure in Northwestern Ontario: refraction seismology, Can. J. Earth Sci., 6, 81-99 (1969).

6. Hall, D.H. and Hajnal, Z., Deep seismic crustal studies in Manitoba, BSSA, 63, 885-910 (1973).

7. Homeniuk, L.A., A near-vertical-incidence reflection survey conducted over the Precambrian Shield area of Southeastern Manitoba, Unpublished M.Sc. Thesis, University of Manitoba, Winnipeg, Canada (1972).

8. Jenkins, G.M. and Watts, D.G., Spectral Analysis and its application (Holden-Day, Calif: 1968) p.21